

**CHARACTERISTICS AND PROPERTIES OF NATURAL
HYDROXYAPATITE DERIVED FROM BOVINE BONE FOR
BIOMEDICAL APPLICATIONS**

ALIASGHAR NIAKAN

**FACULTY OF ENGINEERING
UNIVERSITY OF MALAYA
KUALA LUMPUR**

2016

**CHARACTERISTICS AND PROPERTIES OF NATURAL
HYDROXYAPATITE DERIVED FROM BOVINE BONE FOR
BIOMEDICAL APPLICATIONS**

ALIASGHAR NIAKAN

**THESIS SUBMITTED IN FULFILLMENT OF THE REQUIREMENTS
FOR THE DEGREE OF DOCTOR OF PHILOSOPHY**

**FACULTY OF ENGINEERING
UNIVERSITY OF MALAYA
KUALA LUMPUR**

2016

UNIVERSITI MALAYA

ORIGINAL LITERARY WORK DECLARATION

Name of Candidate: ALIASGHAR NIAKAN



Registration/Matric No: KHA1200006

Name of Degree: DOCTOR OF PHILOSOPHY

Title of Project Paper/Research Report/Dissertation/Thesis ("this Work"):

CHARACTERISTICS AND PROPERTIES OF NATURAL HYDROXYAPATITE DERIVED FROM BOVINE BONE FOR BIOMEDICAL APPLICATIONS

Field of Study: MANUFACTURING PROCESS

I do solemnly and sincerely declare that:

- (1) I am the sole author/writer of this Work;
- (2) This Work is original;
- (3) Any use of any work in which copyright exists was done by way of fair dealing and for permitted purposes and any excerpt or extract from, or reference to or reproduction of any copyright work has been disclosed expressly and sufficiently and the title of the Work and its authorship have been acknowledged in this Work;
- (4) I do not have any actual knowledge nor do I ought reasonably to know that the making of this work constitutes an infringement of any copyright work;
- (5) I hereby assign all and every rights in the copyright to this Work to the University of Malaya ("UM"), who henceforth shall be owner of the copyright in this Work and that any reproduction or use in any form or by any means whatsoever is prohibited without the written consent of UM having been first had and obtained;
- (6) I am fully aware that if in the course of making this Work I have infringed any copyright whether intentionally or otherwise, I may be subject to legal action or any other action as may be determined by UM.

Candidate's Signature

Date

Subscribed and solemnly declared before,

Witness's Signature

Date

Name:

Designation:

UNIVERSITI MALAYA

PERAKUAN KEASLIAN PENULISAN

Nama: ALIASGHAR NIAKAN

No. Pendaftaran/Matrik: KHA120006

Nama Ijazah: DOCTOR OF PHILOSOPHY

Tajuk Kertas Projek/Laporan Penyelidikan/Disertasi/Tesis ("Hasil Kerja ini"):

CIRI-CIRI DAN SIFA HYDROXYAPATITE ASLI DARI BOVINE BONE ANTUK APLIKASI BIOPERUBATAN

Bidang Penyelidikan: MANUFACTURING PROCESS

Saya dengan sesungguhnya dan sebenarnya mengaku bahawa:

- (1) Saya adalah satu-satunya pengarang/penulis Hasil Kerja ini;
- (2) Hasil Kerja ini adalah asli;
- (3) Apa-apa penggunaan mana-mana hasil kerja yang mengandungi hakcipta telah dilakukan secara urusan yang wajar dan bagi maksud yang dibenarkan dan apa-apa petikan, ekstrak, rujukan atau pengeluaran semula daripada atau kepada mana-mana hasil kerja yang mengandungi hakcipta telah dinyatakan dengan sejelasnya dan secukupnya dan satu pengiktirafan tajuk hasil kerja tersebut dan pengarang/penulisnya telah dilakukan di dalam Hasil Kerja ini;
- (4) Saya tidak mempunyai apa-apa pengetahuan sebenar atau patut semunasabahnya tahu bahawa penghasilan Hasil Kerja ini melanggar suatu hakcipta hasil kerja yang lain;
- (5) Saya dengan ini menyerahkan kesemua dan tiap-tiap hak yang terkandung di dalam hakcipta Hasil Kerja ini kepada Universiti Malaya ("UM") yang seterusnya mula dari sekarang adalah tuan punya kepada hakcipta di dalam Hasil Kerja ini dan apa-apa pengeluaran semula atau penggunaan dalam apa jua bentuk atau dengan apa juga cara sekalipun adalah dilarang tanpa terlebih dahulu mendapat kebenaran bertulis dari UM;
- (6) Saya sedar sepenuhnya sekiranya dalam masa penghasilan Hasil Kerja ini saya telah melanggar suatu hakcipta hasil kerja yang lain sama ada dengan niat atau sebaliknya, saya boleh dikenakan tindakan undang-undang atau apa-apa tindakan lain sebagaimana yang diputuskan oleh UM.

Tandatangan Calon

Tarikh

Diperbuat dan sesungguhnya diakui di hadapan,

Tandatangan Saksi

Tarikh

Nama:
Jawatan:

ABSTRACT

Bovine bone is a hierarchically structured natural composite material, consisting of collagen as an organic phase, hydroxyapatite as a mineral phase, and hydroxyl. The aim of this research is to study the properties of natural hydroxyapatite (HA) developed from bovine bone. Sintering process was used to transform the bovine bone constituents into pure HA mineral phase which makes bovine bone such a unique biological material. Femur cortical bone was harvested from local slaughterhouse, cleaned and subsequently sintered in air atmosphere at different temperatures ranging from 200°C to 1300°C with heating ramp rate of 10°C for 2 hours. The samples were characterised through bulk density measurement, X-ray diffraction, Micro X-ray Fluorescence, Fourier transforms infrared spectroscopy analysis, simultaneous thermal analyser, differential scanning calorimeter, Vickers hardness and fracture toughness determination. In addition, the microstructural evolutions of the sintered bodies were also examined by field emission scanning electron microscopy and transmission electron microscopy. The results revealed that the thermal stability of the HA matrix was not disrupted and that all of the sintered samples exhibited phase pure HA. Nevertheless, sintering at 750°C was identified as the optimum temperature to produce a well-defined porous HA body with a relative density of 50% and Vickers hardness of 172 MPa. In addition, a natural interconnected porous structure was clearly visible, and the pores were distributed homogeneously throughout the matrix. Uniform pores with a mean size of approximately 152 nm and HA grains sizes ranging from 111 nm to 248

nm were obtained. Finally, biocompatibility of the bovine-derived samples was evaluated via *in vitro* human osteocalcine cells test. Cell viability and cell attachment were undertaken by human bone marrow stem cell. The results of cell viability, cell attachment and osteocalcine test on sintered samples indicated minor cytotoxic response. Thus, this research proved that natural hydroxyapatite developed from sintered bovine bone could be a suitable bioceramic for use in clinical application.

University of Malaya

ABSTRAK

Tulang lembu adalah bahan komposit semulajadi berstruktur hierarki, yang terdiri daripada kolagen sebagai fasa organik, hydroxyapatite sebagai fasa mineral, dan hidroksil. Tujuan kajian ini adalah untuk mengkaji sifat-sifat semula jadi hydroxyapatite (HA) yang diperbuat daripada tulang lembu. Proses pensinteran digunakan untuk mengubah jujuk tulang lembu ke fasa mineral HA tulen yang menjadikan tulang lembu seperti bahan biologi yang unik. Tulang kortikal tulang paha dituai dari rumah sembelih tempatan, dibersihkan dan kemudiannya disinter dalam suasana udara pada suhu yang berbeza antara 200°C hingga 1300°C dengan pemanasan kadar tanjakan 10°C selama 2 jam. Sampel telah dicirikan melalui pengukuran ketumpatan pukal dan dianalisis menggunakan *X-ray Diffraction*, *Micro X-ray Fluorescence*, *Fourier Transforms Infrared Spectroscopy*, *Simultaneous Thermal Analyser* *Differential Scanning Calorimeter*, kekerasan Vickers dan penentuan ketahanan patah. Di samping itu, evolusi mikrostruktur daripada bahan-bahan yang telah disinter juga diperiksa dengan menggunakan *Field Emission Scanning Electron Microscopy* dan *Transmission Electron Microscopy*. Keputusan menunjukkan bahawa kestabilan matriks HA itu tidak terganggu dan bahawa semua sampel yang telah disinter mempamerkan fasa tulen HA. Walau bagaimanapun, pensinteran pada 750°C telah dikenal pasti sebagai suhu optimum untuk menghasilkan badan HA berliang yang jelas dengan kepadatan relatif 50% dan kekerasan Vickers 172 MPa. Di samping itu, struktur berliang semulajadi yang saling bersambung adalah jelas kelihatan, dan liang telah diselaratakan secara seimbang ke atas seluruh matriks. Liang seragam dengan saiz purata kira-kira 152 nm dan HA

bijirin saiz antara 111 nm hingga 248 nm diperolehi. Akhir sekali, keserasian biologikal sampel lembu yang diperolehi telah dinilai melalui ujian in vitro sel *osteocalcine* manusia. Daya keupayaan sel dan pelekatan sel telah dijalankan ke atas sel stem tulang sumsum manusia. Keputusan ujian ini menunjukkan tindak balas sitotoksik yang berskala kecil. Oleh itu, kajian ini membuktikan bahawa hydroxyapatite semula jadi yang dihasilkan daripada tulang lembu yang telah disinter boleh menjadi bahan bioseramik yang sesuai untuk digunakan dalam aplikasi klinikal.

University of Malaya

ACKNOWLEDGEMENTS

I would like to thank my mother for giving me the drive to attempt to obtain my Ph.D. for being there for me throughout completion of my degree. In addition, foremost I would like to express my sincerest gratitude and appreciation to my project supervisor, Prof. Ir. Dr. Ramesh Singh, for his valuable and insightful advice, discussion, comments and encouragement throughout this research endeavor. Throughout my tenure as a postgraduate student, he has not only shared with me his vast technical knowledge but more importantly, has moulded me to be a better individual.

In addition, I am also deeply appreciative of the marvelous support and goodwill I have been given by Associate Professor Dr. Tan Chou Yong. It is a genuine honor to know you and to learn from you. I have also been truthfully blessed to be supported by Dr. Poo Balan.

During my program, I have been very fortunate to have a best cordial relationship with Dr. Kelvin Chew. You are truly my best friend. Please accept my sincere gratitude and extend it to your parents.

I would also like to take this opportunity to thank:

- University of Malaya (UM) for the HIR funding and the short-term research grant (PG 079-2013A).
- Tissue Engineering Group (TEG) at the Department of Orthopedic Surgery, Faculty of Medicine, University of Malaya.
- My friends in UM for their constant support and encouragement.

Last but not least, I would like to dedicate this work to the soul of my father and may he rest in peace. While he is no longer with me, I owe a debt of gratitude to him. He could not support me through this endeavor because he left. But I know he would be truly ecstatic to see me here today. He saw himself in me in many ways (not just in research), and I know he would be sincerely proud to see me finish this process.

Table of Contents

Title Page	i
Original Literary Work Declaration Form	ii
Abstract	iv
Abstrak	vi
Acknowledgements / Dedication	viii
Table of Contents	ix
List of Figures	xiii
List of Tables	xvi
List of Abbreviations	xvii
List of Appendices	xviii
CHAPTER 1	1
1.1 Biomaterials	1
1.2 Bone substitution	2
1.3 Scope and objectives of the research	4
1.4 Structure of the thesis	6
CHAPTER 2	7
LITERATURE REVIEW	7
2.1. Bone graft	7
2.2. Structure and composition of bone as natural hydroxyapatite precursor	15
2.2.1. Mechanical and physical characteristics of bone	15

2.2.2. Mineral composition of bones and hard tissues	18
2.3. Calcium phosphate bioceramics	19
2.4. Hydroxyapatite	20
2.4.1. Hydroxyapatite crystallography	21
2.4.2. Comparison between hydroxyapatite and bone	23
2.5. Synthesis of hydroxyapatite	24
2.5.1 Precipitation technique	25
2.5.2. Hydrothermal reaction	26
2.5.3. Solid state reaction	27
2.5.4. Sol-gel route	28
2.6. Synthesis of HA from natural source	30
2.7. Use of natural bone as a bone replacement material	31
2.7. Cell cultural behavior and attachability of HA based ceramics	34
CHAPTER 3	40
3.1 Introduction	40
3.2. Sample preparation	40
3.3 Sintering of the bone	42
3.4 Surface preparation and polishing	43
3.5 Phase analysis	43
3.6 Bulk density measurement	44
3.7 Thermal analysis	44
3.8 Fourier transforms infrared spectroscopy analysis (FTIR)	45
3.9 Micro X-ray Fluorescence (Micro-XRF)	45
3.10 Microstructural evolution	46
3.11 Vickers hardness and fracture toughness measurements	46

3.12 Biocompatibility study	48
3.12.1 Cell viability and cytotoxicity	48
3.12.2 Cell attachment	50
3.12.3 Alkaline phosphate activity (ALP)	50
3.12.4 Osteocalcin	50
3.12.5 Statistical analysis	51
CHAPTER 4	52
Results and Discussion	52
4.1 Introduction	52
4.2 Physical observation	52
4.2.1 TGA analysis	54
4.2.2 Phase analysis and thermal stability	55
4.2.3 FTIR analysis	60
4.2.4 Micro-XRF analysis	62
4.2.5 Microstructural evolution	65
4.2.6 Average grain size and porosity	70
4.2.7 Relative density	72
4.2.8 Micro hardness and fracture toughness	74
4.3 Biocompatibility evaluation	76
4.3.1 Alamar blue assay for cell proliferation	76
4.3.2 SEM analysis of cultured scaffold	78
4.3.3 Chemical analysis by EDX	83
4.3.4 Confocal microscopy of cultured scaffold	85
4.3.5 ALP and osteocalcin assays	88
CHAPTER 5	91

5.1 Conclusion	91
5.2 Recommendation for further work	93
REFERENCES	95
List of Publication and Award	116
APPENDIXES	

University of Malaya

List of Figure	Page
Figure 2.1: Three main categories of bioceramic materials	14
Figure 2.2: The main characteristics of bioceramic materials	14
Figure 2.3: Femoral bone (A) and arrangement of cortical bone (cross section, B), osteon (C), collagen fiber (D, E and F), biologic apatite (G) and crystal structure of hydroxyapatite in bone	16
Figure 2.4: Schematic representation of the hydroxyapatite lattice.	22
Figure 2.5: SEM of porous structure of hydroxyapatite from calcined bovine cancellous bone	33
Figure 2.6: Porous HA structure produced from sintered bovine bone powder.	33
Figure 2.7: Rounded cell (RC) and spread cell (SC) morphology of human osteoblasts cells on implant surface.	35
Figure 2.8: The ESM images of HA scaffold; (a) undoped HA scaffold and (b) Ca-doped HA scaffold.	37
Figure 2.9: SEM images of porous calcium phosphate with (a) 45.9% porosity, (b) 43% porosity, (c) immersion of (a) in HBSS, and (d) immersion of (b) in HBSS after 2 weeks	38
Figure 3.1: cortical bone before (a) and after autoclaving (b).	41
Figure 3.2: The precision saw (a) used to cut the test samples (b).	42
Figure 3.3: The sintering process	42
Figure 3.4: Schematic diagram showing the Vickers indentation.	47
Figure 4.1: Colour change due to sintering of bovine bone at various temperatures.	53
Figure 4.2: The TG and DTA curve of as-received bovine bone as measured from room temperature to 1000°C.	55

Figure 4.3: The XRD patterns of the un-sintered bone sample at 30°C and as-sintered samples from 200°C to 600 °C.	56
Figure 4.4: XRD patterns of bovine bone sintered from 700°C to 1200°C calcined for 2 hours.	57
Figure 4.5: XRD patterns showing the presences of β -TCP in bone samples sintered at 1250°C and 1300°C.	59
Figure 4.6: XRD patterns of sintered bovine samples at 750°C	60
Figure 4.7: FTIR spectrum of un-sintered bovine bone and sintered samples at 750°C.	61
Figure 4.8: FTIR spectrum of sintered bovine bone at 1250°C and 1300°C.	62
Figure 4.9: The variation in the Ca/P ratio with increasing sintering temperature.	64
Figure 4.10: FESEM images of un-sintered sample and sintered samples at (a) 30°C and (b) 200°C.	66
Figure 4.11: Surface microstructure of the sintered samples at (a) 600°C and (b) 700°C.	68
Figure 4.12: Micrograph of the sintered samples at (a) 1000°C, (b) 1100°C, (c) 1200°C and (d) 1300°C.	70
Figure 4.13: The variation of average grain size at different sintering temperatures.	71
Figure 4.14: Effect of sintering temperatures on pore size.	72
Figure 4.15: Relative bulk density of bone samples sintered at different temperatures.	73
Figure 4.16: Variation in Vickers hardness with sintering temperatures.	75
Figure 4.17: The relationship between the relative density and Vickers hardness for sintered samples.	75
Figure 4.18: hMSCs proliferation of sintered bovine bone scaffold sintered at different sintering temperatures with significant value at $P < 0.05$.	77

Figure 4.19: SEM picture of scaffold sintered at 600°C showing hMSCs activity after day 11.	79
Figure 4.20: SEM pictures of exposed scaffolds sintered at (a) 700°C and (b) 750°C revealing hMSCs activity after day 11.	80
Figure 4.21: SEM pictures of exposed scaffolds sintered at (a) 800°C and (b) 900°C revealing hMSCs activity after day 11.	81
Figure 4.22: SEM pictures of exposed scaffolds sintered at (a) 1000°C and (b) 1150°C revealing hMSCs activity after day 11.	82
Figure 4.23: SEM picture of exposed scaffolds sintered at 1250°C revealing hMSCs activity after day 11.	83
Figure 4.24: EDX of bovine scaffold infiltrated with hMSCs	84
Figure 4.25: Confocal microscopy of cell attachment on bovine scaffolds prepared at varying sintering temperature from 600°C to 1000°C.	86
Figure 4.26: Confocal microscopy of cell attachment on bovine scaffolds prepared at sintering temperature of 1150°C and 1250°C against control scaffold without cells.	87
Figure 4.27: Early hMSCs differentiation and ALP of bovine scaffold prepared from 700°C to 900°C with significant value at $P < 0.01$ and $P < 0.05$.	89
Figure 4.28: Production of osteocalcin (OC) on bovine scaffold prepared from 700°C to 900°C with significant value at $P < 0.01$.	90

List of Table	Page
Table 2.1: Mechanical Properties of human wet cortical bone	17
Table 2.2: Comparison of chemical composition in bone, enamel, dentin, bone and HA	19
Table 4.1: Physical Observation of Bovine Bone with Increasing Temperature.	53
Table 4.2: Chemical elements of samples as determined from micro XRF	63

University of Malaya

List of Abbreviations

Polyglycolic acid	(PGL)
Hydroxyapatite	(HA)
Amorphous Calcium Phosphate	(ACP)
beta-Tricalcium phosphate	(β -TCP)
alpha-Tricalcium phosphate	(α -TCP)
Biphasic Calcium Phosphate	(BCP)
Tetracalcium Phosphate	(TTCP)
X-ray diffraction	(XRD)
Micro X-ray Fluorescence	(Micro-XRF)
Field Emission Scanning Electron Microscopy	(FESEM)
Fourier Transforms Infrared Spectroscopy	(FTIR)
Simultaneous Thermal Analyser	(STA)
Differential Scanning Calorimeter	(DSC)
human Mesenchymal Stromal Cells	(hMSCs)
Fetal Bovine Serum	(FBS)
Phosphate Buffered Saline	(PBS)
Critical Point Drying	(CPD)
Alkaline Phosphatase	(ALP)
Nitrophenyl Phosphate	(NPP)
Standard Deviation	(SD)
Extracellular Matrix	(ECM)

List of Appendix

APPENDIX A	(Equipments and Instruments)
APPENDIX B	(JCPDS cards)
APPENDIX C	(Density table of distilled water)

University of Malaya

CHAPTER 1

INTRODUCTION

1.1 Biomaterials

Biomaterials are materials used as a template to guide tissue reorganization, as a matrix that provides optimum micro-environmental conditions to cells, as a delivery vehicle to carry bioactive factors which can be released in a controlled manner, and as a temporary or permanent scaffold to spur *in situ* tissue regeneration. There are many biomaterials, varying in geometrical structure, physical form, chemical properties, and bio-functionality being developed for skeletal muscle tissue engineering applications (Daglilar and Erkan, 2007; Qazi et al., 2015). According to Hing (2004), during the 1960 and 1970 the first generation of biomaterials was developed to accomplish a suitable arrangement of physical properties to match those of the substitute tissue with a negligible negative reaction with the host. Inert materials were utilized to manufacture implant parts that could perform biomechanical requirements (e.g. alumina, metals and polymers). Although these inert implants display better performance when implanted in some patients, but they often have limited lifetime and requires replacement which can be troublesome to the patients (Katti, 2004; Mitragotri and Lahann, 2009). In addition, there were also reports that some implants could not be fully integrated into the body (Mitragotri and Lahann, 2009).

In order to improve the limitations of these biomaterials, research work was directed to develop the second generation biomaterial having longer lifetime and being compatible with biological environment (Hench and Polak, 2002; Navarro et al., 2008). Amidst 1980s bioactive materials were used and found to be acceptable by the living tissues, particularly as fillers for bone defect (Vogel et al., 2001; El Gannham, 2005). Although the second era of biomaterials had attained numerous advances, but there was a weakness of low bioactivity rate with cell proliferation for these biomaterials (Navarro et al., 2008). As a result, the third generation of biomaterials were developed which have the ability to simulate cellular activities at the molecular level (Hench and Polak, 2002; Navarro et al., 2008). In these materials, the interconnected porous structure allows cell migration into the materials, thus promoting attachment, vascularisation, nutrition delivery and facilitate in the healing of damaged tissues and reproduction of new tissues (Agrawal and Ray, 2001). The research has also focused on new methods in which functional implants are created by seeding stem cells onto biocompatible and interconnected porous substrates materials that become as platform, and permit transmission of supplements to the cells and the cell-to-cell contact that prompts the arrangement of new tissue (Weiner and Dove, 1986; Weiner, 2008). The tissue engineered constructs are then implanted into the patients to replace contaminated or damaged tissues (Hench and Polak, 2002).

1.2 Bone substitution

The quest for the ideal bone repair or substitution material was a result of the early work reported in 1892 which concentrated on the suitability of calcium sulphate as a bone substitution material (Georgiade et al., 1993; Sousa and Evans, 2003). Resulting to this, numerous advances have been made in bone substitution innovation; however a

few key issues still remain, particularly on the easy accessibility of viable grafts materials.

Autografts, which are parts of bone that taken from patients themselves are known as the “gold standard” of bone substitution material for the restorative action and provided excellent biocompatibility, while their availability are limited (Giannoudis et al., 2005). The autogenous grafts could be utilized to increase the extremely atrophic bones edges, to recreate alveolar absconds in patients, or to extension absconds that are the consequence of trauma surgery or ablative. On the other hand, autogenous bone grafts are typically adjusted to the beneficiary site and fuse well into the imperfections. A layer of connective tissue will basically blanket the grafts structure. Therefore, the interface between the beneficiary bone and the joining revascularisation happens at last prompting the framing of new bone (Artico et al., 2003). However there is little tissue excess inside living organisms, which confines the accessibility of such material. Implanted autografts contain surviving cells and inductive proteins, which can fortify osteogenesis. From an organic and biologic perspective, it is the best material accessible since it is no immunogenic and it can bind with bone quickly after transplantation. Besides, morbidity at the site of evacuation is obstacle in 10-25% of cases, with patients who have experienced bone extraction for transplantation on occasion reporting extensive and delayed torment, showing indications of nerve harm and experiencing disease at the site of evacuation (Tuominen et al., 2001; Tadic and Epple, 2004; Hing 2005). Consequently, autograft implantation is a tough process and in perspective of these realities, it is obvious that autografting is not a complete answer for fulfil the therapeutic interest for bone substitution material.

The utilization of allografts is a possible solution to the issue of material accessibility. Allografts are gathered from an alternate part of the same species (from individuals for this situation) and are accordingly available in numerous supplies.

However, their utilization has the capability of presenting different inconveniences which the most relating to the hepatitis, HIV and genetic disease exchange (Chen et al., 2009). In spite of this, the vicinity of natural material as protein or fat in allografts raises the likelihood of evoking antigenic invincible and immune reactions after implantation into the body (Trentz et al., 2003; Chen et al., 2009). A method for minimizing such immunological issues is to utilize xenografts and engineered materials without organic substance.

Xenografts and alloplastic including synthetic and engineered bio-materials, for instance ceramics, are easy to produce. In the preparation procedures of these materials, it is possible to develop different micro-structural, physical and mechanical properties (Pinchuk and Ivanchenko 2003). However, the difficulties remain in the capability to match all specific properties and some biocompatibility issues to support certain bone requirements in the body (LeGeros et al., 2008).

The other restriction in the creation of an artificial bone substitute material is the selection of the starting bone source and the lack of proper production method, which permits the synchronous production of suitable internal structure and porosity, chemical composition particularly the calcium to phosphorus ratio and a microstructure that mimics the natural bone.

1.3 Scope and objectives of the research

Sintered bones from biogenic source such as from biowastes which include fish bones, corals, bovine bones, eggshells etc. are biomaterial that contains natural calcium phosphate compounds, is perceived to be better accepted by the living tissues because of its physiochemical similarity to the human bone. Sintered bone is made of hydroxyapatite (HA), which is the most stable phase of calcium phosphate apatite that has demonstrated excellent biocompatibility and bioactivity with hard tissues

(Taniguchi et al., 1999). Studies have shown that the physiochemical property of hydroxyapatite, for example grain size and surface morphology are paramount variables that effect on bio-resorbability of HA (Nayar and Guha., 2009; Mucalo and Worth, 2008; Hasegawa et al., 2003; Joschek et al., 2000; Barralet et al., 2002; Albrektsson et al., 2001).

In particular interest, the bovine bone represents a huge biowaste of xenogeneic material as a potentially viable source of biomaterial for clinical application (Tuominen et al., 2001; Worth et al., 2005; Worth et al., 2007; Pinchuk and Ivanchenko 2003; Chau and Mobbs, 2009). Therefore, in this research, the scope of the work is confined in converting bovine bone into a natural porous biomaterial characterised by having suitable mechanical properties via employing the sintering process. This research work aim to demonstrate that interconnected micropores structure could be directly derived from sintered cortical bovine bone, having proper mechano-chemical properties, excellent biocompatibility without any cytotoxicity react, as it is readily integrated with the human marrow cells providing a natural tendency for osteoblast formation.

Therefore, the objectives of this research are as follows:

1. To convert bovine bone through a sintering process to form the stable phase of calcium phosphate hydroxyapatite (HA).
 - The bone samples were sintered under atmospheric conditions at various temperatures ranging from 200°C to 1300°C.
2. To identify the optimum temperature to produce bovine-HA with natural interconnected pores, fine microstructure and good mechanical properties without compromising on HA phase stability in the bone matrix.
 - Samples characterization and mechanical properties of the as-sintered samples were undertaken by X-ray diffraction (XRD), Micro X-ray

Fluorescence (Micro-XRF), field emission scanning electron microscopy (FESEM), Fourier transforms infrared spectroscopy (FTIR) analysis, simultaneous thermal analyser (STA), differential scanning calorimeter (DSC), Vickers hardness and fracture toughness determination.

3. To evaluate the biocompatibility of the derived bovine-HA using cell culture and cytotoxicity studies with human osteoblasts cells.
 - The biocompatibility and cytocompatibility of the as-sintered samples were examined through *in vitro* assessment.

1.4 Structure of the thesis

This thesis is divided into five main chapters. Chapter 1 presents a brief overview of biomaterials, identifying the gaps in the literatures and establishing the objectives of this research. The literature review is presented in Chapter 2. This chapter deliberates on the findings of the literatures on the concept of HA bioceramic and strategies that have been employed for its use as a potential biomaterial. The materials and experimental procedures employed in this research are presented in Chapter 3. The results obtained in this research and discussions are presented in Chapter 4. In this chapter, the effect of sintering temperature on the thermal stability of HA derived from bovine bone as well as their mechanical properties are discussed. The resulting microstructure of the bovine HA as a function of sintering temperature is also deliberated. In addition, the biological response to the bovine HA scaffolds derived in the present research is analysed. Finally, the conclusions drawn from the present research are presented in Chapter 5. The appendices contain some important data to support the results discussed in Chapter 4.

CHAPTER 2

LITERATURE REVIEW

2.1. Bone graft

Bone graft implant is described as a piece of bone that is transplanted from one area of the skeleton system to another for the purpose of bone replacement, filling cavities, repairing the biological defects of the skeleton system and regenerate the holding support for bone growing (Giannoudis et al., 2005). After that the bone graft is exchanged with natural bone, or remains in the structure permanently and connected to natural hard tissues. The bone replacement materials must be accepted by the hard tissues at the implanted site with no act of rejection or evoking an immunologic response. The artificial bone graft must also have ability to supply quick percolation of osteogenesis from the host to the main structure of the bone implant (Miyazaki et al., 2009). Fischgrund et al. (2002) reported that three critical factors were necessary for bone regeneration. First, is the osteogenic cells with the ability of new bone forming, second, is osteoinductive factors such as growth factors and cytokines that encourage the osteoblastic from pluripotent cells and the third, is osteoconductive scaffold that boosts neovascularization and supports the bone growing process. The most favourable replacement graft is the one which is morphologically close or similar to human bone tissue and a material composition of bone graft must be bioactive and biocompatible. In

general, Hing (2004) outline four clinical steps process that fractured bone or bone grafting heals through ossification as follows:

- i. Firstly, a stimulation of fractured bone and healing of fractures, both fresh and untreated fractured or those defects that have broken down to heal after treatment effort.
- ii. As a consequence a stimulation of healing between two bones is required.
- iii. In response to generate the new bone which is damaged or missed due to harm, infection and disease, settings are needed for reconstruction or repair of missing bone. This setting can be change from filling of small cavities, to replacing large sections more than 12 inch in length.
- iv. In point of improving the bone healing reaction and regeneration of new bone and tissues around substitute implanted parts such as artificial joints substitutes like hip joint and knee joint replacement, plates and screws used to keep the bone in position.

Bone graft replacement materials should offer those properties related to human hard tissue and bone such as: (i) Bone graft materials should offer enough strength to support the movements, protect the skeleton system and its function. (ii) Bone graft substitutes should contain a mixture of pores with different size to permit the movement of body enzyme that act as bone growth factors. On the other hand, porosity structure is also required to carry the nutrition and blood vessels to the osteon cells and other structures. (iii) Another important and basic property that should provide from graft materials is their biological compatibility. It means that any bone graft must be made of those kinds of materials that are body friendly and compatible with skeleton system, so as to ensure that skeleton system admit the graft material. (iv) The bone graft should provide the substance to encourage the bone formation which is called catalysts to bone

growth. The catalysts to bone growth could be through different ways such as adding the artificial growth factors or by natural procedures like use of patient bone marrow or guide the blood vessels to the substitute. According to Salgado et al. (2004) and Schieker et al. (2006) there are millions of skeleton system defect per year that needs repairing or replacing with bone graft operation worldwide, especially in America and Europe countries mainly due to increasing population and aging.

Current treatment of biomaterials are based on naturally extracted bone graft substitute that have been used for years as the core source of grafts materials which include autografts, allografts and xenografts (Joschek et al., 2000; Thomas, 2008; Ruehe et al., 2009). Each type of these bone grafts has its own advantages and disadvantages. In addition, some alternative materials such as metals, polymer and ceramics are also used for biomedical applications (Petite et al., 2000; Rose et al., 2002; Jensen et al., 2006).

Autograft or endogenous bone graft is a process that bones are transplanted directly from one area of an individual's skeleton into his or her own defected part (Vacarro, 2002). Autograft remains as the gold standard for bone substitute and replacement graft. The autograft is normally derived in the form of trabecular shape from the patient's body of large area like hip, ribs or leg. Autograft is one of the safest bone grafts to repair the defected bone due to the low risk of virus and disease transfer. Salgado et al. (2004) reported that the cortical bone can be used to harvest the autograft. Truumees and Herkowits (1999) reported that the autograft implant provides a better chance of response and strength in the transplant location due to the osteon cells, nutrients and proteins that is provided from patient's body. In general, the penetration of blood vessels into the graft for revascularization is easy, but the graft can offer low mechanical stress and strength. In addition autograft harvesting is associated with difficulties including body deformation, blood loss, nerve injury, hernia formation,

infection, arterial injury, urethral injury, fracture, pelvic instability, cosmetic defects, tumors transplantation, and sometimes constant pain for patient (Gunzburg et al., 2004; Giannoudis et al., 2005). In many situations allografts or exogenous bone tissues is chosen as an alternative graft where autografts are not suitable.

Allograft is the most often chosen bone alternative and is regarded as the surgeon's second option. The current increasing availability of allograft tissue has made it possible to manufacture customized parts such as dowels strips, and chips. Allografts bones are taken from the other skeleton system. It is normally from cadaver's donor who have volunteered to donate their bone or from bone harvested during other operations, such as allografting during hip or knee surgery operation. The reduction of expenses of operative procedures and the elimination of second surgery operation on patient body can be the advantages of allografts bone. However, fresh allografts are seldom used due to biological effect, risk of transferring viral diseases or immune response and pathogen transmission from donor to host that could occur in the patient's body after the transplantation. Another disadvantage of the allografts is that it's considered to have weak osteoinductive capabilities and its consolidation rate is also worse than autograft (Petite et al., 2000; Rose and Oreffo 2002; Simon et al., 2002; Salgado et al., 2004).

Xenograft bone substitute is derived from animals bones and implanted to human body. For the long time, xenografts bone is used for orthopedics and clinical applications. Xenografts bone substitute are obtained from animals bones including ivory, cow horn and bovine bone or pig that have lattice structures similar to human bones (Reynolds et al., 2010). Compared to other bone grafts substitute, xenogenic bone such as bovine is easier to obtain, lower in cost and it is available in huge amount. From material viewpoint, bovine bone contained organic and inorganic elements. The organic part composes of collagen and the inorganic part is primarily hydroxyapatite (HA)

including low weight percentages of other ions such as fluoride, carbonate and magnesium. The part of bone that contains the inorganic component will be used for xenograft (Wenz et al., 2001; Bloemers et al., 2003; Ooi et al., 2007).

Based on the many issues highlighted with regards to the extraction procedure as well as the many problems reported with regards to autografts and allografts that derived from human bone, the development and production of artificial bone replacements have become very important. At this level, metals, polymers and ceramics are chosen as an alternative to autografts and allografts bone substitute. However, these alternative materials have several advantages and disadvantages. Metals have been suggested and used for handling of load bearing and also offering instant mechanical support at the transplanted area in orthopedic applications. In general, metals implant demonstrated poor biocompatibility with the hard tissues and might cause breakdown for reason of infection or due to fatigue loading (Salgado et al., 2004). Metals implants are typically made from stainless steel, cobalt alloys, titanium and its alloy (Suchanec and Yoshimura, 1998; Agrawal, 1998; Vallet-Regi, 2001; Salgado et al., 2004; Vallet-Regi et al., 2010). Stainless steel is used to stabilise the fractures fixation, since it provide the high elastic modulus and tensile strength including good ductility which allows them to be cold work and is bioinert. Stainless steel is among the expensive metals and also it has low fatigue resistance that could be disadvantages of using stainless steel as biomaterial. Cobalt and its alloys have also seen chosen to manufacture artificial parts of joints prostheses and for dental applications. Cobalt and its alloys possess high elastic modulus, hardness, strength and corrosion resistance, but they have low ductility and difficult to machine. Another alternative metal which is used as a bone substitute is titanium and its alloys. These days most of the bone substitutes that need to bear the load are made from titanium and its alloy even in dental implant due to its biocompatibility properties.

According to Katia et al. (2008), polymeric materials have been widely studied and chosen as alternative for bone replacement for medical applications. Polymeric bone substitute can be used and manufacture for prostheses implants, dental implants and materials, craniofacial applications, extracorporeal devices, polymeric drug delivery system (Burg et al., 2000; Salgado et al., 2004; Katja et al., 2008). Polymeric bone substitutes can be produce in various forms of film, fibers, sheet, latex and etc due to their ease of manufacturability, reasonable production cost and they can offer desired behaviour and properties needed for biomaterials such as biocompatibility, sufficient medical and mechanical properties (Burg et al., 2000). According to Salgado et al. (2004), polymeric bone substitute can be categorized into natural polymers and synthetic polymers materials. They have been used in wide range of operation and application such as facial prostheses and dental plate, kidney and liver parts, ear components, tracheal tubes, hip and joints (Agrawal and Ray 2001 ; Katja et al., 2008). Natural polymers materials can be found in gelatin and collagen, starch, chitin and chitosan that have been widely used to replace and repair skin, nerves, cartilage and hard tissues. The negative aspect of natural polymers substitute is low mechanical and physical properties for implantations. Synthetic resorbable polymers, such as polyglycolic acid (PGL), polylactic acid, gelatin and collagen are categorized as biodegradable polymers and have been used to support bone repair (Eppley and Prevel, 1997; Wei and Ma, 2004). The synthetic resorbable polymers are degraded by body enzyme through enzymatic or hydrolysis reaction. Furthermore, synthetic resorbable polymers have been used as a temporary implant in drug delivery systems (Wei and Ma, 2004; Tian et al., 2012).

Ceramics materials are defined as solid components that are formed through the heat treatment method and sometimes under the combination of heat and pressure. Ceramics are comprised of non metallic elements or a compounding of at least one

metallic and non metallic solid elements (Barsoum et al., 2002). Bioceramics can be defined as ceramics that have been used for clinical applications as implants materials. Various ceramic materials such as zirconia, alumina, titania, tricalcium phosphate, dicalcium phosphate dehydrate, dicalcium phosphate anhydrous, tetra calcium phosphate, octacalcium phosphate, sintered hydroxyapatite and bioactive glasses can be classified as bioceramics materials (Hench, 1998; Billote, 2000; Vallet-Regi, 2001; Vallet-Regi et al., 2010). In general, bioceramics are categorized as refractory materials and offers high compression strength and hence suitable for replace or repair bones defects, joints failure and teeth. On the other hand, Vallet-Regi (2010) reported that there are three main categories of bioceramics materials i.e. resorbables bioactive ceramics, bioinert and bioactive surface as depicted in Figure 2.1.

Bioinert ceramics do not react with living tissue and alumina is a good example of bioinert ceramics. Resorbable bioactive ceramics would degrade after implantation as the bone heals and replaced by new tissues. Bioactive ceramics are the most chemically and physically stable bioceramics which are able to attach with living osseous cells and tissues. Most of the calcium phosphates ceramic exhibit this attribute (Kalita et al., 2007; Kalita et al., 2010; Tian et al., 2012).

According to Kalita et al. (2010), calcium phosphate-based bioceramics can be used for medical application and implants without rejection due to their biocompatibility, chemical stability within human body fluid and pH. They offer both low and high density structures, higher wear resistance and have a chemical composition similar to the mineral phase of human bone. The main characteristics of bioceramic for use in biomedical application are shown in Figure 2.2.

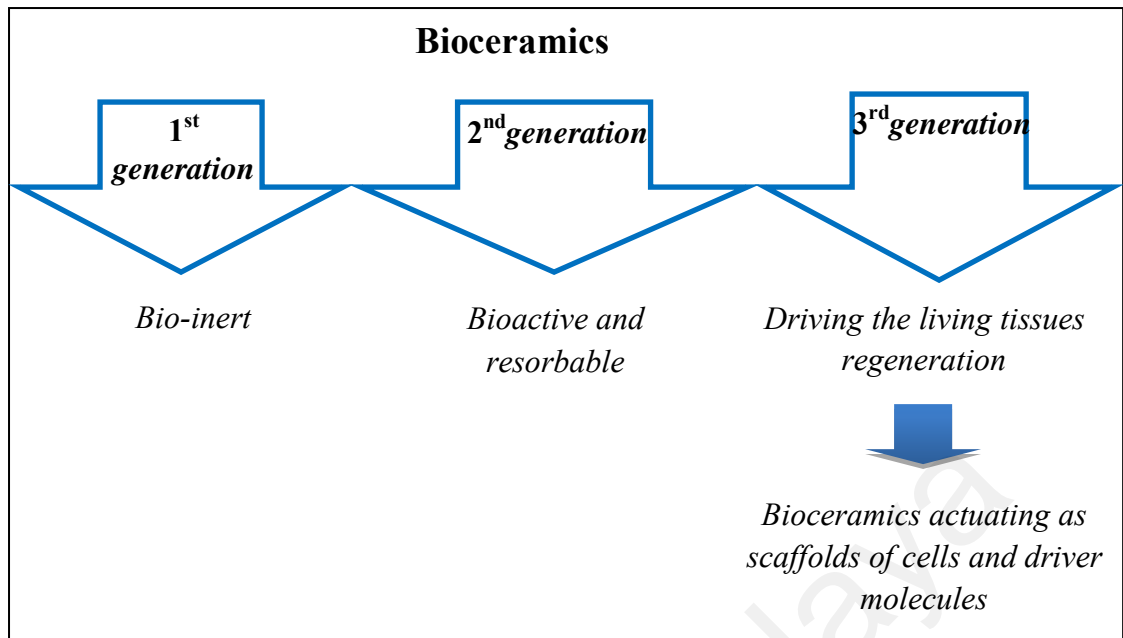


Figure 2.1: Three main categories of bioceramic materials (Vallet-Regi et al.,2010).

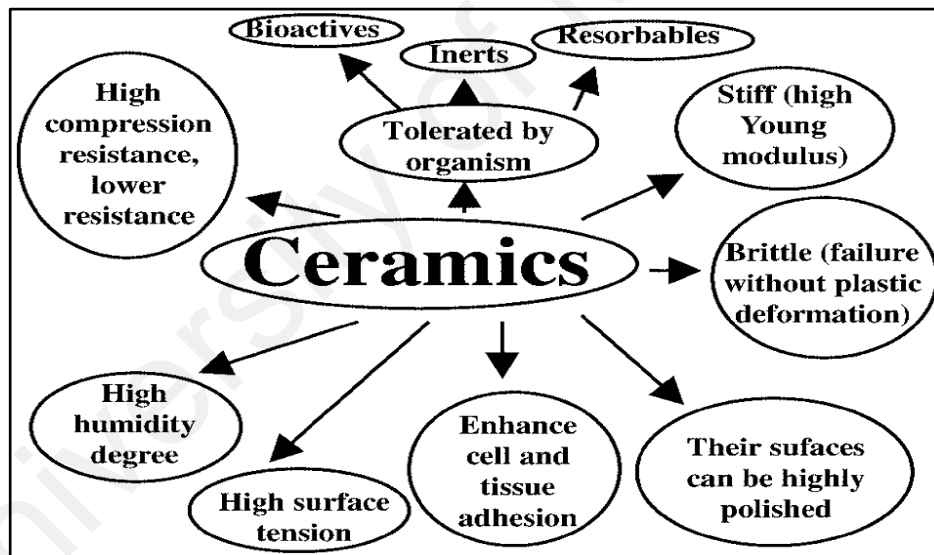


Figure 2.2: The main characteristics of bioceramic materials (Vallet-Regi (2001).

At the clinical level and biocompatibility studies, hydroxyapatite (HA, $\text{Ca}_{10}(\text{PO}_4)_6(\text{OH})_2$) has been considered as a most suitable bioceramic material and used for bone implants and various medical applications. The mineral phase of bones and hard tissues are consisted of HA compound. Hydroxyapatite ceramic does not show any cytotoxicity effect in contact with collagen and osteon cells. Furthermore it can be used

to repair the damaged skin, muscle and also can be used as a bone substitute due to its excellent biocompatibility and bonding properties with hard tissue. These are the most important requirements of any biomaterials developed for bone substitute (Hench, 1998; Hojo et al., 2005; Vallet-Regi et al., 2010). On the other hand, hydroxyapatite ceramic have been offering the desirable properties due to their chemical stability and high degree of crystallinity (Bigi et al., 2005; Bigi et al., 2007; Kumar et al., 2010).

Unfortunately there are some issues with hydroxyapatite ceramics that have been reported by researchers such as low mechanical properties, low reliability, some infection risk and high production cost (Chesnutt et al., 2009; Zhou and Lee, 2011; Shepherd et al., 2012). Hydroxyapatite has been produced in different form of dense and porous structure with variety shape of thin film, granules for coating, block or plate for bone implants and orthopedic applications. The structural studies and properties of natural bone and hard tissue are very important in order to develop and fabricate hydroxyapatite having better biological response and mechanical properties.

2.2. Structure and composition of bone as natural hydroxyapatite precursor

It is very important to identify the characteristics of bones that affect their chemical, physical and mechanical behaviour. These characteristics and properties are important parameters which must be controlled during the production of artificial bone implants and substitutes.

2.2.1. Mechanical and physical characteristics of bone

The principal inorganic constituents of bone are made of carbonate hydroxyapatite (65-70 wt. %), and organic part (20-30 wt. %) and water (5-9 wt. %), respectively. The organic component of bone is composed of collagen with a group of macromolecules such as lipids, polysaccharides, and protein (Salgado et al., 2004;

Vallet-Regi and Gonzalez-Calbert, 2004; Kalita, 2007; Dorozhkin, 2010). Collagen as a small microfiber can be viewed as the bone matrix; however, observing collagen fibers is obviously hard because of its net- like appearance as indicated in Figure 2.3.

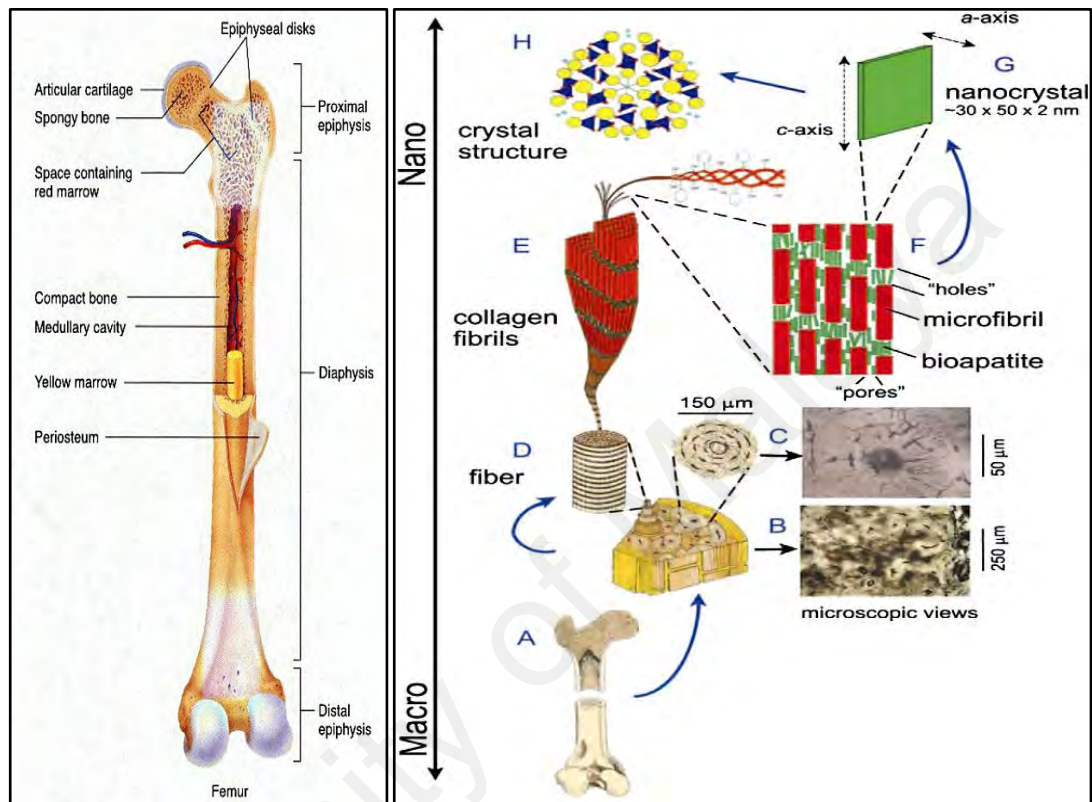


Figure 2.3: Femoral bone (A) and arrangement of cortical bone (cross section, B), osteon (C), collagen fiber (D, E and F), biologic apatite (G) and crystal structure of hydroxyapatite in bone (Dorozhkin, 2010)

According to Dorozhkin (2010), the size of collagen microfibers' diameter varies from 100 to 200 nm. These organic constituents of bone will potentially contribute to the high toughness, the low modulus and the other different characteristic properties of polymers for bone. Crystallized hydroxyapatite (HA) as a mineral component of bone and amorphous calcium phosphate (ACP) will contribute to the bone stiffness. The nano crystallized apatites are present in the form of plates or needles with a length about 50 nm, wide dimension about 30 nm and thickness of 2 nm.

Dorozhkin (2010) also reported that the lamellar sheets thickness of mammalian bone could vary between 3-7 mm thick which hold and arrange the mineral fibers as well as keeping the osteons in the form of concentric circles structure as it is indicated by the inset figures (B) and (C) in Figure 2.3.

Figure 2.3 shows the main section of the femoral bone which consisted of periosteum, yellow and red marrow, compact bone (cortical), spongy bone (cancellous) and articular cartilage. The two main parts of each mature bone are compact bone (cortical) and spongy bone (cancellous) that formed the harversian system and cylindrical osteons. Both cortical and cancellous bones have contained porosity. The porosity in bone appears at varying hierarchical levels from 50 nm to 250 μm (Dorozhkin, 2010) that affect mechanical properties. The mechanical properties of human compact bone are given in Table 2.1.

Table 2.1: Mechanical Properties of human wet cortical bone (by Suchanek and Yoshimura, 1997)

Human compact bone	Test direction related to bone axis
Tensile strength (MPa)	49
Compressive strengt (MPa)	133
Bending strength (MPa)	-
Shear strength (MPa)	-
Young's modulus (GPa)	11.5
Work of fracture (J/m^2)	-
K_{Ic} ($\text{MPam}^{1/2}$)	-
Ultimate tensile strain	0.007
Ultimate compressive strain	0.028
Yield tensile strain	0.004
Yield compressive strain	0.011

The spongy bones (cancellous or trabecular) consisted of connected open porous network including cellular material. While compact bones (cortical) are consisted of dense and close osteon structures. This dense structure is varying from low stress to high stress region. According to Zioupos (2001), the mechanical properties of bones are basically dependent on age, type of bone, humidity of surrounding bone area and load bearing application and direction. From microscopic point of view, the strength and mechanical properties of both compact and spongy bones are also dependent on density, porosity, amount and direction of collagen fibers, osteons structure (close or open), amount of apatites and their crystalline form.

2.2.2. Mineral composition of bones and hard tissues

Chemical studies of inorganic phase in bones and hard tissues are essential for the development of standard bone substitute and replacement materials such as hydroxyapatite that could offer the similar chemical composition and properties of inorganic phase of bones. Table 2.2 shows the chemical composition of inorganic phase in bone in compare with hydroxyapatite. Its shows that inorganic phase in bone are consisted from calcium (Ca) and phosphorous (P) as main elements and some other compound such as chlorine (Cl⁻), fluorine (F⁻), potassium (K⁺), sodium (Na⁺), magnesium (Mg²⁺), carbonate (CO₃²⁻) and water (H₂O) (Dorozhkin et al., 2010) . The presence of all these elements at the substitute materials can provide the better biocompatibility and properties similar to bone.

Table 2.2: Comparison of chemical composition in bone, enamel, dentin, bone and HA (Dorozhkin, 2009).

Composition, wt.%	Enamel	Dentin	Bone	HA
Calcium (Ca)	36.5	35.1	34.8	39.6
Phosphorous (P)	17.7	16.9	15.2	18.5
Ca/P (molar ratio)	1.63	1.61	1.71	1.67
Sodium	0.5	0.6	0.9	-
Magnesium	0.44	1.23	0.72	-
Potassium	0.08	0.05	0.03	-
Carbonate (CO_3^{2-})	3.5	5.6	7.4	-
Fluoride	0.01	0.06	0.03	-
Chloride	0.300	0.01	0.13	-
Pyrophosphate ($\text{P}_2\text{O}_7^{4-}$)	0.022	0.10	0.07	-
Total inorganic	97	70	65	100
Total organic	1.5	20	25	-
Water	1.5	10	10	-

2.3. Calcium phosphate bioceramics

Calcium phosphate (CaP) apatite is a promising bone replacement material mainly due to its excellent biocompatibility with hard tissues. Vaccaro (2002) reported that calcium phosphate apatite has been utilised in dentistry since the early 1970s and then in orthopedic applications since 1980s. In another research, Kalita et al. (2007) discussed that calcium phosphate bioceramic is preferred in hard tissue engineering as a bone graft material because of its outstanding characteristics such as being a light-weight composition similar to that of the mineral phase of bone.

Calcium phosphate bone substitutes are generally fragile and they possess poor tensile strength compared to the bone, however the mechanical properties of the

ceramic will improve after implantation due to its porous structure that allows the penetration of blood vessels and nutrition into the pores to form tissue. Thus, the mechanical characteristic of calcium phosphate bone substitute will become similar to the mechanical characteristic of cancellous bone once it is bonded to the surrounding hard tissue (Skedros et al., 2005; Vreken et al., 2010; Low et al., 2010).

According to Hench (1998) and Ooi et al. (2007), processing temperature, the presence of additional elements or compounds as impurities and Ca/P ratio are significant factors that affect the calcium phosphate phases. Therefore calcium phosphate bioceramics can exist in different forms and phases such as hydroxyapatite, beta-tricalcium phosphate (β -TCP), alpha-tricalcium phosphate (α -TCP), biphasic calcium phosphate (BCP) and monocalcium phosphate monohydrate (MCPM). Different phases of calcium phosphate bioceramic will be used in different applications depending upon whether a restorable or bioactive material is desired (Billote, 2000). Among those calcium phosphate bioceramics, hydroxyapatite has been extensively studied and used as synthetic calcium phosphate bioceramic for bone graft purpose during the last decade (Langstaff et al., 2001; Lee and Oh, 2003; Bigi et al., 2005; Ramesh et al., 2012; Dorozhkin, 2012).

2.4. Hydroxyapatite

Hydroxyapatite (HA), $\text{Ca}_{10}(\text{PO}_4)_6(\text{OH})_2$, is a principal mineral and apatite factor of inorganic components of hard tissues of vital organs such as teeth and bone. HA and the other calcium phosphate minerals have been used widely as implants materials since many years ago because they are highly biocompatible and have similar chemical composition with natural bone (LeGeros, 2002; LeGeros et al., 2008).

Hydroxyapatite in granular and bulk shapes with porous and dense structures is generally utilized to fill the cavity space in bones defects, and related to this application

several clinical successes have been reported in the literatures (Deisinger et al., 2004; Jokanovic et al., 2006). In addition, hydroxyapatite coating is utilized frequently in metallic prostheses to improve their biological characteristics (Liu et al., 2001; Kwok et al., 2009). From the phase stability point of view, hydroxyapatite is the most stable biomaterial at the body pH, in the presence of water, temperature of the body and physiological environment (DeGroot 1988; Correia et al., 1996; Jayabalan et al., 2010). In fact, the biocompatibility of hydroxyapatite provides a unique advantage for its usage in medical and orthopedic aspect over other biomaterials and bone substitutes such as polymeric substitute or metallic implants (Suchanek nad Yoshimura, 1998; Qian et al., 2008). Moreover, hydroxyapatite promotes osteoconduction that prepares the bone matrix for regeneration of new bone due to chemical and biophysical reactions that resulted in bone bonding. Accordingly, it rapidly combined with nanofibers and fibro-vascular tissues to encourage the better bonding and repair of damaged area without incurring any inflammatory reaction with the host tissue after implantation (Park et al., 2003; Porter et al., 2004; Yeong et al., 2004; Oh et al., 2006;).

2.4.1. Hydroxyapatite crystallography

The atomic lattice structure of hydroxyapatite as shown in Figure 2.4, consist of hexagonal arrangement of six fold synchrony axis with a three twisted fold and micro plates (Dorozhkin, 2007; Dorozhkin 2010; Silvester et al., 2014). The green line shows the crystallite surface division through Ca atoms and the red line shows the theoretical crystallite division through P atoms.

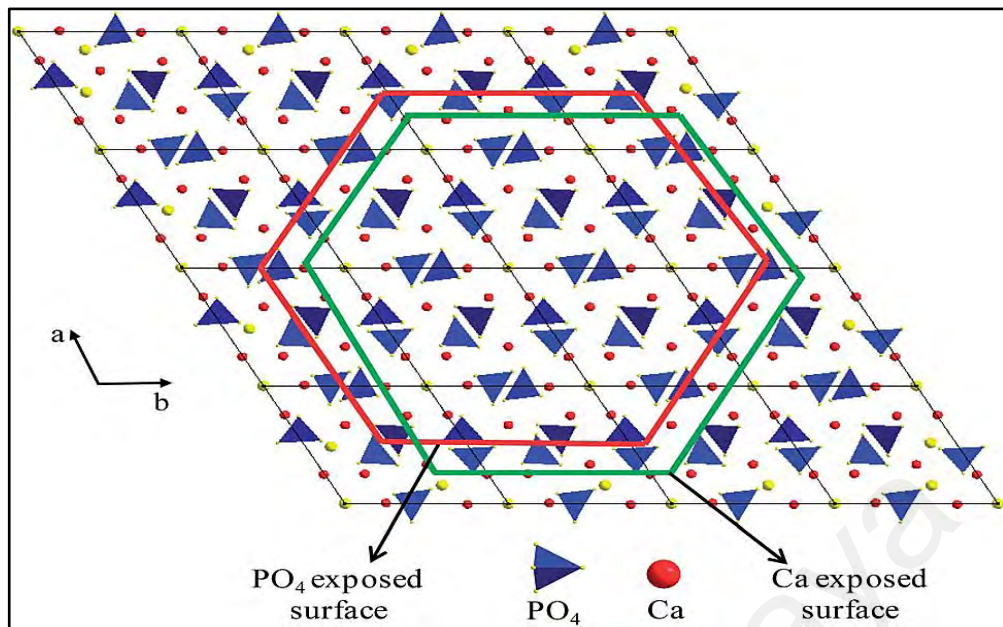


Figure 2.4: Schematic representation of the hydroxyapatite lattice.

(Silvester et al., 2014)

The main ions elements of hydroxyapatite atomic lattice are (PO_4^{2-}), (Ca^{2+}) and (OH). The substitutions of these ions result in changes in morphology, lattice structure, acidity and solubility of final product within the same hexagonal symmetry (Vallet-Regi and Gonzalez-Calbet, 2004).

These ions substitutions in lattice arrangement and sintering temperature including Ca/P ratio have produced the other phases of calcium phosphate biomaterials such as α -TCP and β -TCP. There is high positional risk of transformation from hydroxyapatite to other phases at higher temperature that affects the Ca/P ratio value. The ideal Ca/P ratio value for hydroxyapatite is 1.67 and the calculated density is 3.219 g/cm^3 . If the Ca/P ratio of calcium phosphate compound is lower or higher than 1.67, HA may transform to β -TCP, α -TCP for Ca/P ratio lower than 1.67 or Tetracalcium phosphate (TTCP) may be formed at higher ratios (Dorozhkin 2010).

2.4.2. Comparison between hydroxyapatite and bone

The most important dissimilarities between natural bone minerals and heat treated hydroxyapatite are the higher crystallite size and lack of carbonate component compared to bone (Tadic et al., 2004). Dorozhkin et al. (2010) indicated that similarity of chemical composition of synthetic calcium hydroxyapatite and mineral phase of bone is the most significant factor that affects the biocompatibility properties of synthetic HA. However, it was found that the presence of carbonate ions and mineral component in natural bone or natural HA derived from natural sources such as bovine bone, sheep bone, chicken bone and fish bone play a very important role in the biological activity. Table 2.2 in section 2.2.2 shows the chemical composition of human bone mineral and hydroxyapatite bioceramic.

Many researchers have studied the mechanical properties and clinical application of calcium phosphate based materials and hydroxyapatite. Charriere et al. (2003) reported that hydroxyapatite is a fragile material and its fracture strength is about 120 MPa which is low for load bearing applications. In addition, Muralithran and Ramesh (2000) reported that HA possessed low fracture toughness (K_{Ic}) i.e. of about 0.8-1.2 MPam^{1/2} as compared to human bone which vary from 2 MPam^{1/2} to 12 MPam^{1/2}. Based on the preparation and sintering temperature, the tensile strength, bending strength and compressive strength of the synthetic dense hydroxyapatite ceramics are reported in the variety range of 38-300 MPa, 38-250 MPa and 120-900 MPa respectively. However, these values are in the range of 2-100 MPa, 2-11 MPa, and 3MPa for porous hydroxyapatite (Suchanek and Yoshimura, 1998; Dorozhkin, 2007). However, the fracture toughness and strength of porous hydroxyapatite implant would be expected to increase after bone infusion and tissue migration into the porous structure of the HA (Dorozhkin, 2007).

2.5. Synthesis of hydroxyapatite

The preparation and synthesis of hydroxyapatite can be form two main routes which are by chemical processing and extraction from natural biological sources such as natural calcite corals, natural gypsum, cuttlefish shells, eggshells, and bovine bone. Various techniques have been used for synthesis of hydroxyapatite biomaterial (Suchanek and Yoshimura, 1998; Orlovskii et al., 2002; Zakharov et al., 2004; Kannan et al. 2007; Ramesh et al., 2007). However, the two main proven techniques for preparing HA are the wet chemical methods and dry chemical method through solid state reactions. The wet chemical method can be further divided into three main groups: precipitation method, hydro-chemical reaction of other calcium phosphate and hydrothermal technique.

Depending on the techniques, calcium phosphate based biomaterial with various morphologies, level of crystallinity and stoichiometry can exist. The advantage of wet chemical methods is the use of water as a main part of mixture which resulted in low contamination during preparing. Other advantages of wet chemical methods are low and reasonable production cost and can be easily be implemented at low temperature range of 40 to 100°C (Raynaud et al., 2002; Santos et al., 2004; Kumar et al., 2004). While the solid state route gives a stoichiometric and better crystallized structure in final HA, it requires a higher temperature and long heat treatment times compared to wet chemical methods coupled with the high risk of contamination during mixing. Furthermore, low sinterability and phase decomposition of the prepared powders have been reported (Suchanek et al., 2004; Mostafa, 2005). Some of the most important synthesis techniques to produce hydroxyapatite as reported by various researchers are presented in subsequent section.

2.5.1 Precipitation technique

Precipitation technique is the simplest procedure and regular method that used to produce hydroxyapatite with wide range of particle sizes and morphology structure through an aqueous solution. In general, precipitation technique or wet chemical technique involved a mixed of aqueous solution at the $\text{pH} > 7$ that contained the Ca^{2+} and PO_4^{3-} compounds ions. The source of Ca^{2+} ion may include $\text{Ca}(\text{NO}_3)_2$, CaCl_2 , $\text{CaSO}_4 \cdot 2\text{H}_2\text{O}$, $\text{Ca}(\text{OH})_2$ and $(\text{CH}_3\text{CO}_2)_2\text{Ca}$. while the PO_4^{3-} ion is usually taken from Na_3PO_4 , $\text{NH}_4\text{H}_2\text{PO}_4$, H_3PO_4 , K_3PO_4 , and $(\text{NH}_4)_2\text{HPO}_4$. In addition, ammonia (NH_4OH) is normally used to maintain the pH of slurry above 7 during reaction.

The quality and phase purity of hydroxyapatite obtained are dependent on the reaction rate, sequence and mixing rate of Ca^{2+} and PO_4^{3-} compounds, a molar concentration of each element, pH value of slurry, stirring time, applying pressure, and temperature of reaction (Riman et al., 2002; Ramesh et al., 2004). Therefore, close control over all parameters are critical to obtain a well-defined HA. Hydroxyapatite obtained through the precipitation technique often result in the retention of secondary phases such as TCP or CaO due to uncontrolled pH of mixture resulting in a deviation in the Ca/P ratio from 1.67.

Akao et al. (1981) presented the two main chemical equations to obtain the hydroxyapatite by precipitation technique as follows:



In the equation (2.1), hydroxyapatite is obtained from the chemical reaction between orthophosphoric acid (H_3PO_4) and calcium hydroxyl ($\text{Ca}(\text{OH})_2$) slurry. In the

second equation (2.2), the calcium nitrate ($\text{Ca}(\text{NO}_3)_2$) and ammonium phosphate ($(\text{NH}_4)_2\text{HPO}_4$) are diluted with water separately. Then the aqueous ammonium phosphate is slowly titrated into the calcium nitrate slurry under stirring condition.

There is no any formation of secondary phases of calcium phosphate due to presence of ammonium ions in the slurry as a necessary factor to control and adjust the P^{H} of mixture but these ions will be involved in the reaction and hence included in the HA structure. The presence of these ions might affect the mechanical and biocompatibility properties of the final HA product.

2.5.2. Hydrothermal reaction

Hydrothermal method is the reaction that needs to apply pressure and high temperatures within a controlled environment. This technique works based on exchange reaction to transform the substance phases or convert it to another material with higher crystallinity compare to using common wet chemical methods. This can be one of the main advantages of this method as well as maintaining high purity of final product due to the use of pressure and higher temperatures (Yoshimura et al., 2004; Guo and Xiao, 2006; Montazeri et al., 2010; Guo et al., 2011).

Hydroxyapatite powder can be obtained with hydrothermal technique by applying pressure about 80 MPa to 100 MPa within temperatures range of 250°C to 300°C. Although this route is relatively time consuming, it has the added benefit of preserving the original architecture as illustrated by the production of porous HA from calcium carbonate corals (Porter et al. 2008).

Della Roy and Linnehan (1974) were amongst the pioneer to use the hydrothermal route to obtain hydroxyapatite from coral, as a natural resource of calcium carbonate (CaCO_3) material.

This was soon followed by other studies to synthesize hydroxyapatite from seashells, eggshell and natural gypsum through hydrothermal route (Zaremba et al., 1998; Xu et al., 2001; Rocha et al., 2005; Lemos et al., 2006; Sasikumar and Vijayaraghavan, 2006; Zhang and Vecchio, 2007; Vecchio et al., 2007). The advantage of hydrothermal method is its ability to provide a pure hydroxyapatite without presence of any secondary phases. For instance by Jingbing et al. (2003) and Neira et al. (2008) reported that the processing temperature and pH value of mixture are the two main controlling factors to obtain pure hydroxyapatite with desirable morphology. They reported that a well elongated HA particles with typical length of 600 nm and diameter of 40 nm could be obtained via hydrothermal method at the pH of 9 and heat treatment at 120°C.

2.5.3. Solid state reaction

The influence of heat treatment and temperature on heterogeneous mixture of proper solid component can provide a suitable structure through solid state diffusion of the ions. This process is categorized as dry chemical method known as mechanochemical technique which normally requires the high temperature processing at 1000°C to 1300°C to enable the solid state diffusion between calcium and phosphorus ions (Orlovskii et al., 2002; Nasiri-Tabrizi et al., 2009). Wide range of calcium phosphate and calcium compound have been used in solid state reaction such as dicalcium phosphate dehydrate ($\text{CaHPO}_4 \cdot 2\text{H}_2\text{O}$), monocalcium phosphate monohydrate ($\text{Ca}(\text{H}_2\text{PO}_4)_2 \cdot \text{H}_2\text{O}$), dicalcium phosphate anhydrous (CaHPO_4), calcium hydroxide ($\text{Ca}(\text{OH})_2$), calcium pyrophosphate ($\text{Ca}_2\text{P}_2\text{O}_7$), calcium carbonate (CaCO_3) and calcium oxide (CaO) (Rhee, 2002). Hydroxyapatite is synthesized through reaction between stoichiometric mixing of calcium and phosphorous compound at optimum temperatures.

Solid state reaction technique provides a synthetic hydroxyapatite with Ca/P=1.67 and increase the kinetic and thermodynamic reactions between solids powers (Suchanek et al., 2002; Mochales et al., 2004; Salas, et al., 2004; Nasiri-Tabrizi et al., 2009). The hydroxyapatite obtained by solid state reaction technique is stable at high temperature of 1300°C, that can be advantage of this technique but its required long heat treatment times and extra instrument to supply the evaporated water. Since the synthesis of hydroxyapatite through this method requires high temperatures, therefore H₂O vapour must be applied continuously to supply the OH⁻ group in the reaction (Chen et al., 2004; Nasiri-Tabrizi et al., 2009). Suchanek (2004) and Chen (2004) indicated that sinterability and homogeneity of product are observed due to the high temperature and pressure that required in mechanochemical process.

This is important to understand the difference between the mechanochemical synthesis technique and mechanochemical hydrothermal synthesis technique. Mechanochemical technique only involved the solid state reactions while mechanochemical hydrothermal technique (wet mechanochemical method) incorporates an aqueous phase and slurry form of compounds. In comparison to the solid state reaction technique, wet mechanochemical method provides a highly active reaction due to the present of slurry form and aqueous phase of components that accelerate the process in terms of crystallization, adsorption, dissolution and diffusion. This highly active reaction can provide a fast react zones with the temperature about 700°C due to adiabatic heating of gas bubbles and friction of particles that normally present during reaction.

2.5.4. Sol-gel route

Sol-gel routes have been employed to synthesis hydroxyapatite (Hsieh et al., 2001; Liu et al., 2002; Ramanan et al., 2004; Bigi et al., 2005; Fathi and Hanifi 2007;

Padmanabhan et al., 2009; Sanosh et al., 2009). The advantages of using this route includes the high purity of hydroxyapatite produced, controllability of the process parameters, fully homogenized composition of final product, higher reaction rate compared to other methods such as mechanochemical synthesis technique, hydrothermal and wet chemical precipitation, and the production of nanosized HA particles (Ramanan et al., 2004; Fathi and Hanifi, 2007; Padmanabhan et al., 2009; Chen et al., 2011). On the other hand, hydroxyapatite can be obtained at lower sintering temperature due to higher reaction rate of the sol-gel process. Based on these advantages, sol gel method is use to synthesis the hydroxyapatite mostly for surface coating purpose. The calcium alkoxides, phosphorous alkoxides, metals salts, calcium salts or mixture of stoichiometric calcium alkoxide with phosphorus alkoxide are frequently employed as the main elements in the sol-gel processing (Ramanan et al., 2004; Bigi et al., 2004).

However, the drawbacks of sol-gel processing of hydroxyapatite includes the use of expensive metal salt and alkoxide component, the purity and phase stability of hydroxyapatite is based on absolute dissolution of the alkoxide component after sintering process, and long preparation time of more than 24 h (Kim and Kumta, 2004; Fathi and Hanifi, 2007; Chen et al., 2011). In order to obtain the desirable morphology of hydroxyapatite by sol-gel process, higher sintering temperature with longer holding time requires to active and increases the reaction rate (Jillavenkatesa and Condrate, 1998).

Jillavenkatesa and Condrate (1998) also mentioned that the prepared hydroxyapatite partially decomposed to calcium oxide (CaO) and other calcium phosphate phases. Fathi and Hanifi, (2007) also observed the secondary phase of calcium phosphate (β -TCP). This secondary phase can be removed through the use of diluted hydrogen chloride (HCl) or water instead of strong acids.

In addition, Hsieh et al., (2001), suggested using proper aging steps prior to the drying process followed by washing with water.

2.6. Synthesis of HA from natural source

There are several methods adopted to synthesize HA from natural sources. Hu et al. (2001) produced highly crystalline HA with homogeneous size and shape by hydrothermal processing of corals. HA, thus synthesised allows quick tissue in growth. Sivakumar et al. (1996) and Chattopadhyay et al. (2007) have also reported a simple method of converting the calcium carbonate skeletons of corals available in the Indian coast into HA granules.

Conversion of conch and clam seashells into hydroxyapatite by hydrothermal method for load bearing applications and conversion of sea urchin spines to resorbable Mg-substituted tricalcium phosphate by hydrothermal reaction have been reported Vecchio et al. (2007). A nano-powder of HA prepared by hydrothermal transformation of milled oyster shell powders were obtained by Lemos et al. (2006).

The synthesis of HA using eggshells and phosphoric acid has also been reported (Kamalanathan et al., 2014; Balazsi et al., 2007). Siva Rama Krishna et al. (2007) have synthesized nanocrystalline HA from microwave processing of eggshell waste and synthetic calcium hydroxide. HA platelets of length 33–50 nm and width 8–14 nm were obtained. Sasikumar et al. (2006) have also synthesized HA from the CaCO_3 present in egg shells by combustion method.

Ivankovic et al. (2009) have produced HA structures for tissue engineering by hydrothermal treatment of aragonite in the form of cuttlefish bone at 200°C. Aragonite (CaCO_3) monoliths were completely transformed into HA after 48 hours of hydrothermal treatment. Pena et al. (2000) have reported preparation of biphasic materials by microwave processing from natural aragonite and calcite. Prabakaran and

Rajeswari (2006) have reported the development of HA powder from fishbone as a natural apatite rich substance through heat treatment method.

HA synthesized from natural sources, which are available in abundance, has better tissue response by virtue of its porosity, chemical and structural similarity to that of the mineral phase of bone, and easily bonds with natural bone (Ben Nissan 2003; Murugan and Ramakrishna, 2005; Balazsi et al., 2007) .

2.7. Use of natural bone as a bone replacement material

Xenogeneic bone has been used to repair bone defects and grafting material for long time. It is easy to obtain and has a lower cost than autogenic or allogenic bone graft. However, the clinical application of xenograft has been limited because it involves numerous problems such as infection, disease transfer and immunological defensive reaction. To overcome these problems, various treatments and observation have been conducted with the aim of removing the strongly antigenic proteins and the cellular elements of xenogenic bone (Tadic et al., 2006; Ooi et al., 2007; Deatherage et al., 2010). Among other xenogenic, the crystalline phase composition of sintered bovine cancellous bone is very similar to natural bone mineral.

Sintered bovine bone maintains the porous network characteristic of bone matrix material. This natural bone structure represents an initial step towards a successful substitute material. Sintered bone is composed mainly of hydroxyapatite (Deatherage et al., 2010).

The mineral component in living bone structure is a carbonated apatite, with the sintering process leading to a decomposition of the carbonate component to release CO_2 gas and CaO as the remaining solid (Barralet et al., 2002). Similarly, elemental analysis of the sintered bone produced by Foster (2004) and Ooi et al. (2007) showed calcium to phosphorus molar ratio of 2.10 to 1.00.

Other studies have shown that physicochemical properties of the sintered bone such as grain size, sintering temperature and porosity percentage are important variables that affect the biocompatibility of sintered bone (Joschek et al., 2000; Kim et al., 2014). Sintered bovine bone has a porous structure that allows the migration of cells into the centre of the structure. This porous structure is expected to increase the cell attachment rate of bone cell and implant resorption. It has been shown that in a synthetic hydroxyapatite ceramic bone replacement implant with insufficient porosity or unsuitable structure, cell cultural test may not process rapidly enough to yield the homogenous connection of the scaffold into the living bone cells (Akazawa et al., 2005).

Recently, a pure mineral bone has been developed by sintering method to remove all organic components of bovine bone and burning remnant material constitution by high temperature heat treatment (Lin et al., 1999; Ooi et al., 2007; Hai-Bo et al., 2010). The sintering process leads to the removal of organic material, and a fusing of the mineral component into crystals of bone mineral (HA), while the interconnecting macroporous architecture is remain (Gross and Rodriguez., 2004; Akazawa et al., 2005; Hai-Bo et al., 2010).

Lin et al. (1999) and Hai-Bo et al. (2010) developed a porous structure of hydroxyapatite by calcined cancellous bovine bone. The calcined cancellous bone maintained the spongy structure of natural bone, which has an interconnecting porous structure, high porosity level about 70 vol% as shown in Figure 2.5. In comparison to the synthesis of porous ceramics, the sintered cancellous bone due to natural porous structure would be much superior to the synthetic porous hydroxyapatite ceramics.

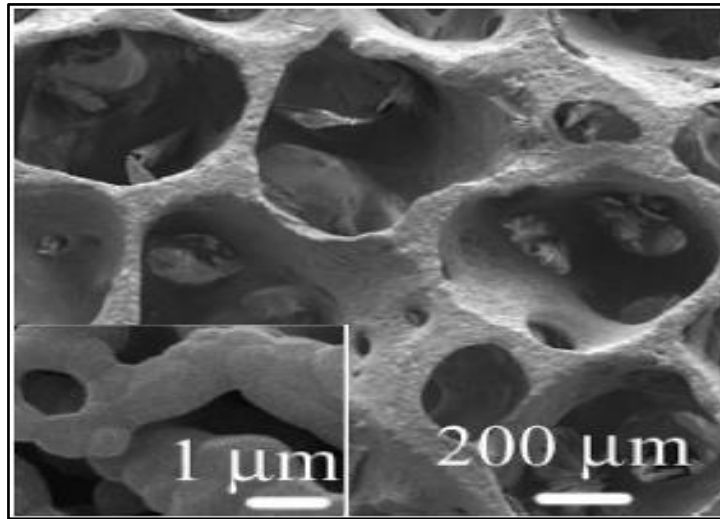


Figure 2.5: SEM of porous structure of hydroxyapatite from calcined bovine cancellous bone. (Hai-Bo et al., 2010)

Ooi et al. (2007) have used sintered cortical bovine bone as a raw material to produce porous HA by calcination process. They have achieved the porous structure as shown in Figure. 2.6 after annealing the bone powder and sintered at temperature about 900°C. Herliansyah et al. (2009) also used bovine bone powder to produce the porous HA structure with using pore creating particles which burn out during sintering.

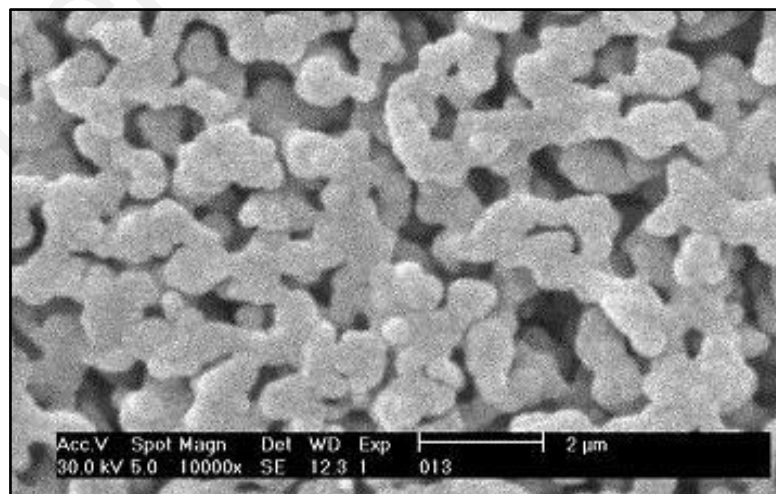


Figure 2.6: Porous HA structure produced from sintered bovine bone powder. (Ooi et al. 2007)

To prepare the porous structure, bovine bone powder was mixed with sucrose ($C_{12}H_{22}O_{11}$) as progen material and then the mixed powder was palletized into green bodies by using a uniaxial press. The compacted green body was sintered at $1200^{\circ}C$ to remove the progen and produce the porous HA structure. Nevertheless, the production of porous HA structure with use of HA powder has some issues. For example the surface of final product contains bubbles with some close pore and non-uniform porous structure. Thus the structural study of sintered bovine bone that can lead to produce an acceptable and uniform porous structure has attracted more attention in recent years.

Porosity, as one of the most important demands that is defined as a percentage of empty space in a solid material and it is a morphological feature that is irrespective of the presence of pores materials. Porous structure is a necessary property for the bone formation through the bone cells migration and cell proliferation of osteoblasts. In addition, porous surface facilitates mechanical bonding between implanted biomaterials and surrounding of natural bone. However porosity has a significant influence on the mechanical properties of a ceramic as its presence tends to intensify stresses applied to the material (Park et al., 2008). The influence of porosity on the flexural strength of a ceramic can be quite dramatic as increase in porosity of 10% could reduce the mechanical strength by over 50% (Park et al., 2008).

Most used techniques for inducing porosity within the biomaterial are salt leaching, gas formation, phase separation, freeze drying and the sintering depending on the material used for obtaining a scaffold.

2.7. Cell cultural behavior and attachability of HA based ceramics

Currently, the study of both *in vivo* and *in vitro* interaction between osteoblasts cells and implant surfaces is considered. Osteoblasts cells may first attach to the surface of biomaterial and bone substitute instead of direct binding between proteins cells and

implant surface (Boyan et al., 2001). Then interactions of protein cell would occur from selective fused osteoblasts cells and proteins that bond to the bone substitute surface as shown in Figure 2.7. This fused and combination of cells would determine the immunological responses of the implants and affect cell attachability (Rizzi et al., 2001). However, the chemical composition and morphology structure of implants would also affect the cell attachability.

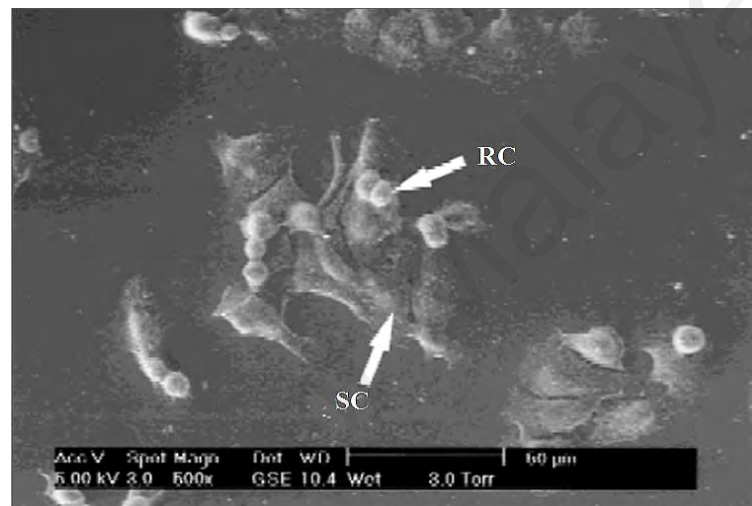


Figure 2.7: Rounded cell (RC) and spread cell (SC) morphology of human osteoblasts cells on implant surface. (Rizzi et al., 2001)

Differentiation of bioactivity and biocompatibility exist among calcium phosphate bioceramics due to their effects in contact with bone, cell culture and osteoblasts cells (Wang et al., 2004; Balasundaram et al., 2006; Shi et al., 2009; Li et al., 2009; Li et al., 2011). For example, Yuasa et al. (2004) compared the cell attachability and cell cultural of apatite cement and sintered hydroxyapatite. Cell culture results of sintered hydroxyapatite shows better attachment and proliferation compared to apatite cement, probably due to chemical composition and low crystallinity of apatite cement.

Cell cultural study and osteoblast response on different phases of calcium phosphate bioceramics was studied by Wang et al. (2004). They have examined

different phase composition of calcium phosphate such as hydroxyapatite (HA), tricalcium phosphate (TCP), biphasic calcium phosphate I (HA/TCP: 70/30 wt%) and biphasic calcium phosphate II (HA/TCP: 35/65 wt%). Highest cell adhesion on sintered hydroxyapatite samples were reported after six days in culture environment compared to tricalcium phosphate samples. However, the cell adhesion rate of calcium phosphate, biphasic calcium phosphate and TCP were increased between day six to day nine due to TCP properties that dissolve in wet and culture environment.

On the other hand, cells response and cells attachment, specifically for cells proliferations are influenced by some critical factors such as crystallinity level, phase purity and Ca/P ratio of calcium phosphate bioceramics (Best et al., 1997; Best et al., 2008). For example, the cell attachment of TCP was reduced during cell culture test (using bone cells) after day nine of exposure (Wang et al., (2004).

The Ca-doped hydroxyapatite has been investigated to improve the biocompatibility of HA bioceramics. Doping of HA with various chemical elements (Zn, La, Y and Bi) also has been reported with positive outcomes during the *in vitro* and *in vivo* studies (Webster et al., 2004; Evis et al., 2011). Figure 2.8 shows the osteoblast cells activity of 2 mol% Ca-doped hydroxyapatite (Figure 2.8 (b)), that was increased due to more calcium deposition that increased the alkaline phosphates activity. It was also determined that positively adding of C is resulted in improvements of osteoblasts cells attachment and enhances the properties of HA. However, the Ca should not be added into HA more than 1-2 mol% because further additions may result in decomposition of HA at high sintering temperatures.

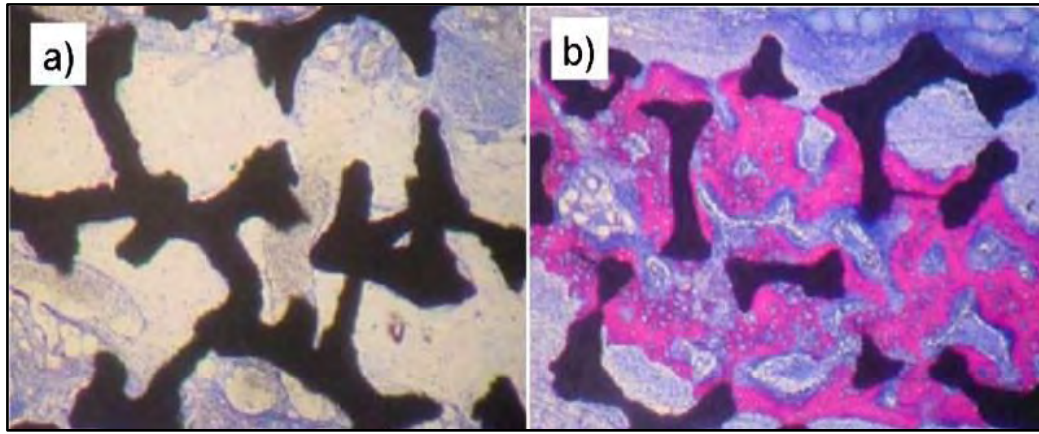


Figure 2.8: The SEM images of HA scaffold; (a) undoped HA scaffold and (b) Ca-doped HA scaffold. The red colour region in (b) shows new bone infiltration that appears after doping. (Evis et al, 2011)

Wang et al. (2010) found that the proliferation of MC3T3-E1 cells (osteoblast precursor cell line derived from rat musculus) was increased for low percentage of zinc (Zn) doped TCP (Ito et al., 2000). However, Kim et al. (2003) reported that there was not any significant improvement in cell proliferation on fluorine-doped HA (FHA). Additionally the results indicated that alkaline phosphates activity and cell proliferation behavior of FHA was similar to pure HA. The different zirconium dioxide (ZrO_2) percentages of FHA- ZrO_2 composites were also investigated. It is found that the high ratios of zirconium dioxide (50% ZrO_2) have a negative influence on cell behavior and their response to the substitute. Both the chemical compositions and physical properties of doped hydroxyapatite affect the cell attachability and cell proliferation. According to Boyan et al. (2001) and Zhao et al. (2006), cell interaction results between osteoblast cells and substrate including cell attachments and proliferations are closely affected by surface morphology.

Cellular attachments and their response on the substitute materials are also depended on porosity level of the material. Therefore, the presence of porous structure with 40% to 50% porosity would provide better cell response, while low porosity offers

better mechanical properties. Kim et al. (2014) used Hanks' balanced salt solution (HBSS) which is an extracellular solution with an ionic composition similar to human blood plasma for osteoconduction test for porous calcium phosphate. Figure 2.9 shows that the osteoconduction can be observed with increasing the porosity due to larger surface area available for protein adsorption and cell adhesion (Wei et al., 2004; Wei et al., 2008; Kim et al., 2014).

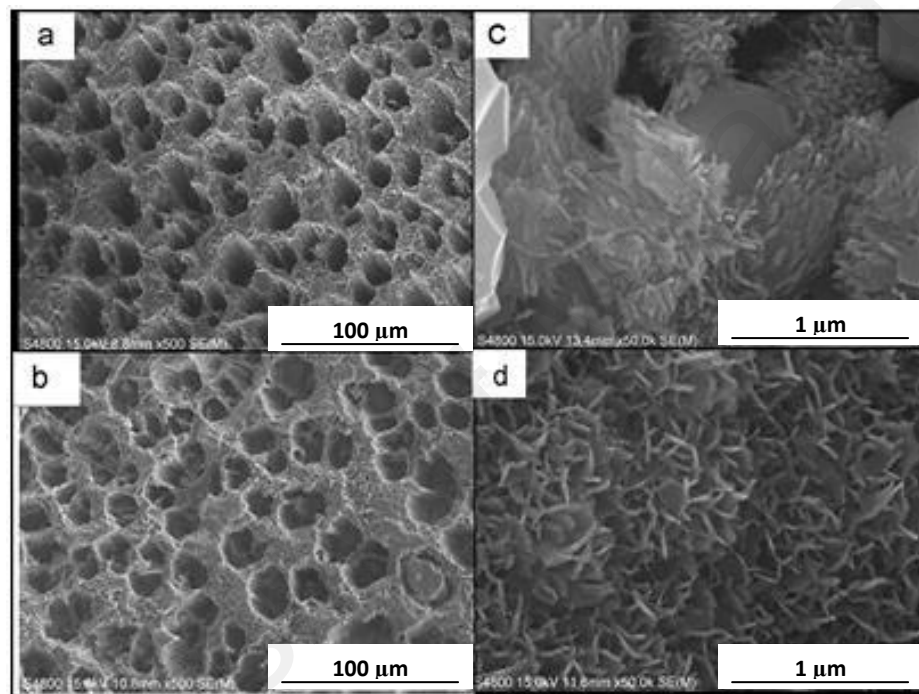


Figure 2.9: SEM images of porous calcium phosphate with (a) 45.9% porosity, (b) 43% porosity, (c) immersion of (a) in HBSS, and (d) immersion of (b) in HBSS after 2 weeks (Kim et al., 2014)

Similar results were also reported by Deligianni et al. (2005). They indicated that osteoblast differentiation and osteoconduction activity of human bone marrow were increased on sintered porous HA (Deligianni et al., 2005; Kokkinos et al., 2012).

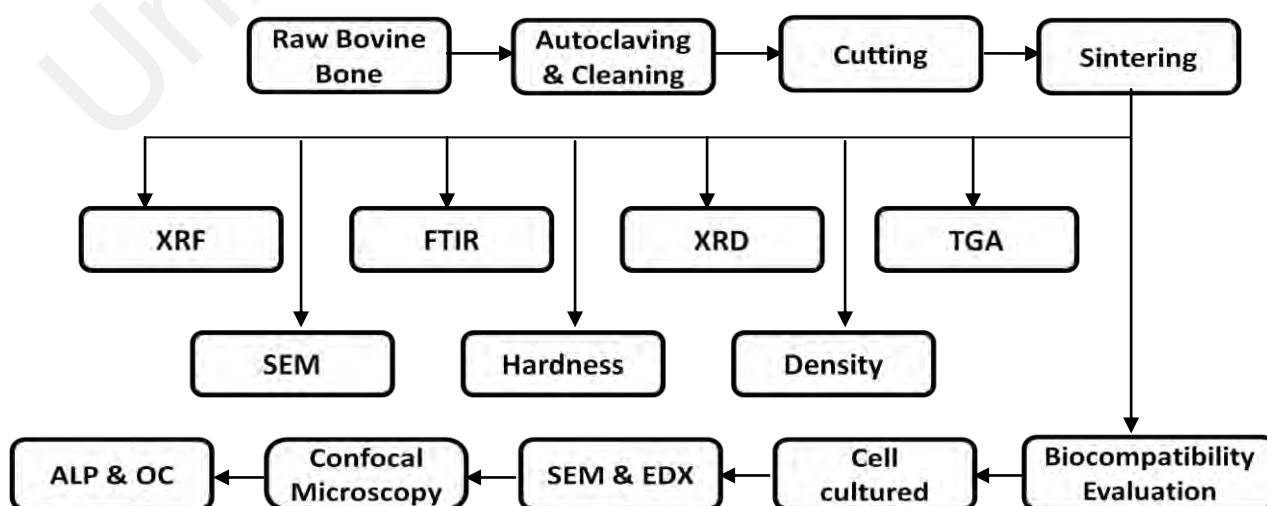
In summary this chapter has provided the investigations about various techniques that have been employed to synthesis hydroxyapatite with the aim of producing a pure mineral and single phase hydroxyapatite from natural source for bone graft purpose. HA synthesized from natural sources that are available in abundance, has better tissue response by virtue of its porosity, chemical and structural similarity to that of the mineral phase of bone and easily bonds with natural bone. Several important parameters which include crystallinity level, phase purity and porosity level as well as distribution within the matrix have been identified as key that affects the bioactivity and cells response of calcium phosphate bioceramics. The challenge would be to select a proper starting material and subsequently tailoring the processes to produce a viable HA scaffold matrix that are bioactive and possessed the mechanical characteristic of cancellous bone.

CHAPTER 3

METHODS AND MATERIALS

3.1 Introduction

This chapter describes the process and equipments by which cortical bovine bone was harvested from waste bovine bone, and processed to derive porous bone graft from sintered bovine bone samples. This process included cutting the raw bone, autoclaving to remove the external fat and protein from bone and then sintering at various temperatures. In addition to this, characterization and mechanical properties of the as-sintered samples were undertaken by X-ray diffraction (XRD), Micro X-ray Fluorescence (Micro-XRF), field emission scanning electron microscopy (FESEM), Fourier transforms infrared spectroscopy (FTIR) analysis, simultaneous thermal analyser (STA), differential scanning calorimeter (DSC), Vickers hardness and fracture toughness determination. The biocompatibility and cytocompatibility of the as-sintered samples was examined through *in vitro* assessment.



3.2 Sample preparation

Femur bone of a bovine (aged between 2-3 years old) was obtained from a local slaughterhouse. Sample preparation began with removal of the connective tissue from bone. The bone was thoroughly cleaned with water.

The as-received bones were cut by handsaw to separate the cancellous bone from cortical part and all cortical parts were cleaned thoroughly to remove the protein externally through an autoclave process. Sufficient quantities of bones (about 2 kg) were placed in a 7 liter capacity domestic autoclave. Water was added to the autoclave container until the bones were covered by water. With the pressure lid secured, the autoclave was placed on top of stove, which was set to full heat. The autoclave process containing steam at 100°C allowed cooking for one hour before cooling and removal of the bone from the rest of the protein substance.

The clean bare bone was subsequently rinsed with warm water, followed by soaking in acetone for 30 minutes to remove residual proteins and impurities. The clean bone was then dried for 2 hours at 100°C in a box oven. The cortical bone before and after autoclaving is shown in Figure 3.1.

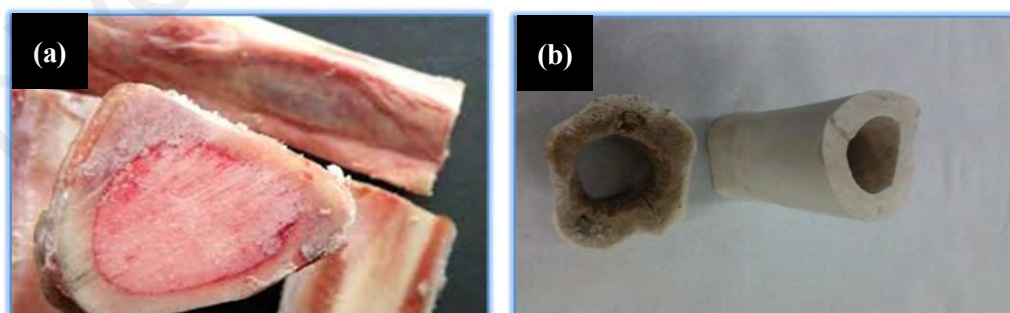


Figure 3.1: cortical bone before (a) and after autoclaving (b).

A Linear precision saw (Buehler Isomet 4000-USA, Appendix A) with 2 mm diamond toothed saw, commonly used to cut ceramics and hard minerals was used to cut the dried cortical bone into smaller pieces as shown in Figure 3.2. A constant flow

of cooling water was sprayed on either side of the saw to prevent friction induced heating during the cutting process. The total numbers of 115 samples were prepared for mechanical properties tests, microstructural analysis, biocompatibilities and *in vitro* assessment.



Figure 3.2: The precision saw (a) used to cut the test samples (b).

3.3 Sintering of the bone

Heat treatment and sintering process refer to the heating operation required to modify the properties of ceramic materials. In general, the stages of sintering include atomic diffusion, recrystallization, pores elimination and grain growth by controlling the temperature and holding time as the most important factor of sintering process as typically shown in Figure 3.3 (ASM Handbook, Volume 04 - Heat Treating).

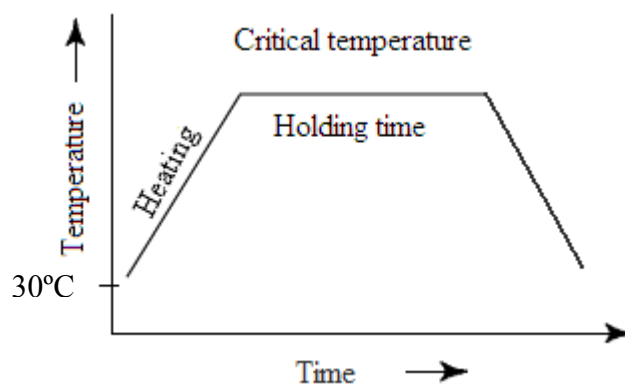


Figure 3.3: The sintering process.

In this research, a laboratory electric furnace (LT Furnace-Malaysia, Appendix A) was used to evaluate the influence of heat exposure and heating regimes on mechanical properties and morphology structure of the bovine bones. For the sintering process, pieces of dried bone formed into specific angular shapes were placed in an alumina crucible for sintering. The bone samples were sintered under atmospheric conditions at various temperatures ranging from 200°C to 1300°C using a standard (heating and cooling) ramp rate of 10°C/min. with 2 hours of soaking time. Five samples were tested for each sintering temperature and average value was taken.

3.4 Surface preparation and polishing

The as-received sintered samples were ground using (LT Grind-Polisher-Malaysia, Appendix A). The silicon carbide (SiC) papers of varying grades from 600 (rough) to 1200 (fine) were used for grinding process. After the grinding, the samples were polished down to 1µm using diamond paste to obtain a smooth reflective surface. Prior to testing, the polished samples were dried at 70°C for 1 hour in a standard electric oven.

3.5 Phase analysis

The phases present in the raw piece of bovine bone as well as the sintered samples were analyzed at room temperature by X-ray diffraction (XRD; PANalytical Empyrea-Netherland, Appendix A). The XRD operated at 45 kV and 40 mA using Cu-K α as the radiation source at a scan speed of 0.5° per minute and a step scan of 0.02°. The crystalline phase compositions were identified with reference to the standard JCPDS (Joint Committee of Powder Diffraction Standard – International Center for

Diffraction Data) cards no. 01-074-0565 and 09-432 for hydroxyapatite (HA), 09-0169 for β -TCP, 09-348 for α -TCP and 25-1137 for TTCP available in the system software. The details of these JCPDS reference files are presented in Appendix B.

3.6 Bulk density measurement

Bulk density measurement of sintered samples was carried out based on the Archimedes principle using distilled water as an immersion medium. A standard weighing balance was used to measure the dry weight of the sintered sample in air. Then the weighing balance was set to zero and the sample was placed in a stainless steel plate immersed into the distilled water. The weight of the sample in water is recorded. The temperature of the distilled water was taken and the density of water was obtained as given in Appendix C.

The bulk density (ρ) of sintered samples is calculated using following equation:

$$\rho = \frac{W_a}{W_a - W_w} \rho_w \quad (3.1)$$

where:

W_a = Weight of the sample in air

W_w = Weight of the sample in water

ρ_w = Density of distilled water

The relative density of each sample was calculated by taking the theoretical density of hydroxyapatite as 3.156 g/cm^3 (Champion et al., 1994).

3.7 Thermal analysis

The Thermogravimetric analysis (TGA) was performed using simultaneous thermal analyzer (STA) integrated with differential scanning calorimeter (DSC). The heating influence of different temperatures on the weight-loss over temperature was evaluated by simultaneous thermal analyzer (STA; Perkin Elmer STA6000-USA, Appendix A) on cubic sample derived from un-sintered bone (cleaned bone), whereas a differential scanning calorimeter (DSC; Perkin Elmer-USA, Appendix A) was employed to investigate the phase transitions in the bone sample during the heating process.

To match with the laboratory electric furnace incremental ramp rate setup, the bone sample was heated at a rate of 10°C/min from 30°C to 1000°C in air atmosphere. The weight loss percentages was assessed by the STA curve (Weight% over Temperature), while the phase transitions in the bone sample was investigated by DSC curve (Heat flow over Temperature).

3.8 Fourier transforms infrared spectroscopy analysis (FTIR)

Fourier transforms infrared spectroscopy (FTIR) analysis (FTIR; NICOLET 6700-USA, Appendix A) was performed to identify sample compositions resulting from the sintering process. In order to determine the various composition groups, the piece of un-sintered bone and the sintered bone sample were examined. FTIR spectra were collected in the wave number range of 4000 - 400cm⁻¹.

3.9 Micro X-ray Fluorescence (Micro-XRF)

The chemical elements present in un-sintered bone as well as sintered samples were determined using the bench top Micro X-ray Fluorescence (Micro-XRF; Orbis

EDAX-USA, Appendix A). The instrument was set at low vacuum condition with detector magnification of 15 μm . The calcium to phosphorus (Ca/P) ratio of the product was calculated based on the chemical elements given by the analyser.

3.10 Microstructural evolution

The microstructural evolution of the as-received bovine bone and bone samples after sintering at varying temperatures was examined using a field emission scanning electron microscope (FESEM; Zeiss Merlin-Germany, Appendix A). Prior to FESEM examination, the polished samples was thermally etched at temperature 50°C below the sintering temperature, using a ramp rate of 10°C/min. and 30 min soaking time in order to delineate the grain boundaries. The average grain size of hydroxyapatite derived from sintered bone was defined from FESEM image using the image analyzer software.

3.11 Vickers hardness and fracture toughness measurements

The Vickers hardness of the sintered bovine-HA was obtained using a pyramidal diamond indenter (HMV-2, Shimadzu-Japan, Appendix A). The Vickers microhardness test operated based on an indentation method using a diamond tip, in the form of a square-based pyramid by applying varying loads of 0.05 kgf, 0.1 kgf and 0.2 kgf onto the polished surface of the sample. During the test, the load was applied smoothly, without impact, and was maintained for of 10 seconds prior to examination.

Furthermore, the physical quality of the indenter and the accuracy of the applied load as defined clearly in ASTM E384-99 (2010) must be controlled to obtain correct results. Generally, the Vickers impression (Figure 3.4) appears to be square with the two diagonals having almost similar lengths. The indentation diagonal lengths (d_1 and d_2) and the crack lines emanating from the indentation corners were measured immediately under an optical microscope attached to the instrument. The average of at

least five indentation reading applied for each sample was taken to determine the average value.

Subsequently, the Vickers hardness (H_v) is calculated using the following equation (ASTM E384-99., 2010):

$$H_v = \frac{1.854P}{d^2} \quad (3.2)$$

where

$$d = (d_1 + d_2) / 2$$

P = the applied load

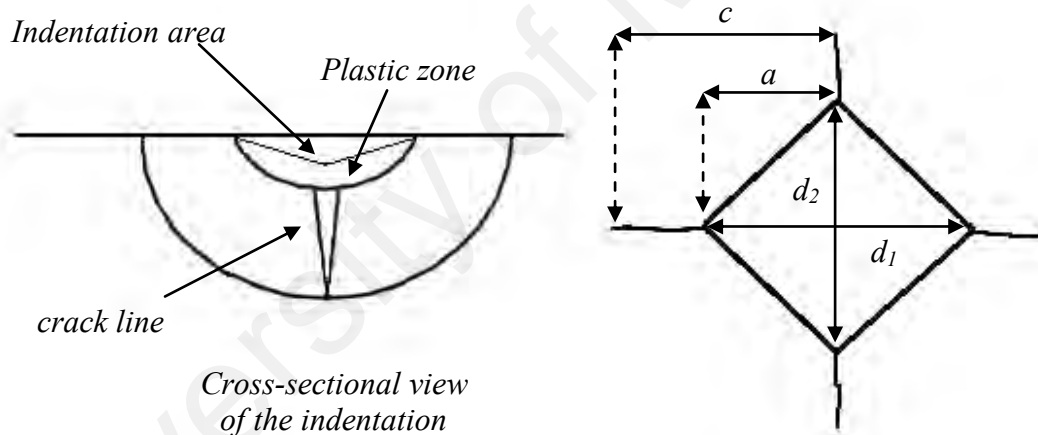


Figure 3.4: Schematic diagram showing the Vickers indentation.

The indentation method has been shown to be useful in determining the fracture toughness of ceramics (Antis et al., 1981; Evans, 1981; lee and Jones 1982; Quinn, 2008; Kruzic et al., 2008). The advantage of this method is the speed, ease of testing and sample preparation, relatively low cost, large numbers of indentation can be made quickly and the small value of material required. Principally, it is the same as the microhardness measurement whereby the Vickers diamond indenter is driven into the

specimen surface by a known load. When the indenter is removed, a characteristic pattern as depicted in Figure 3.4 will be visible, comprising a central indentation with radial cracks emanating from the corners.

The crack system formed by the Vickers indenter are namely, the Median or half-penny and the Palmqvist crack system (Lach et al., 2007; Kruzic et al., 2008; Behnamghader et al., 2011). Previously, Peralta (2004) has established that the crack system for low toughness ceramics such as hydroxyapatite was of Median-type. Thus, the fracture toughness (K_{Ic}) is determined from the equation derived by Niihara et al. (1982):

$$K_{Ic} = 0.203(c/a)^{-1.5}(H_v)(a)^{0.5} \quad (3.3)$$

where

H_v = Vickers hardness

c = The characteristic length of the half penny crack as shown in
Figure 3.4

a = Half diagonal of the indent

3.12 Biocompatibility study

In vitro test was performed on the sintered bone samples that presented single phase porous structure to assess their bioactivity response as a potential graft material. The biological experiments were conducted by Tissue Engineering Group (TEG) at the Department of Orthopedic Surgery, Faculty of Medicine, University of Malaya.

3.12.1 Cell viability and cytotoxicity

The cell viability and cytotoxicity of sintered bone samples was carried out using Alamar Blue assay. The Alamar Blue assay is based on enzymatic reduction of indicator colour by viable cells and serves as an effective method for evaluating cell health and cell proliferation. When cells are alive they maintain a reducing environment within the cytosol of the cell. Resazurin is the active ingredient of Alamar Blue reagent and it is a non-toxic cell permeable compound that is blue in color and virtually non-fluorescent. Upon entering cells, resazurin is reduced to resorufin, a compound that is red in color and highly fluorescent. Viable cells continuously convert resazurin to resorufin, increasing the overall fluorescence and color of the media surrounding cells.

In this research, human mesenchymal stromal cells (hMSCs) provided by Faculty of Medicine, University Malaya was used to investigate its proliferation on sintered bone derived porous hydroxyapatite structure. The as-received cells were placed in cell culture medium flask (10% fetal bovine serum (FBS) and 1% antibiotic) and incubated at 37°C with an atmosphere of 5% CO₂ and 95% humidity.

The sample preparation for cell viability and cell attachment analysis were performed at the same time with following method; The sintered bone samples were washed and sterilized in ethanol 70% (v/v) for 20 mins. Then they had been washed in phosphate buffered saline (PBS) twice to remove the ethanol and neutralize its effects. The sterilized samples were placed into fluorescence microplate reader with excitation 570 nm and emission 600 nm filter pair. The 10,000 hMSCs from cell culture flask were added onto the sterilized samples and incubated for 4 hours. Then the medium was replaced with fresh media containing a 10% Alamar Blue solution. The culture microplate was wrapped in aluminum foil and it was incubated for 4 hours before initial checking of enzymatic reduction of indicator colour.

The cell viability results were performed based on percentage of Alamar Blue reduction on day 0, 3, 6, 9, 12, 15, and 21. The enzymatic reduction of indicator colour was measured using Epoch fluorescence spectrophotometer (BioTek; USA, Appendix A) by Gen5 data analysis software.

3.12.2 Cell attachment

The attachment and spreading of cells on cultured samples were analyzed on day 15 by FESEM and confocal laser scanning microscope (FESEM; Zeiss Merlin-Germany, Appendix A). The cultured samples were taken from well microplate (section 3.4.1). The sample preparation protocols for FESEM imaging were basically included the fixation in 4% glut (Glutaraldehyde; $\text{CH}_2(\text{CH}_2\text{CHO})_2$), critical point drying (CPD) and coated with gold to make the sample surface electrically conductive.

3.12.3 Alkaline phosphatase activity (ALP)

Alkaline phosphatase (ALP) accelerates the hydrolysis of phosphate esters in alkaline buffer and produces an organic radical and inorganic phosphate. The changes in alkaline phosphatase activity are associated with various disease states in the bone.

To measure the ALP activity of hMSCs on sterilized samples, the 1×10^5 cells were washed with PBS and then homogenized in the PBS assay. The homogenized set was centrifuged to remove insoluble material at 10,000 rpm for 3 minutes. The cells were seeded into well microplate after the samples were added. The culture microplate was wrapped in aluminum foil and it was incubated for one hour before initial checking. The ALP activity was measured by Abcam's alkaline phosphatase assay Kit (Abcam ab83369 Kit; UK, Appendix D). The kit used *p*-nitrophenyl phosphate (*p*-NPP) as a phosphate substrate. The ALP activity of hMSCs on samples was performed based on dephosphorylation of *p*-NPP on day 0, 3, 6, 9, 12, 15, 21 and 28.

3.12.4 Osteocalcin

Osteocalcin or bone Gla protein (B.G.P) is the major non-collagenous protein of the bone matrix. Osteocalcin is synthesized in the bone by the osteoblasts. After production, it is partly incorporated in the bone matrix and also it is found in the blood circulation. A large number of studies show that the circulating levels of osteocalcin reflect the rate of bone formation.

Human Bone marrow stem cells were cultured in culture medium and they were grown to confluence within 30 days. Then the medium contained human osteocalcin was stored frozen at -20°C to avoid loss of bioactive human osteocalcin until assay for osteocalcin. The osteocalcin concentration on samples was measured at the end of 14, 21 and 28 days respectively in incubated tissue culture medium. Detection of human osteocalcin was carried out using a Human Osteocalcin Instant ELISA assay Kit (eBioscience BMS2020INST Kit; USA, Appendix D).

3.12.5 Statistical analysis

The Statistical Analysis was used in all results from cell culture experiments and osteocalcin measurements. The values obtained from clinical samples were presented as averaged and expressed as means \pm standard deviation (SD). The statistical calculations with statistical differences were determined using SPSS software version 10. The differences were considered statistically significant if the value of probability levels (p) was less than 0.05.

CHAPTER 4

RESULTS AND DISCUSSIONS

4.1 Introduction

This chapter will present the results and discussions on the characterization techniques and mechanical properties of the sintered bovine bone as a precursor material for producing the natural hydroxyapatite.

4.2 Physical observation

A general visual observation that was made during the sintering of the samples was the colour change of the bone with increasing temperatures. The influence of eleven sintering temperatures is presented in Table 4.1. Figure 4.1 shows that the colour of raw bone changed from light yellow at room temperature to dark black at 400°C to light grey at 600°C. However, the samples became fully white when the annealing was carried out above 700°C, indicating complete removal of organic substance such as protein and collagen (Tadic et al., 2006; Ooi et al., 2007; Deatherage et al., 2010; Niakan et al., 2015).

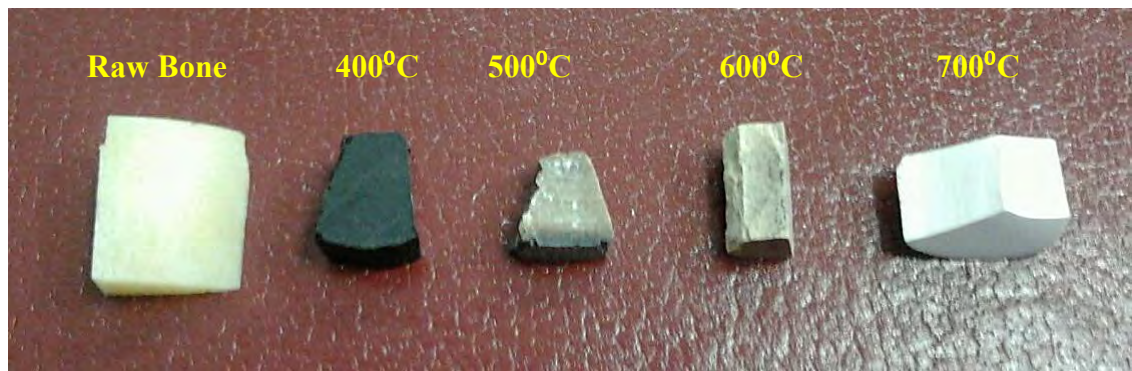


Figure 4.1: Colour change due to sintering of bovine bone at various temperatures.

Table 4.1: Physical Observation of Bovine Bone with Increasing Temperature.

Sample No.	Temperature (°C)	Colour
1	Room temperature	Light yellow
<i>as-received bovine bone</i>		
2	400	Black
3	500	Dark grey
4	600	Light grey
5	700	White
6	800	White
7	900	White
8	1000	White
9	1100	White
10	1200	White
11	1300	White

4.2.1 TGA analysis

The raw bovine bone sample was placed in the TGA machine to determine the effect of different temperatures on the weight loss. The heating ramp rate of 10°C/min. was adopted in this experiment which is the same as that used for the sintering study. The thermo gravimetric analysis of the bone sample was carried out from 30°C to 1000°C in air atmosphere in order to identify the temperature leading to considerable weight loss. The TGA result in Figure 4.2 shows that there are two stages of weight loss that occurred during the heating process. The first weight loss of 8.3 wt% is observed from 30°C to 225°C due to the removal of trapped water in the bone. The second weight loss of approximately 31.6 wt% occurred from 226°C to 900°C and was attributed to the decomposition of organic components, such as collagen and protein in the bone structure. The very small weight loss (approximately 1%) observed from 900°C to 1000°C is not significant, thus indicating that all of the organic components present in the bone structure were completely removed and the remaining structure (approximately 61.1 wt%) was composed of the hydroxyapatite phase as determined from the XRD analysis. The DSC graph presented along the TGA curve in Figure 4.2 shows a short endothermic peak at approximately 54.7°C, and this can be attributed to the heat absorbency of water in the bone structure. In addition, the results confirmed that the two highest exothermic peaks at 122°C and 385°C were associated with the burning of organic and carbonated compounds, respectively. The broad peak observed between 54°C and 226°C in Figure 4.2 corresponded to the burning of collagen in the absence of water (Reyes-Gasga et al., 2008; Herliansyah et al., 2012; Niakan et al., 2015).

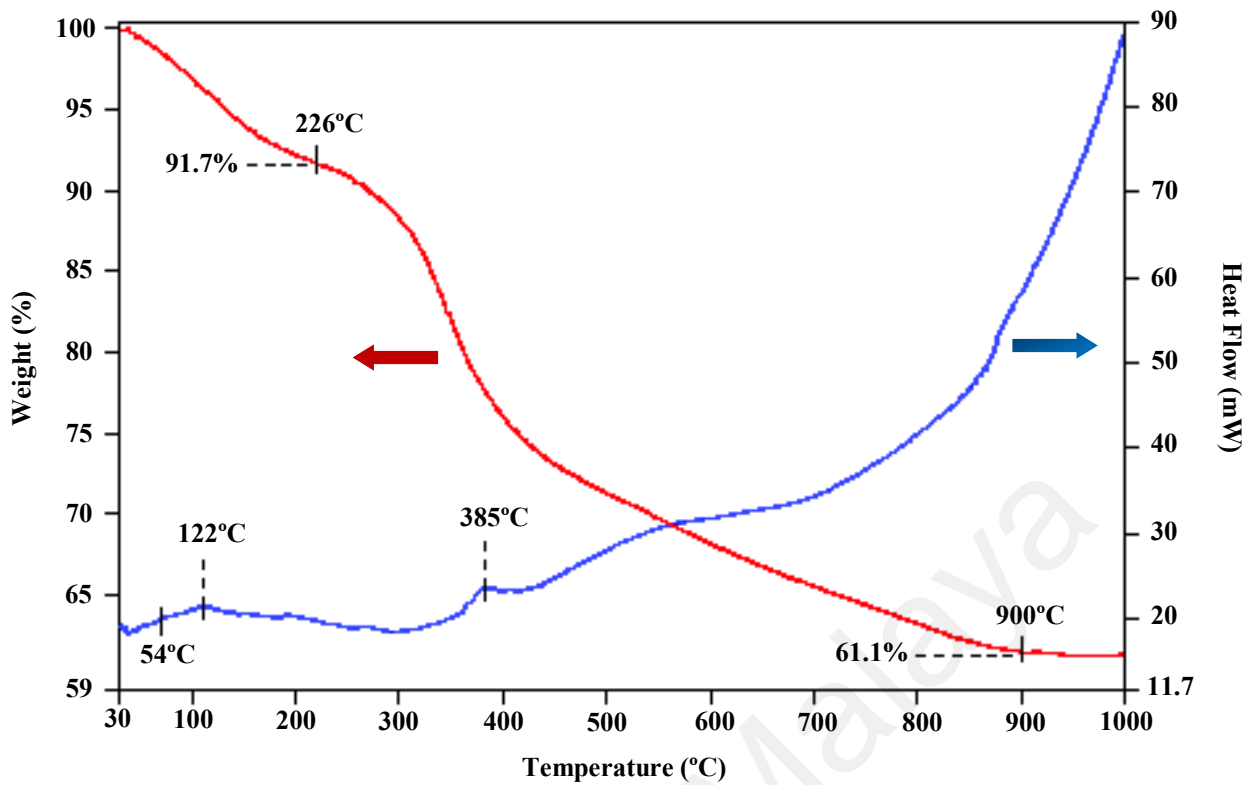


Figure 4.2: The TG and DTA curve of as-received bovine bone as measured from room temperature to 1000°C.

4.2.2 Phase analysis and thermal stability

The XRD patterns of the un-sintered bone sample at room temperature of 30°C and as-sintered samples from 200°C to 600°C are shown in Figure 4.3. The intensity of peaks increased progressively with increasing temperature and became more prominent as the temperature increased beyond 600°C as it is shown in Figure 4.4.

This substantial increase in the peak height and the reduction in the peak width are a reflection of the improved crystallinity and an increased in the crystallite size of the HA phase, respectively. There was no secondary peak associated with TCP detected in the XRD analysis. Furthermore the XRD analysis of all the sintered bodies from 200°C to 1200°C produced only peaks which corresponded to the standard JCPDS card no: 74-566 for stoichiometric HA.

The broad and low XRD peaks observed for the as-received bone sample reflect the low crystallinity of the HA phase in the structure. The crystallinity of the HA phase in the as-sintered samples, however, started to increase with increasing sintering temperatures, as depicted by the increasing intensity of the diffraction peaks.

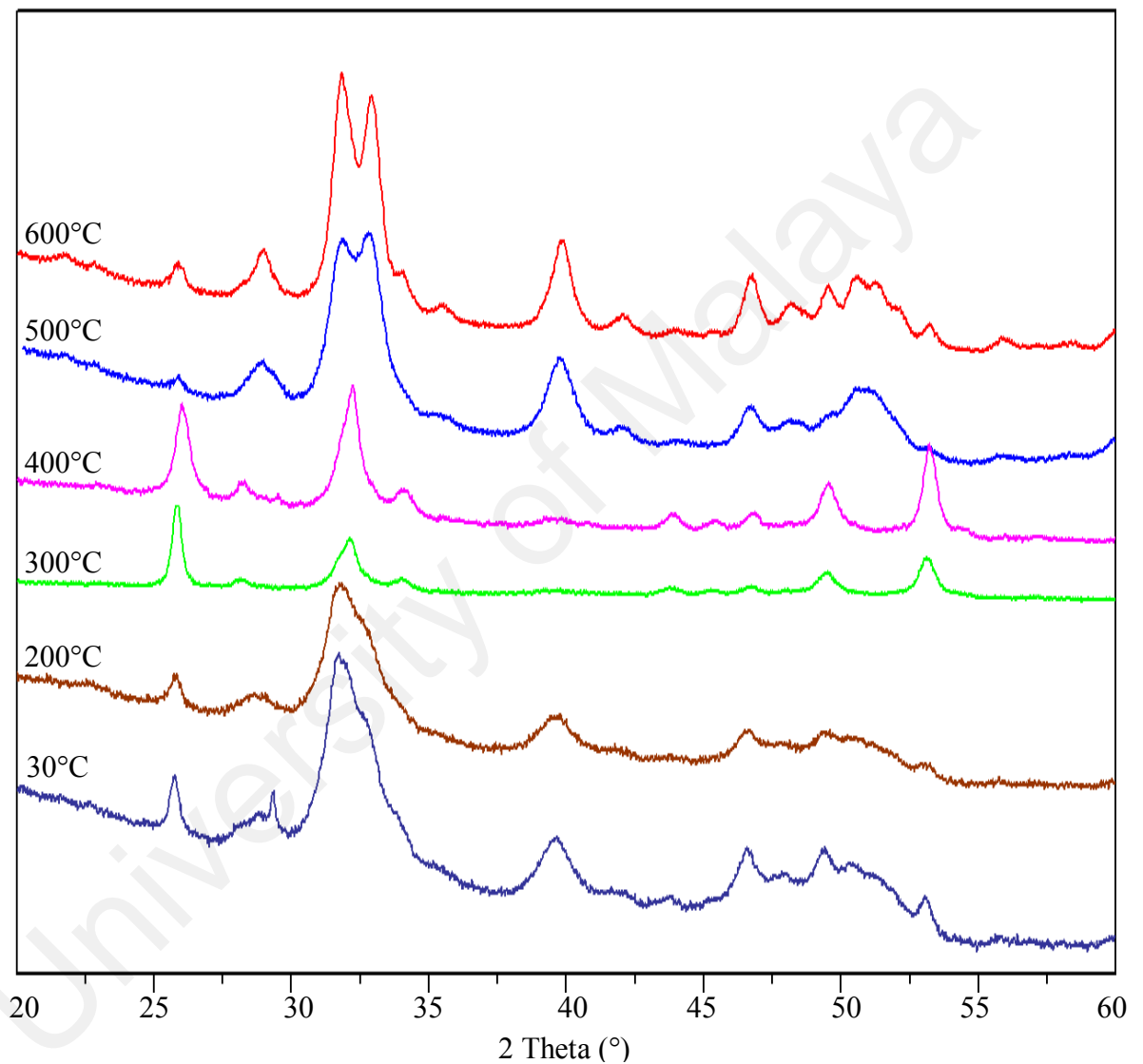


Figure 4.3: The XRD patterns of the un-sintered bone sample at 30°C and as-sintered samples from 200°C to 600 °C. All peaks belong to the HA phase.

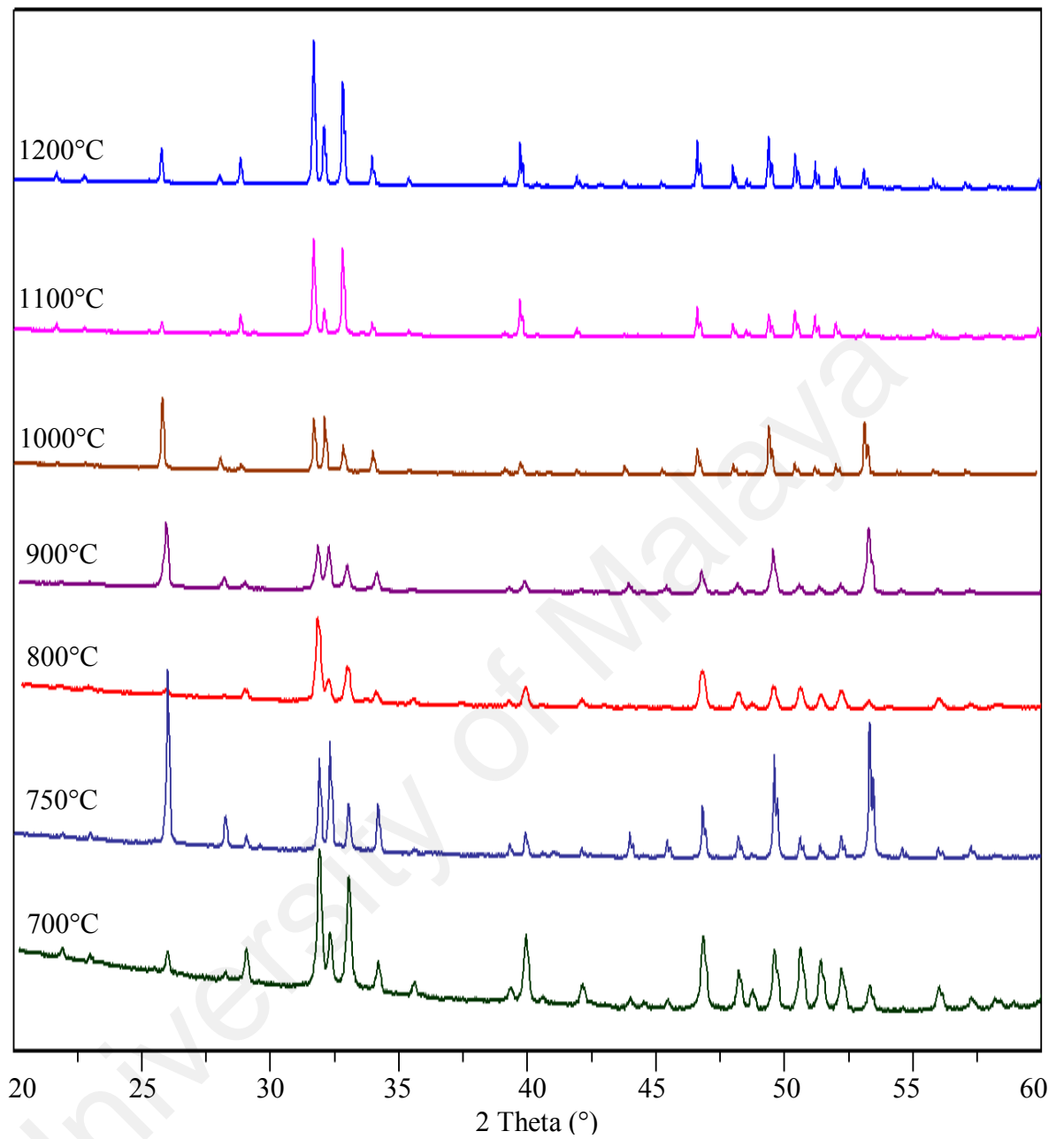
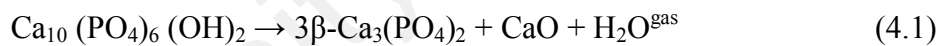


Figure 4.4: XRD patterns of bovine bone sintered from 700°C to 1200°C calcined for 2 hours. All the diffraction lines corresponds to the standard JCPDS card no: 74-566 for stoichiometric HA.

A narrow and sharp XRD peaks observed at 1000°C and 1200°C are a reflection of the highly crystalline HA phase present in the sintered bodies. This observation is not in agreement with some of the literatures, where the decomposition of HA to β -TCP has been reported to occur at low sintering temperatures, below 1000°C (Jinlong et al., 2001; Ugarte et al., 2005) . However, sintering above 1200°C resulted in partial HA phase decomposition to form β -TCP. As the sintering temperature increased to 1250°C, the intensity of the β -TCP peaks located at 2θ of 29.45°, 31.75°, 32.90°, 34.02°, 35.43° and 47.71°, were observed and gradually increased at 1300°C. The β -TCP peaks corresponded well with the standard JCPDS files no: 009-0169 and 009-7500.

Based on the present XRD results the HA stability in the bovine bone matrix was not disrupted when the bone is sintered in air up to 1200°C. According to chemical equation 4.1, dehydroxylation of HA at high sintering temperature will result in phase decomposition and formation of β -TCP:



This phase decomposition for samples observed at 1250°C and 1300°C (Figure 4.5) are attributed to partial dehydration of the hydroxyapatite during heating at high temperature (Bahrololoom et al., 2009; Krishnamurithy et al., 2014).

In the present work, 750°C has been identified as the optimum sintering temperature, as the sample exhibited the highest XRD diffraction intensities and sharp peaks corresponding to the HA phase (see Figure 4.6) compared to all other sintered samples, thus indicating that a highly crystalline HA structure is obtained at this temperature. The present XRD results are consistent with reported literature which states that HA phase is stable in air up to 1200°C (Zhou et al., 1993; Muralithran and Ramesh., 2000).

Furthermore, in comparison with other reported studies (Ooi et al., 2007; Herliansyah et al., 2009) the present results show that the phase stability of HA produced from bovine bone was improved up to 1200°C using the sintering profile with heating rate of 10°C/min and holding time of 2 hours.

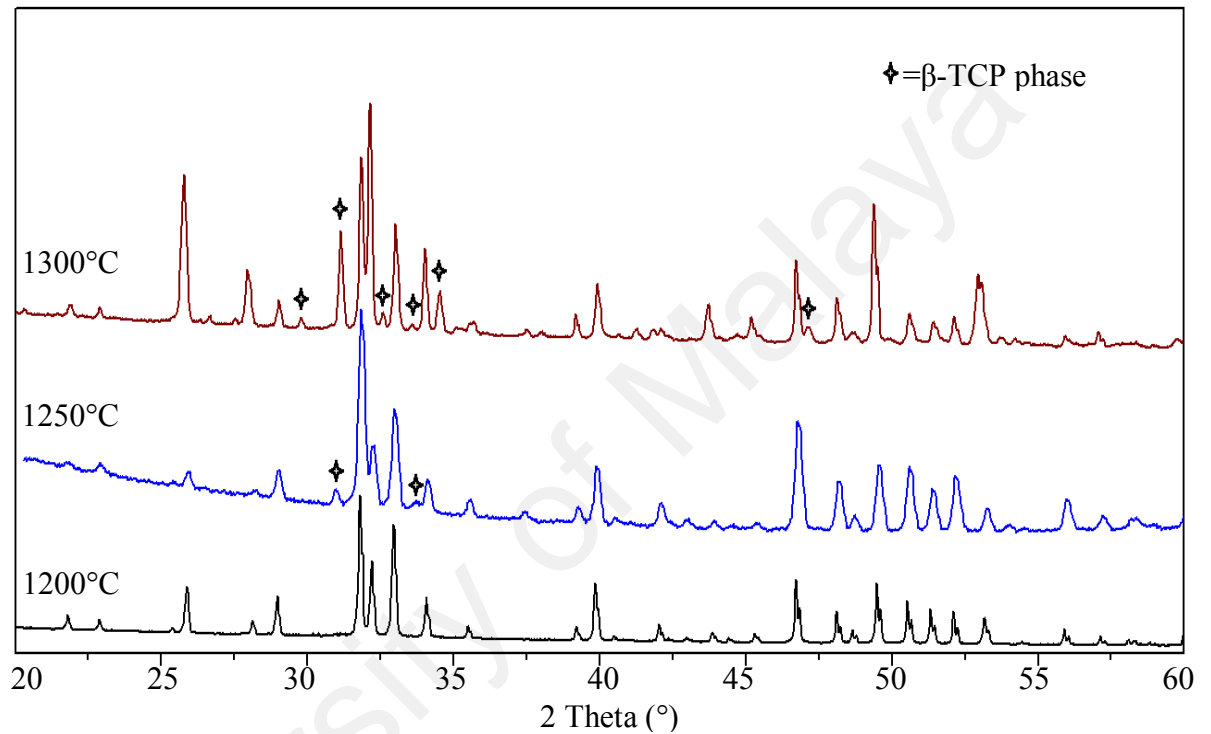


Figure 4.5: XRD patterns showing the presences of β -TCP in bone samples sintered at 1250°C and 1300°C.

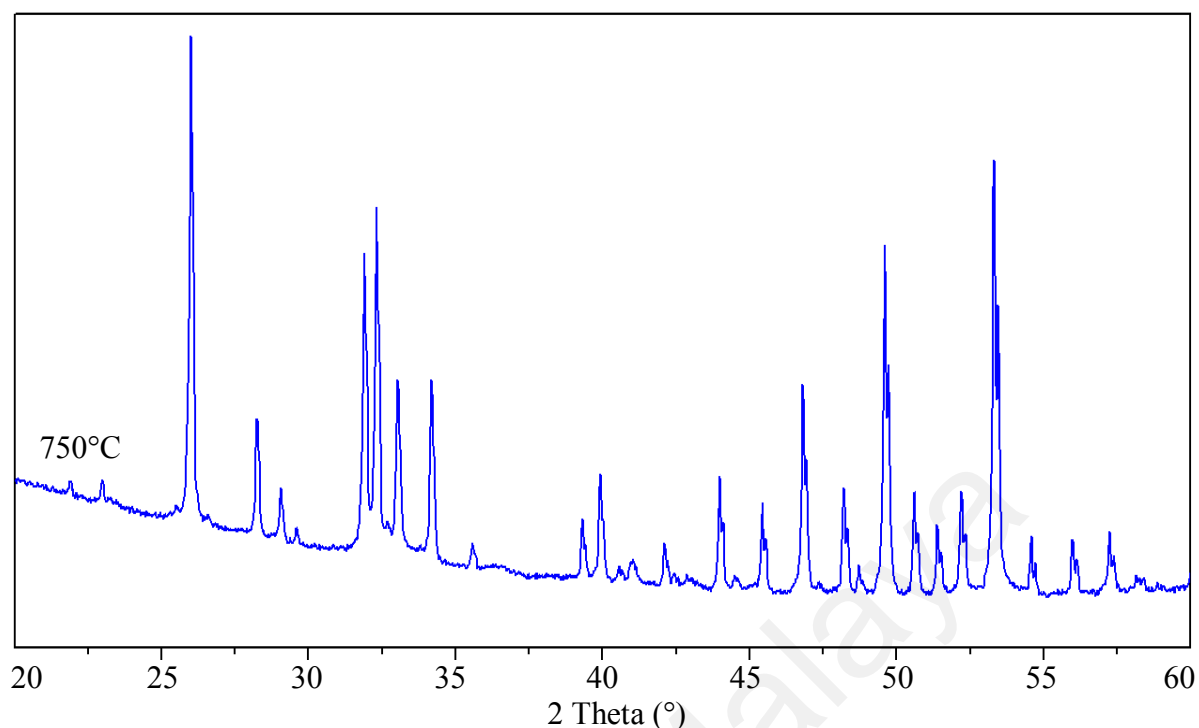


Figure 4.6: XRD patterns of sintered bovine samples at 750°C showing the well-defined and sharp peaks of the HA phase.

4.2.3 FTIR analysis

The FTIR spectrums of the un-sintered bone and bone sample sintered at 750°C are shown in Figure 4.7. In comparison to the un-sintered bone, the FTIR spectrum of the sintered sample shows only the typical absorption peaks corresponding to that of hydroxyapatite, and this is in good agreement with the XRD analysis. The present results indicated that the total organic bands of C–H and C–C observed at 2853, 2920, and 3304 cm^{-1} were removed after the sintering process. These peaks are related to chemical components presents in organic parts such as protein and collagen (Mkukuma et al., 2004; Tripathi et al., 2012; Niakan et al., 2015). A flat line indicates the principal loss of the organic components in sintered bone at 750°C. The most intensive bands in the range of 962.8 – 1087.19 cm^{-1} belongs to PO_4^{3-} ion and it is linked to the mineral elements of bone, which is matched to the asymmetrical stretching peak of P–O, and the

maximum absorption occurs at the wave length of 1013.91 cm^{-1} (Herliansyah et al., 2009; Ooi et al., 2007). The low-intensity bands from 1415 cm^{-1} to 1739 cm^{-1} correspond to the CO_3^{2-} ion, which could have been present in the sample prior to sintering due to lack of control of the atmosphere during. The swing band at 676.9 cm^{-1} and high wave number range at 3304 cm^{-1} correspond to the movement of O–H bonds (Silva et al., 2005; Ugarte et al., 2005; Ooi et al., 2007; Niakan et al., 2015). The FTIR result of the sample that is sintered at 750°C (Figure 4.7) is in good agreement with the result reported by Bahrololoom et al. (2009) for natural hydroxyapatite extracted from bovine cortical bone ash. The FTIR results of sintered samples at 1250°C and 1300°C are shown in Figure 4.8. The vibrations in the range from 1980 cm^{-1} to 2300 cm^{-1} absorption bands are multiple of the fundamental (overtones) related to the functional group PO_4^{3-} and also combinations of other spectral components (Herliansyah et al., 2009; Tripathi and Basu., 2012).

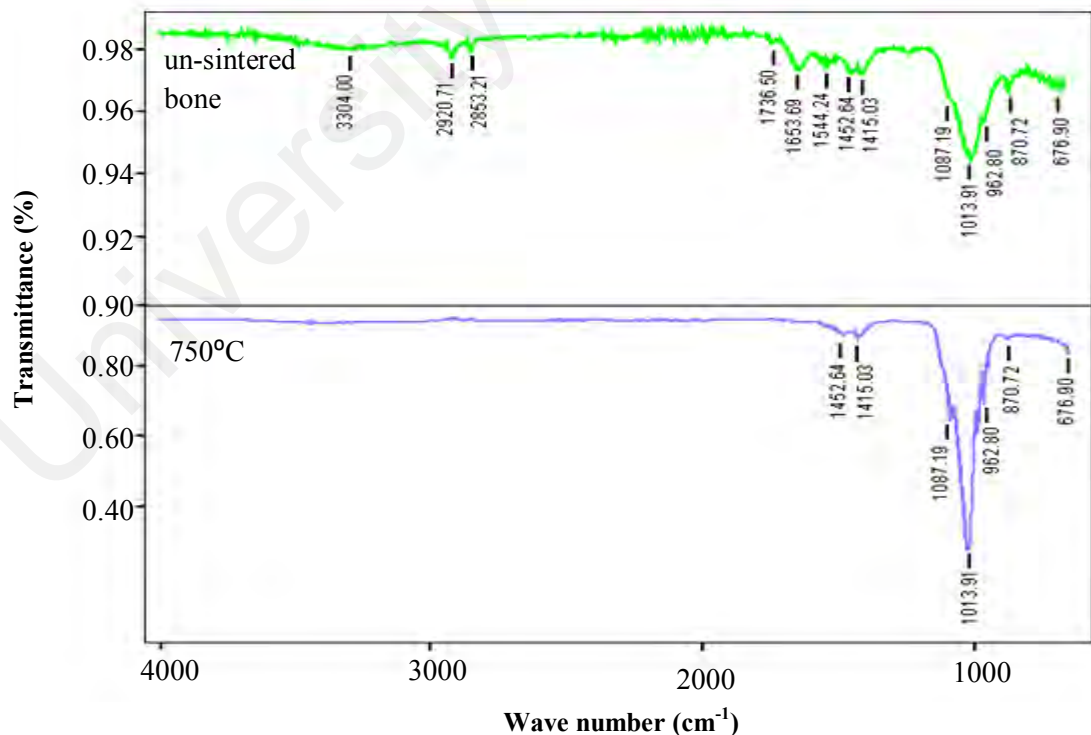


Figure 4.7: FTIR spectrum of un-sintered bovine bone and sintered samples at 750°C .

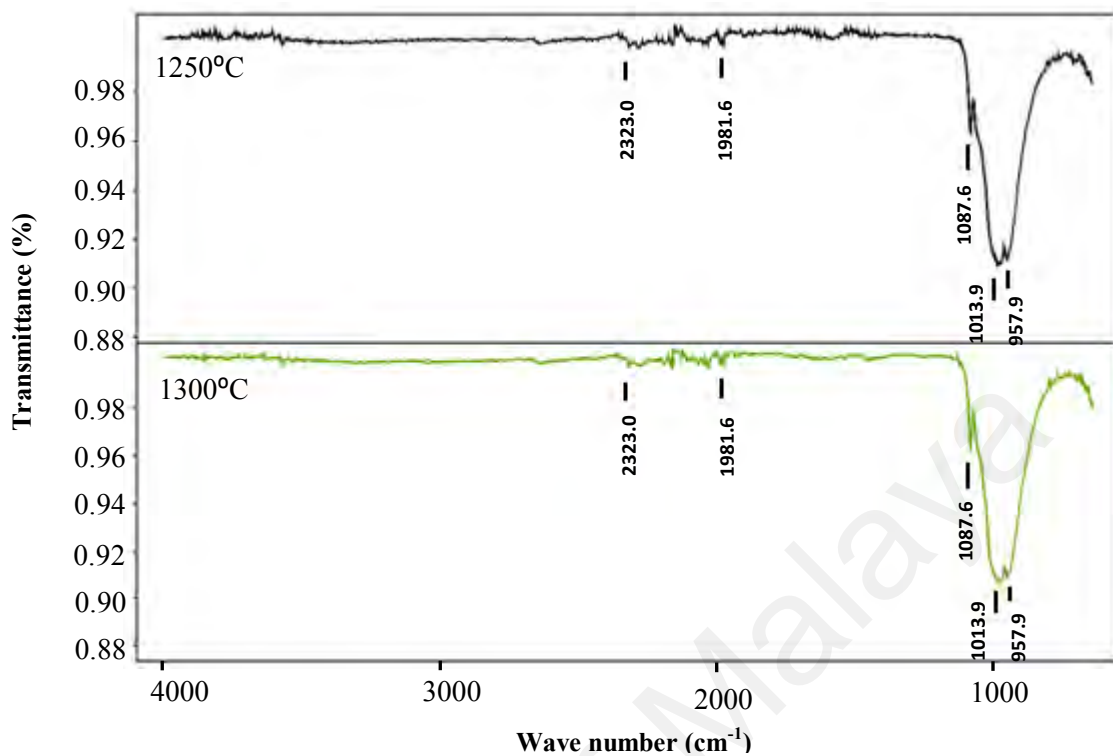


Figure 4.8: FTIR spectrum of sintered bovine bone at 1250°C and 1300°C.

4.2.4 Micro-XRF analysis

The chemical elements of the bone samples sintered at different temperatures as well as un-sintered bone are given in Table 4.2. The two elements of calcium (Ca) and phosphorus (P) are the main elements detected in the micro XRF result of the sintered sample. In addition, the minor percentage of other elements, such as sodium (Na), magnesium (Mg), potassium (K) and strontium (Sr) are part of the chemical composition of the bone itself.

Table 4.2: Chemical elements of samples as determined from micro XRF

Elements (wt%)	P	Ca	Sr	Mg	Na	K
Un-sintered bone	29.1	53.24	10.14	1.55	3.26	2.71
Sintered at 200°C	29.41	53.36	9.29	1.59	3.63	2.72
Sintered at 300°C	29.86	54.09	8.65	1.69	3.96	1.75
Sintered at 400°C	29.92	54.16	8.31	1.7	4.13	1.78
Sintered at 500°C	30.98	56.02	5.01	1.7	4.8	1.49
Sintered at 600°C	31.68	56.94	3.6	1.79	4.96	1.03
Sintered at 700°C	32.63	58.11	1.53	1.79	4.96	0.98
Sintered at 750°C	33.71	58.32	0.21	1.87	5.13	0.76
Sintered at 800°C	33.81	58.43	0.11	1.86	5.13	0.66
Sintered at 900°C	34.46	58.61	0.16	1.4	5.12	0.25
Sintered at 1000°C	34.91	58.81	0.11	0.87	5.14	0.16
Sintered at 1100°C	35.06	58.83	0.11	0.81	5.13	0.06
Sintered at 1200°C	35.18	58.81	0.12	0.89	4.94	0.06
Sintered at 1250°C	35.68	58.73	0.08	0.88	4.6	0.03
Sintered at 1300°C	36.04	58.73	0.08	0.88	4.24	0.03

The average Ca/P ratio of the samples sintered from 200°C to 1300°C, calculated from the micro XRF results, is presented in Figure 4.9. The Ca/P ratio of the un-sintered bone was determined to be 1.83 ± 0.01 . However, when the bone was subjected to sintering, the Ca/P ratio of the sintered samples decreased from 1.78 ± 0.02 (600°C) to

1.68 ± 0.01 (1000°C). Figure 4.9 shows small changes in the Ca/P ratio of the samples at low sintering temperatures between 200°C and 500°C. Figure 4.9 also shows that when sintering at temperatures between 1000°C and 1200°C, the Ca/P ratio did not change significantly. Following sintering, resulted in a decreased in Ca/P ratio, down to about 1.65 ± 0.01 and 1.63 ± 0.01 for sintering at 1250°C and 1300°C, respectively. The Ca/P ratio for the 750°C sintered sample was found to be 1.73 ± 0.02. The lower Ca/P ratio of sintered samples at 1250°C and 1300°C represents that samples are less stable than stoichiometric HA (Ca/P=1.67) and decomposed to form of TCP (Ramesh et al., 2007; Fanovich et al., 1998; Slosarczyk and Piekarczyk., 1999).

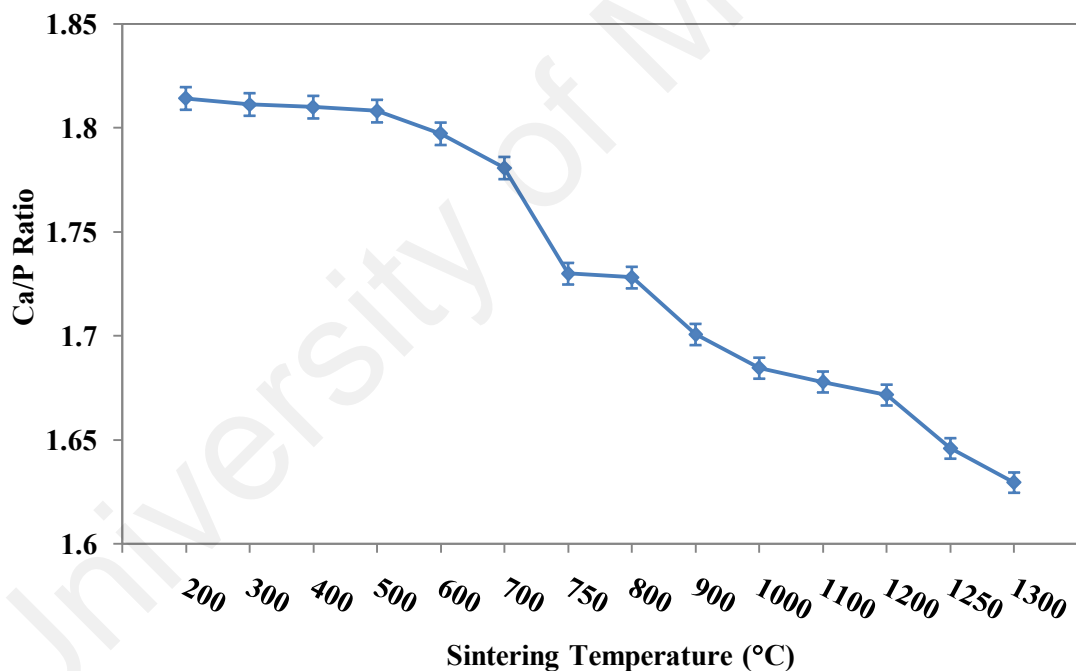


Figure 4.9: The variation in the Ca/P ratio with increasing sintering temperature.

The Ca/P ratio of the sintered bone obtained in the present work deviates from the theoretical Ca/P ratio of 1.667 for pure HA. It should be mentioned that Ca/P ratios as low as 1.61 (Krishnamurithy et al., 2014) and as high as 1.93 (Doostmohammadi et al., 2011) have also been reported in the literature for bovine bone. This deviation in the

Ca/P ratio can be attributed to many factors. For instance, the sintering temperature and sintering atmosphere have an effect on the type and amount of other calcium phosphate phases and/or other Ca compounds which could have been present with the HA phase (Sofronia et al., 2014). The crystal lattice components of bovine HA, such as Ca^{2+} , OH^- and PO_4^{3-} , can readily be exchanged by other ions. Therefore, it is obvious that the composition of the trace elements varies considerably in bone depending on nutrition and the turnover rate of the mineral (Joschek et al., 2000). Commercially available HA can be deficient in phosphorous or in calcium ($\text{Ca/P} \neq 1.67$) while still yielding an X-ray diffraction spectrum identical to that of stoichiometric HA (Muralithran and Ramesh., 2000). Alternatively, powders can have the correct Ca/P ratio but contain a mixture of TCP and CaO (Ooi et al., 207). Although the Ca/P ratio in this study deviates from the theoretical Ca/P for HA, XRD and FTIR analyses proved that the sintering successfully produced a HA matrix from the bone up to sintering temperature of 1200°C.

4.2.5 Microstructural evolution

The microstructural development of the sintered samples from 200°C to 1300°C as well as un-sintered bone at 30°C are shown in Figures 4.10 (a–e), 4.11 (a–e) and 4.12 (a–d). The analysis of these photomicrographs revealed three distinct stages; the first stage is sintering at lower temperatures to 500°C which revealed the presence of collagen, protein and organic substance in the bovine bone lattice. Therefore the surface microstructures of these samples seemed to be dense. The second stage from 600°C to 900°C wherein the samples started to exhibit a reasonable degree of porosity and corresponding to the formation of homogeneous as well as uniform porous structure between 700°C to 800°C.

At the sintering temperatures of $\leq 700^\circ\text{C}$, the HA grains and a porous network structure are not clearly visible; however, as the temperature increases to 750°C, a

natural interconnected porous structure is clearly visible and a well-defined equiaxed HA grain morphology is observed. Bone sample sintered at this temperature provide a more homogeneous porosity distribution and forming an interconnected porous network throughout the matrix. As the sintering temperature was increased further, this was accompanied by a reduction in porosity, accompanied by a rapid HA grain growth as observed in Figure 4.11 (c) for the 900°C sintered sample.

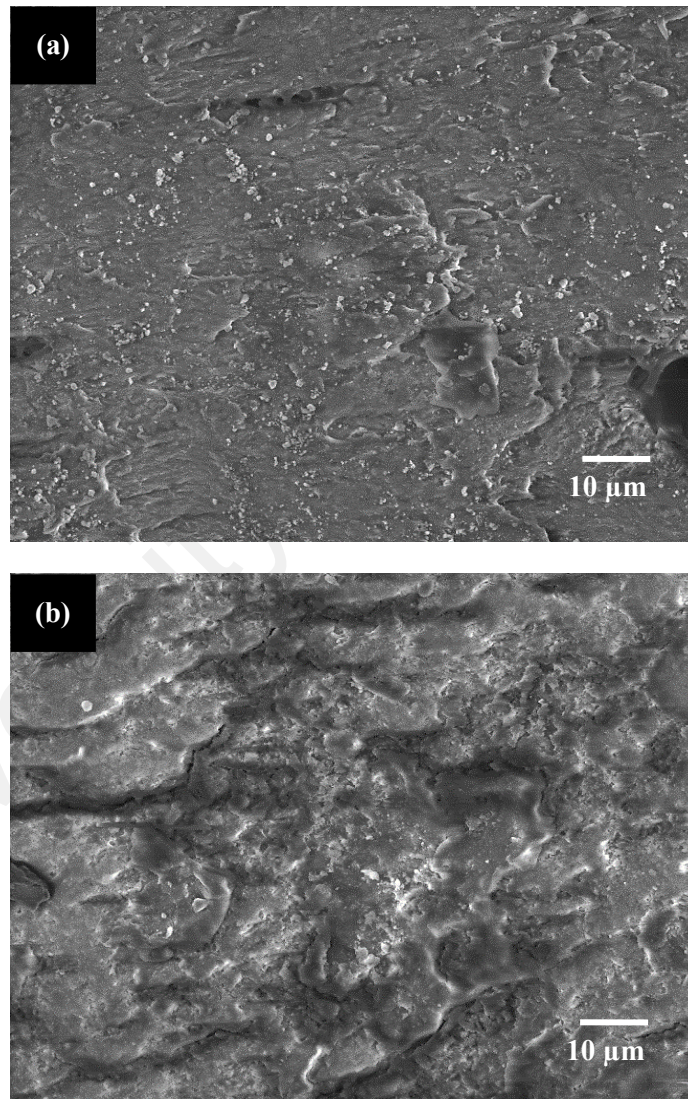


Figure 4.10: FESEM images of un-sintered sample and sintered samples at (a) 30°C and (b) 200°C.

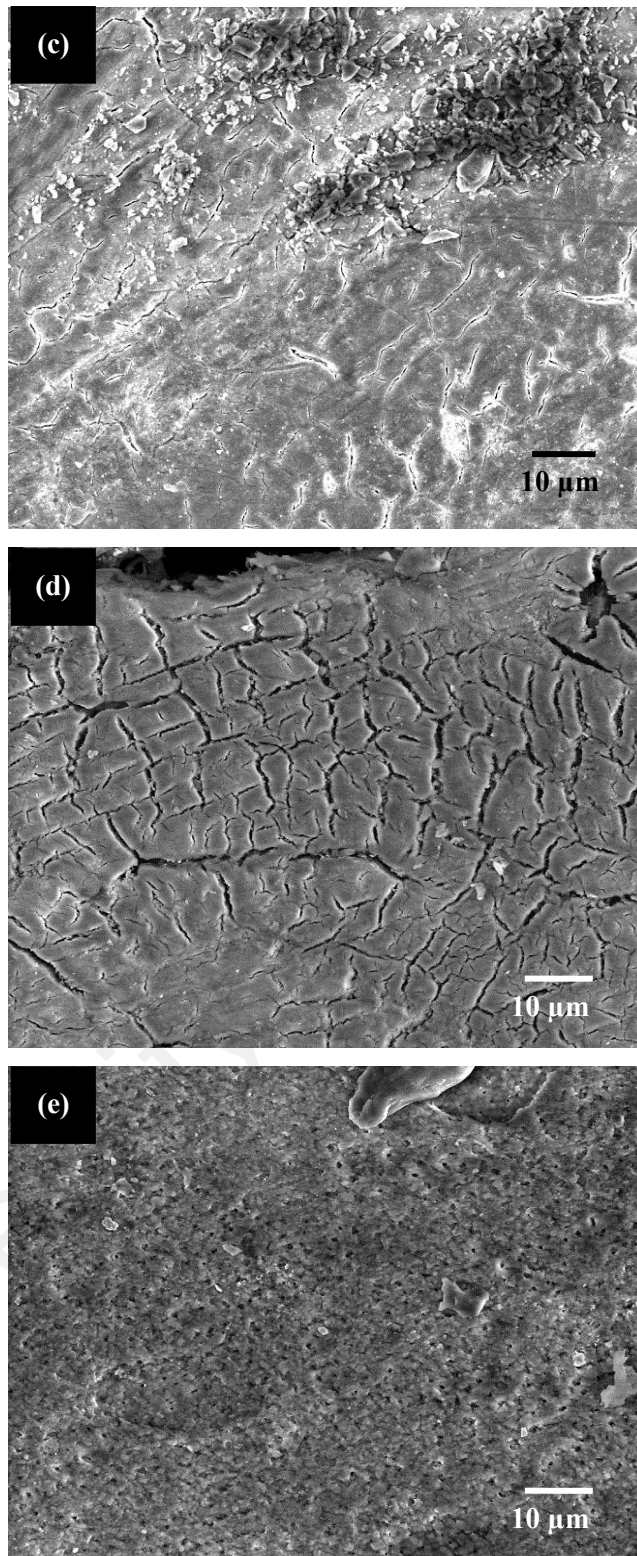


Figure 4.10 (*cont'd*): FESEM images of sintered samples at (c) 300°C, (d) 400°C and (e) 500°C.

At the sintering temperatures $\leq 700^\circ\text{C}$, the HA grains and a porous network structure are not clearly visible; however, as the temperature increases to 750°C, a

natural interconnected porous structure is clearly visible and a well-defined equiaxed HA grain morphology is observed. Bone sample sintered at this temperature provide a more homogeneous porosity distribution and forming an interconnected porous network throughout the matrix. As the sintering temperature was increased further, this was accompanied by a reduction in porosity. Rapid growth of the HA grains as can be observed in Figure 4.11 (c) for the 900°C sample. The results of this study shows that more uniform pores with a mean size of approximately 152 nm and HA grains sizes ranging from 110 nm to 215 nm were measured from the SEM micrographs of the 750°C sintered sample. This porous morphology profile could provide a very good platform for soft tissue attachment and cell proliferation when used in orthopaedic applications (Sopyan and Kaur., 2009).

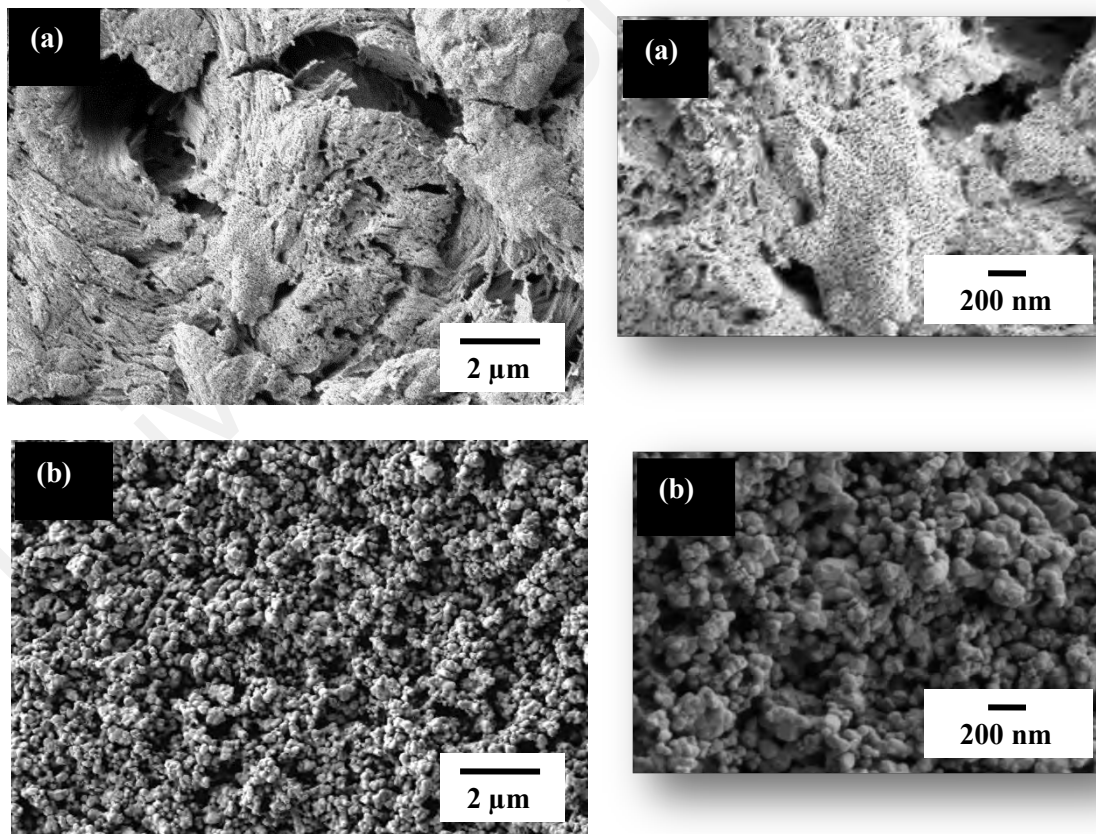


Figure 4.11: Surface microstructure of the sintered samples at (a) 600°C and (b) 700°C.

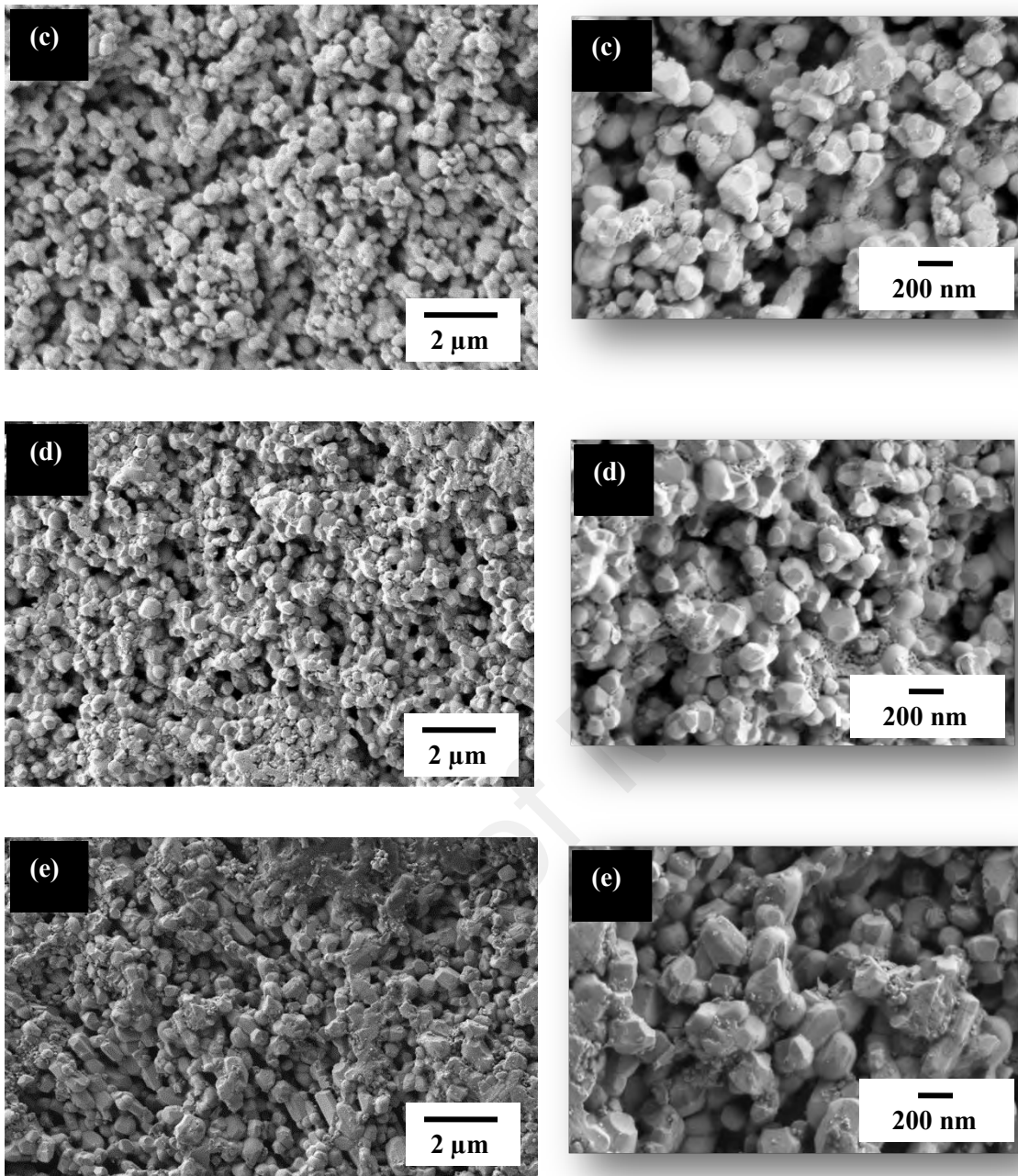


Figure 4.11 (*cont'd*): Surface microstructure of the sintered samples at (c) 750°C, (d) 800°C and (e) 900°C.

The microstructures of sintered samples from 1000°C to 1300°C are shown in Figure 4.12. In general, an equiaxed grain structure can be observed. The micrographs shows that for the sintering temperatures of 1000°C, 1100°C and 1200°C the porosities occurs mainly at grain boundaries. Furthermore, there is a significant increase in

densification from 1000°C to 1300°C and there has been a continuous grain growth from 0.88 microns at 1000°C to 2.41 microns at 1300°C. This increase is related to an average increase in the contact surface area between the grains thus providing an increased mass transfer pathway related to volumetric diffusion phenomena. As a consequence, in this temperature range there is a gradual reduction of porosity, altering the physical and mechanical properties of the material.

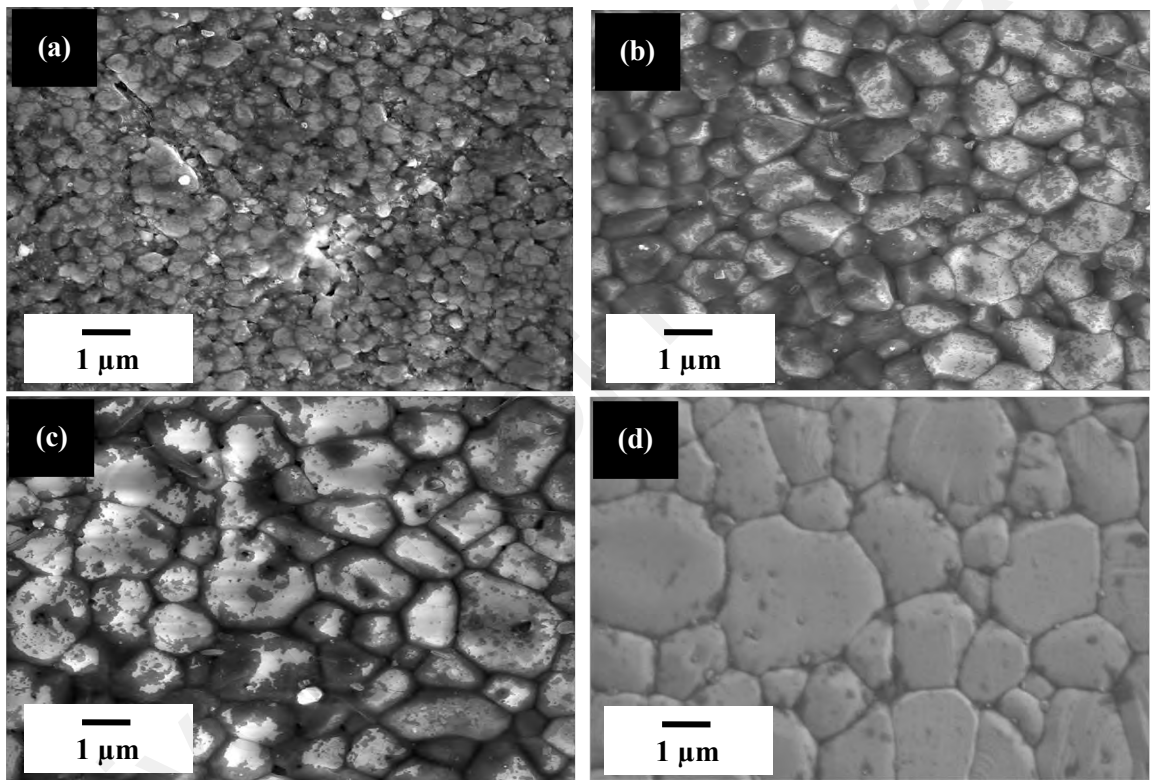


Figure 4.12: Micrograph of the sintered samples at (a) 1000°C, (b) 1100°C, (c) 1200°C and (d) 1300°C.

4.2.6 Average grain size and porosity

With regards to SEM micrographs of sintered bones, in the sintering temperature range between 200°C and 600°C, which corresponds to a low sintering temperature stage, it was not possible to characterize the grain structure and grains growth and porosities. Figure 4.13 shows the variation of average grain size for the temperature

range from 700°C to 1300°C and the effect of sintering temperatures of 700°C to 1000°C on pore size is illustrated in Figure 4.14.

Figure 4.13 shows a steady increase in the average grain size in the range between 700°C and 900°C, in which the average grain size increases by a factor of 86.5%, from 104 nm to 194 nm, whereas the growth rate accelerated from 1000°C to 1300°C resulting in the average grain size increases by 172.9% from 0.88 microns to 2.41 microns. Moreover, at this temperature range there is gradual reduction porosity of 18.7% to 7.4%. Although sintering temperature was found to be significant factor to controlling the grain size.

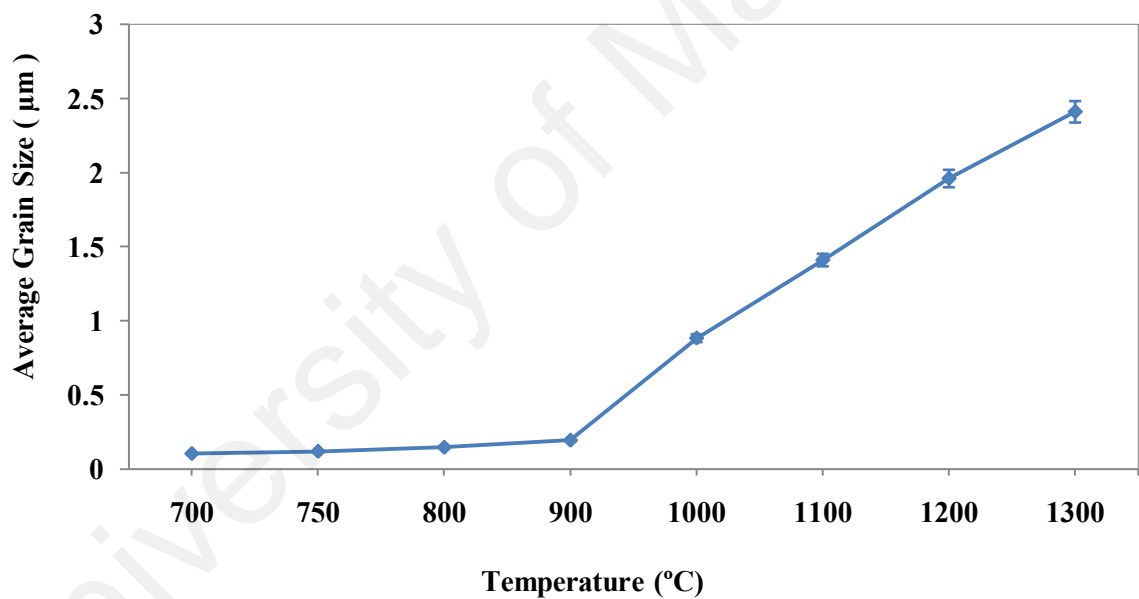


Figure 4.13: The variation of average grain size at different sintering temperatures.

The micrograph of the sintered samples from 700°C to 1000°C (Figure 4.11) shows the high degree of porosity. During this sintering range, the pore size and pore morphology underwent significant changes. As a result, tubular pores were observed along the grain boundaries, which correspond to the intermediate sintering stage. Therefore, the natural interconnected porous morphologies with variation of ultrafine

pore size from 175 nm to 101 nm are reported in this study. Figure 4.14 shows that the pore size and formation of porosity are reduced with increase of sintering temperatures. In the final sintering stage, isolated spherical or quasi-spherical pores were observed at grain boundaries or within grains (Figure 4.12 a, b and c), while the porosity decreased to 101 nm. As results, there is a gradual increase in grain size and decrease in pore size for the bone samples sintered at 1100°C, 1200°C and 1300°C that indicating an increase in the degree of density with increasing sintering temperature (Sopyan and Kaur., 2009; Lh He et al., 2008; Muralithran and Ramesh., 2000).

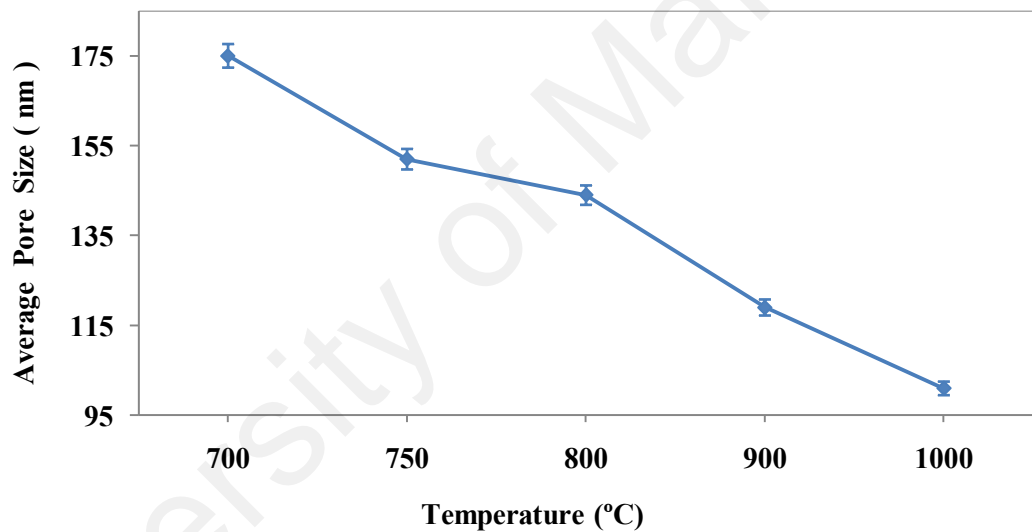


Figure 4.14: Effect of sintering temperatures on pore size.

4.2.7 Relative density

The influence of the sintering temperature on the relative density of sintered samples is shown in Figure 4.15. These values correspond to relative densities that compared to the stoichiometric hydroxyapatite density ($\rho = 3.156 \text{ g/cm}^3$). The percentage of porosity in the un-sintered bone was measured to be approximately 32.6%, which is in close agreement with the 30% porosity found in human cortical bone

(Koester et al., 2008). It is observed an increase in relative density of 39.0% at 400°C to 92.6% for 1300°C. The relative density of the un-sintered bone (67.4%) decreases to 39.0% when sintered at 400°C. This decline in is attributed to the burning of organic compounds and hydroxyls in the porous HA structure. The relative density of the sintered samples was found to increase linearly with increasing temperature, from 41.0% at 500°C to 92.6% at 1300°C. This increase can be associated with consolidation of the HA particles, forming larger grains and reducing the porosity, as shown in Figure 4.11 and Figure 4.12.

The relative density of the sample sintered at 750°C was approximately 50% (i.e., 50% porosity) and hence is reported within the range suitable for use as HA porous scaffolds (Almirall et al., 2004; Porter and McKittrick., 2014).

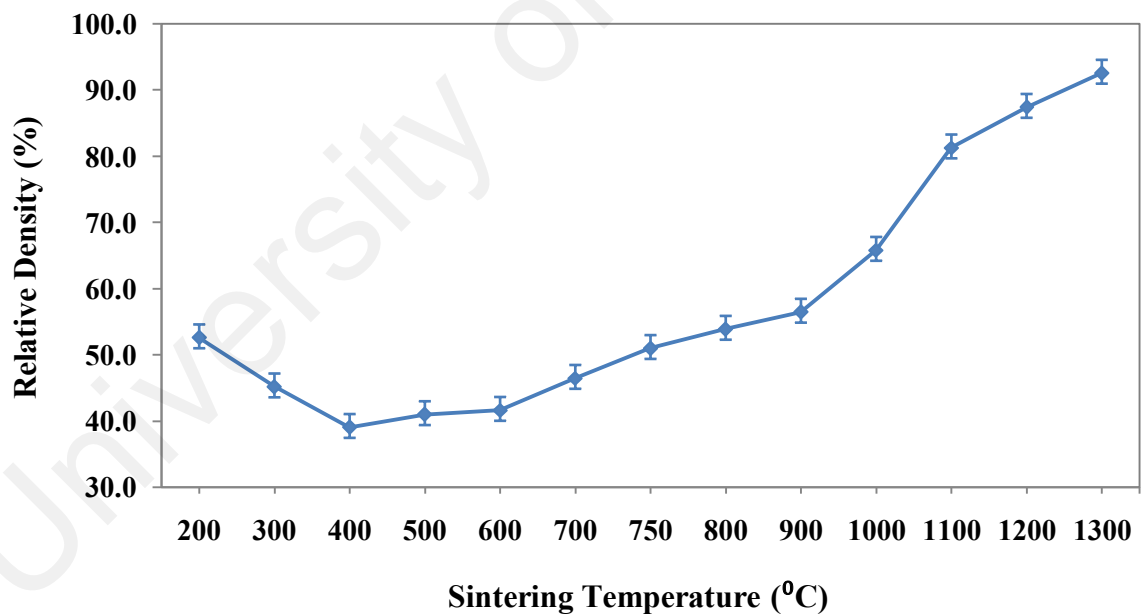


Figure 4.15: Relative bulk density of bone samples sintered at different temperatures.

4.2.8 Micro hardness and fracture toughness

The Vickers hardness (HV) measured for the samples sintered at different temperatures is shown in Figure 4.16. The average HV of the porous HA body increased from 152.2 MPa at 600°C to 172 MPa at 750°C and then start to increased further between 1000°C - 1300°C with maximum HV of 794 MPa being recorded at 1300°C. This increased in hardness can be related to an increased in the relative density and grain growth. Relatively low hardness values of the samples sintered below 1000°C are not related to decomposition of HA but rather to the formation of porous structure, as shown earlier in Figure 4.11. Simultaneously the hardness values of this study are lower than those reported in the literature (Karimzadeh et al., 2014; Muralithran and Ramesh, 2000) for HA prepared using the chemical synthesis route and the different preparation methods. On the other hand, the Vickers hardness obtained in the present work for sintered porous HA is in good agreement with the range reported by Poinern et al., (2012) for biomedical application. It was also found that the hardness of the bovine bone is very much controlled by the relative density of the HA structure, i.e., the hardness increases with increasing sintered density as depicted in Figure 4.17. This can be an advantage because the amount of porosity in the bovine HA could be tailored to suit different biomedical applications which require higher density and hardness.

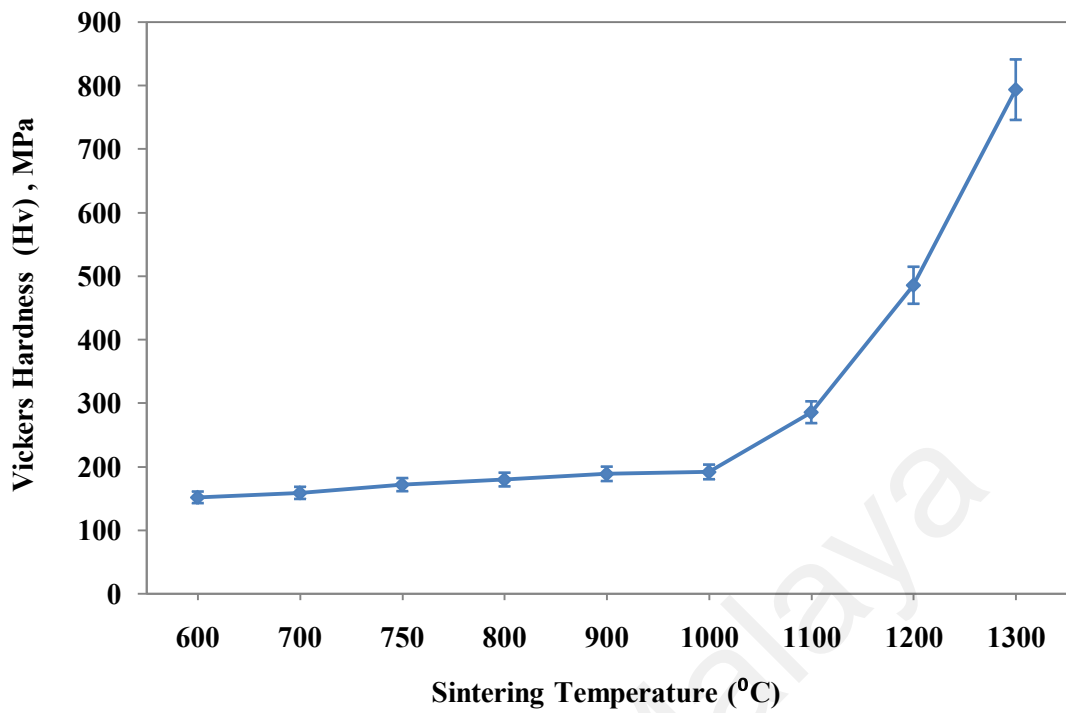


Figure 4.16: Variation in Vickers hardness with sintering temperatures.

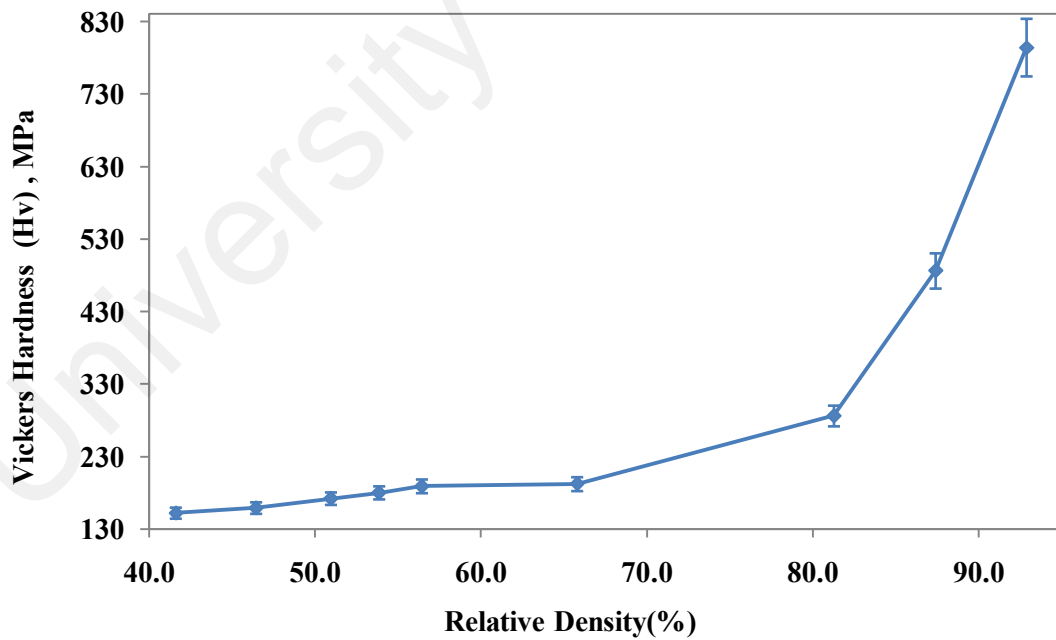


Figure 4.17: The relationship between the relative density and Vickers hardness for sintered samples.

The fracture toughness (K_{Ic}) variation of bulk HA for sintering temperature of 1100°C, 1200°C and 1300°C exhibited values of 0.56, 0.66 and 0.66 MPam^{1/2} respectively, which agrees well with the fracture toughness values reported by both Wang et al., (2009) and Dey et al., (2011). Wang measured toughness of bulk HA specimens using the Vickers indentation method, yielding a toughness value of 0.61 ± 0.04 MPam^{1/2} however, the K_{Ic} values of sintered HA samples below 1100°C could not be measured due to a porous structure exist with relative porosity range of 46.5% to 65.8% for sintering temperature range of 700°C to 1000°C. To the authors' knowledge, no specific data of K_{Ic} for HA with porosity $\geq 47\%$ are available in the literature except for two data points reported by Villora et al. (2004), where the specimens were composite containing both HA and SiO₂ phases.

4.3 Biocompatibility evaluation

In vitro test was performed to investigate the potential ability of the bovine bone scaffold prepared from different sintering temperatures (700°C to 1250°C) to induce osteogenic differentiation of human mesenchymal stromal cells (hMSCs) in the absence of supplemental osteogenic medium.

4.3.1 Alamar blue assay for cell proliferation

Cell proliferation assay was carried out based on the % of Alamar Blue (AB) reduction. As shown in Figure 4.18, the percentage reduction of Alamar Blue was monitored from day 0 to 15, and the data obtained indicated a significant difference in cell proliferation between sintered bovine bone scaffold and monolayer from day 7 to 15. The values obtained were averaged and expressed as means \pm standard deviation (SD). Statistical difference was determined using SPSS software version 10.

The differences were considered statistically significant if the value of p (probability) is < 0.05 . Therefore, the proliferation rate of monolayer is significantly higher on day 11 and 15, when compared with that of scaffold ($p < 0.05$). It can be assumed that the cell viability is not affected in this scaffold and sintered bovine scaffold can be considered as a nontoxic scaffold.

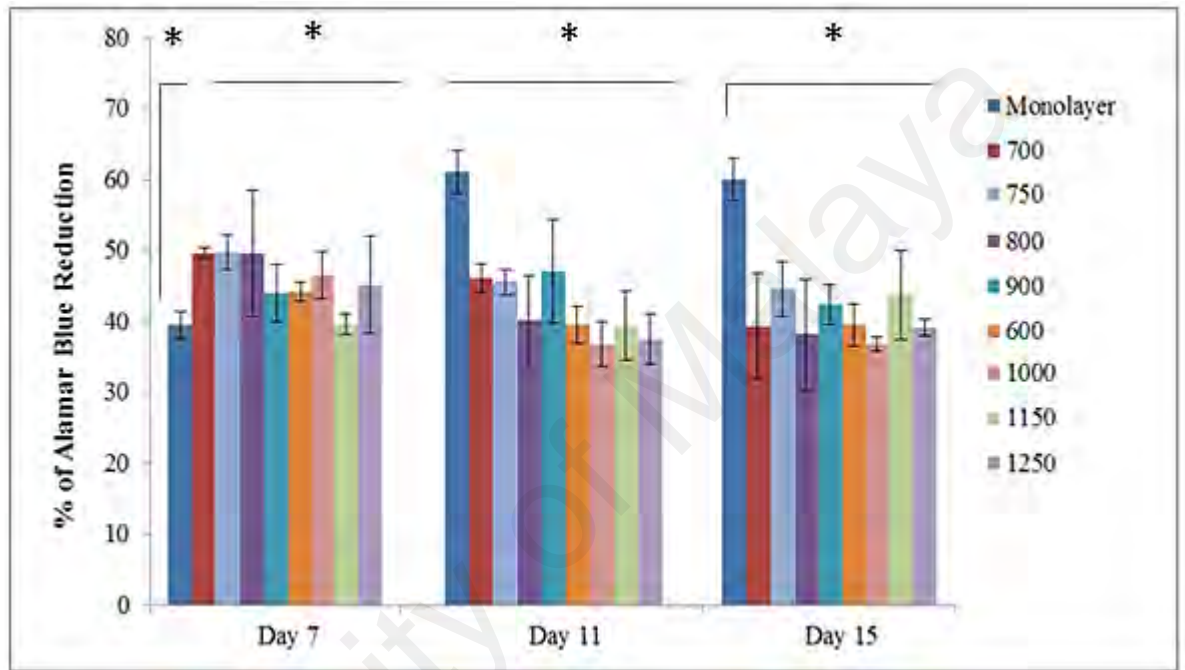


Figure 4.18: hMSCs proliferation of sintered bovine bone scaffold sintered at different sintering temperatures with significant value at $P < 0.05$. The symbol * represent the $P < 0.05$.

The metabolic activities of the cells in the sintered bovine scaffold were found to be statistically different in some time points than those in the monolayer (control). In 7 days, no significant difference was observed between sintered samples except certain groups. As shown in Figure 4.18, sintered bovine scaffold at 700°C, 750°C and 800°C almost presented higher metabolic activities compared with sintered scaffold at 600°C and 1150°C where the sintered bone sample at 1150°C has a significantly lower proliferation rate than all others ($p < 0.05$).

Observations at day 11 and 15 showed a significant difference between the control and all type of sintered samples ($p < 0.05$). On the other hand, significant differences were observed only between certain groups (750:600, 750:1000, 750:1250°C, respectively). There was no significant difference between the groups after day 15 of culture, however, a significant difference was observed between the control and all biomaterials. This increase in cell proliferation can be due to the cell-matrix interaction phenomenon which involves three types of proteins including ECM adhesion proteins, cell membrane proteins and cytoskeletal proteins (Anselme 2000; Anselme et al., 2002). Based on the results obtained, scaffolds from day 11 were chosen for SEM analysis.

4.3.2 SEM analysis of cultured scaffold

SEM analysis was used to determine the cell attachment property of the bovine scaffold seeded with hMSCs. The specimens at day 3 were fixed overnight in 4% glutaraldehyde with 0.1M cacodylate and fixed for 1 h in 1% aqueous osmium tetroxide. These specimens were washed three times in distilled water before being dehydrated through a graded ethanol series (50, 70, 80, 90, 95, 100%, acetone mixture and in pure acetone). The specimens were subsequently dried at a critical point in a critical point drier (Bal Tec, CPD030) supplement with CO₂. The specimens were mounted on the aluminum stub and sputter coated with gold before being examined using a field emission scanning electron microscopy (FESEM).

The SEM analysis confirmed the affinity of surface for cell attachment. Figures 4.19 – 4.23 shows the attachment of cells the surface of the prepared scaffolds at (600, 700, 750, 800, 900, 1000, 1150 and 1250°C). The attached cells are found to extend filopodia to strengthen the attachment between the cells and porous scaffold surfaces at (700, 750, 800 and 900°C). The SEM images show that the architecture around the cells

mimic extracellular matrix (ECM) and form continuous layer of sphere and fusiform over the surface of the scaffold and growth compare to the prepared scaffolds at (600, 1000, 1150, and 1250°C) with higher surface density. The SEM images show that the cellular matrix just dispersed in a layer on the dense surface of prepared scaffolds of 1150°C and 1250°C. This observation also correlates with the Alamar Blue assay. It is well established that the surface characterization influences cell adhesion and growth, and guides cellular differentiation.

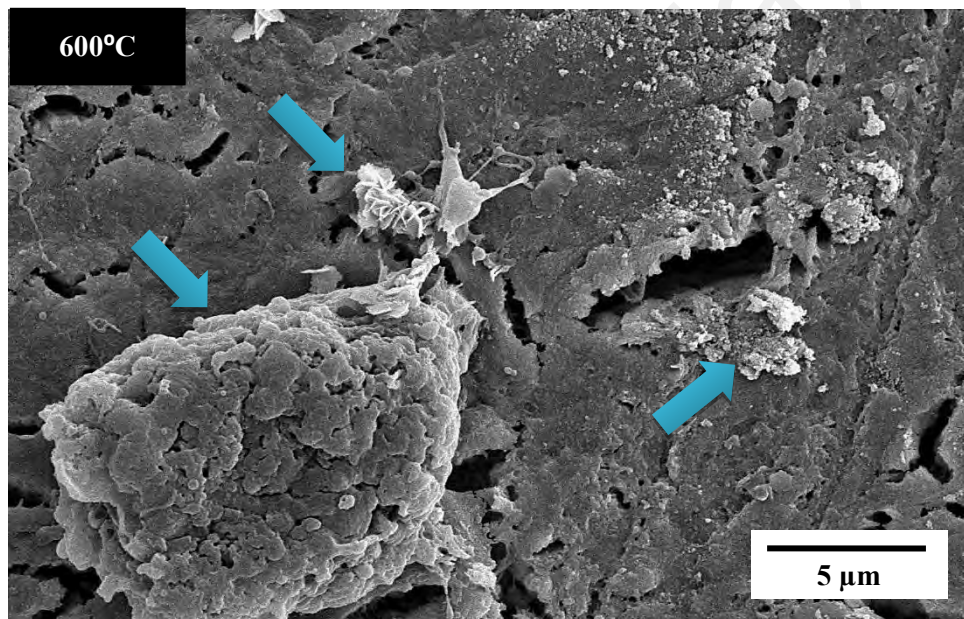


Figure 4.19: SEM picture of scaffold sintered at 600°C showing hMSCs activity (indicated by the arrows) after day 11.

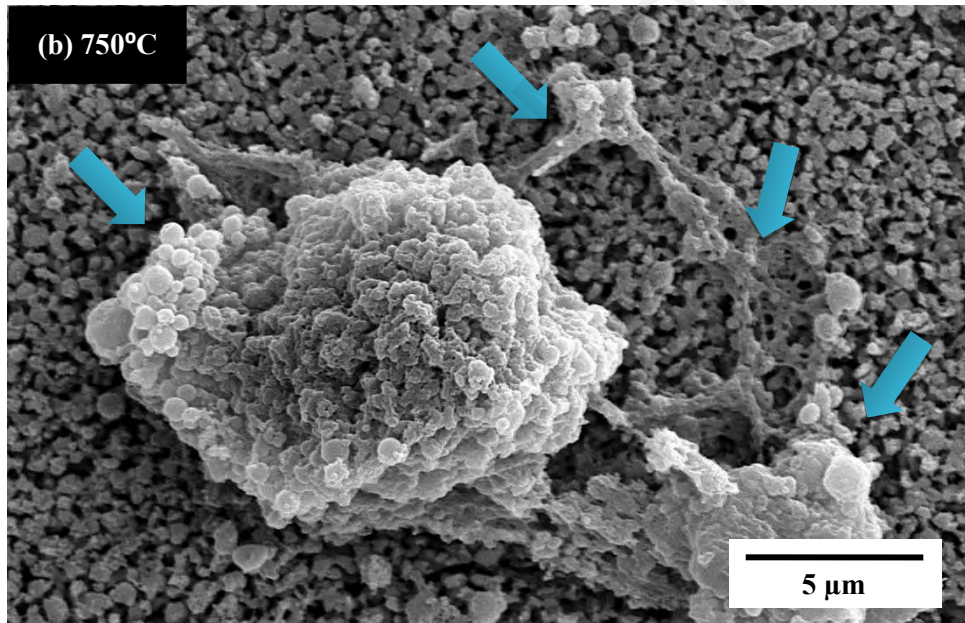
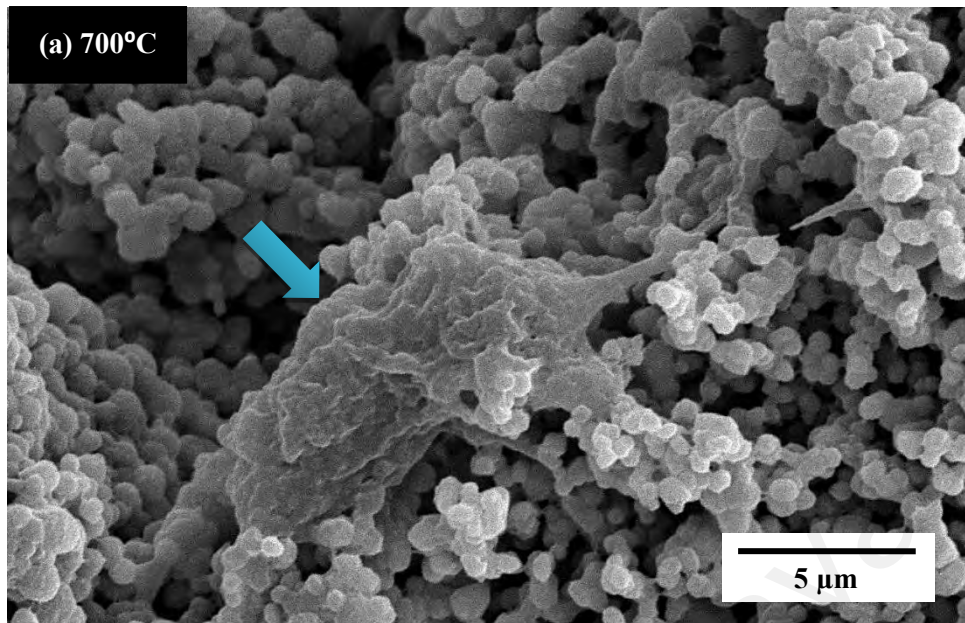


Figure 4.20: SEM pictures of exposed scaffolds sintered at (a) 700°C and (b) 750°C revealing hMSCs activity (indicated by arrows) after day 11.

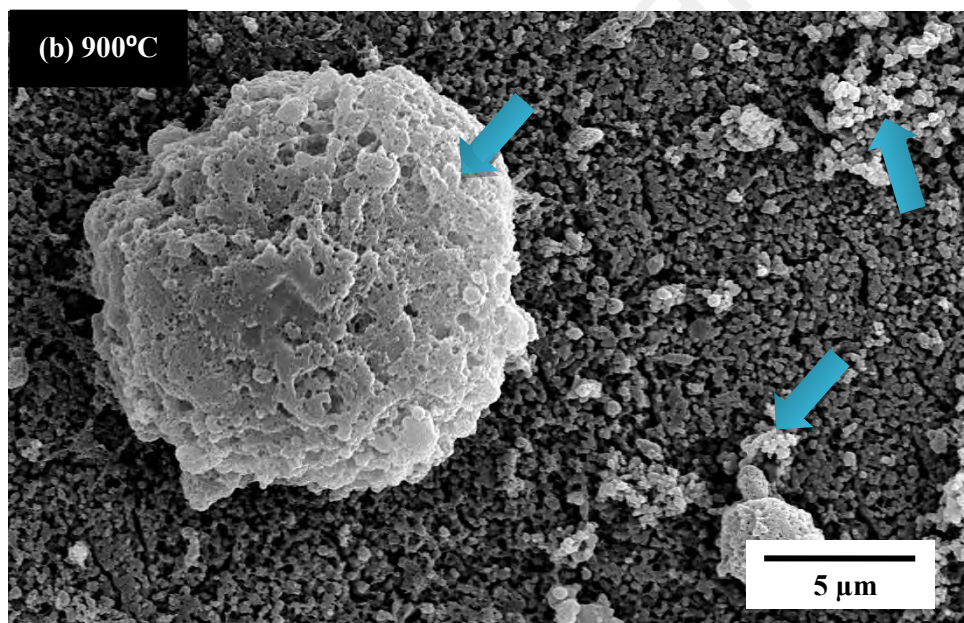
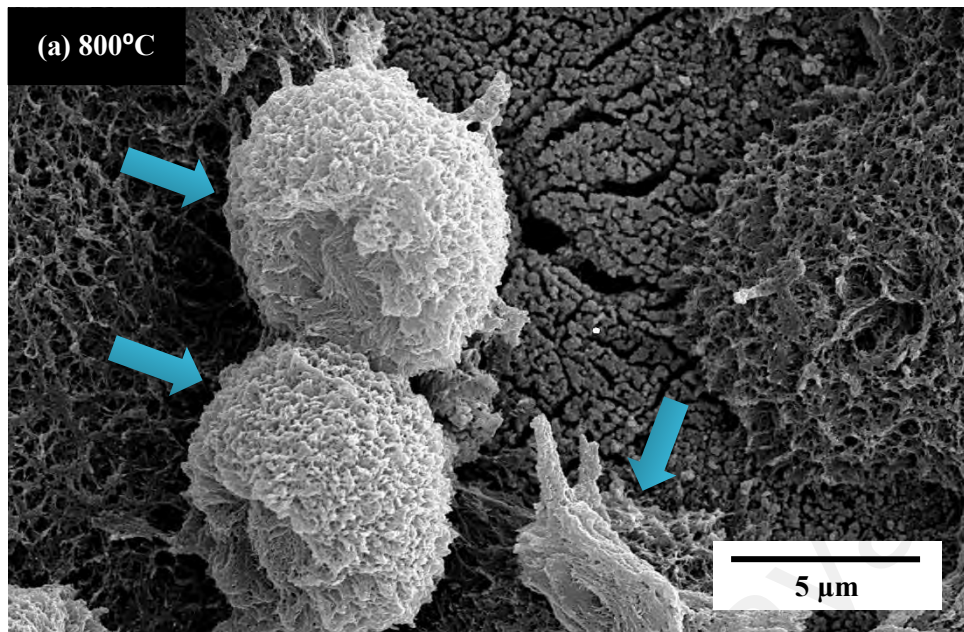


Figure 4.21: SEM pictures of exposed scaffolds sintered at (a) 800°C and (b) 900°C revealing hMSCs activity (indicated by arrows) after day 11.

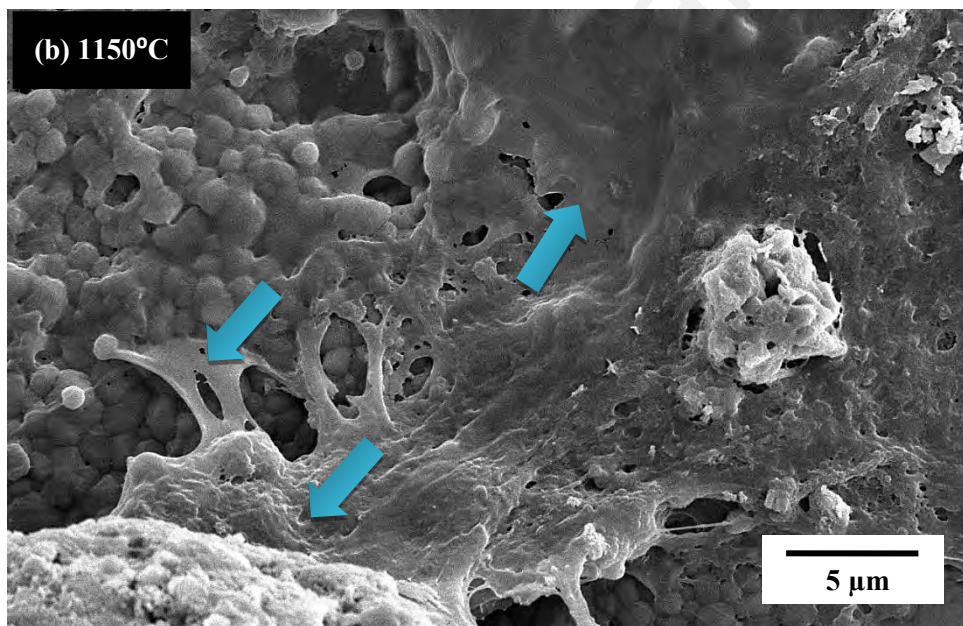
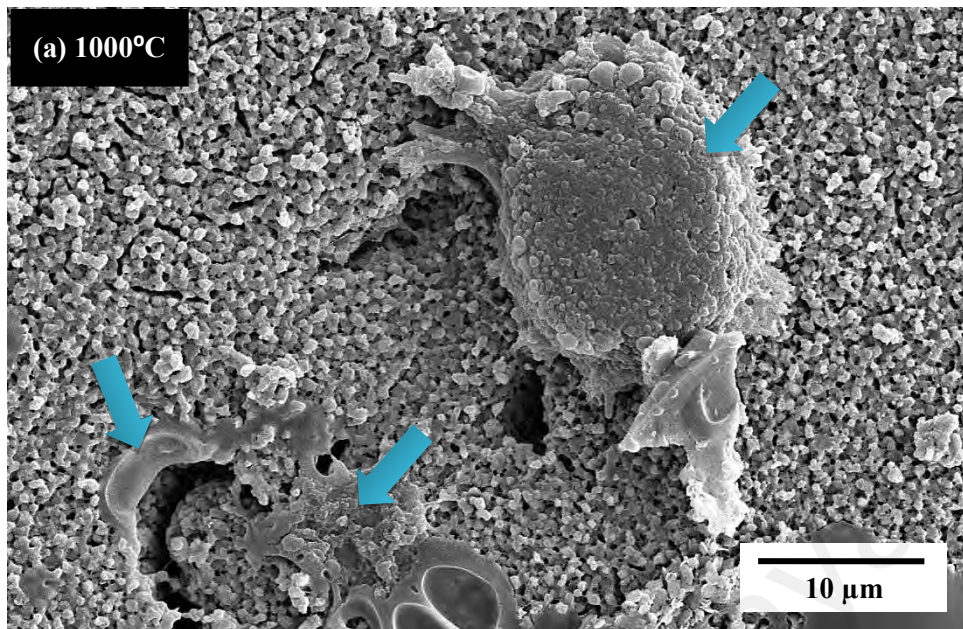


Figure 4.22: SEM pictures of exposed scaffolds sintered at (a) 1000°C and (b) 1150°C revealing hMSCs activity (indicated by arrows) after day 11.

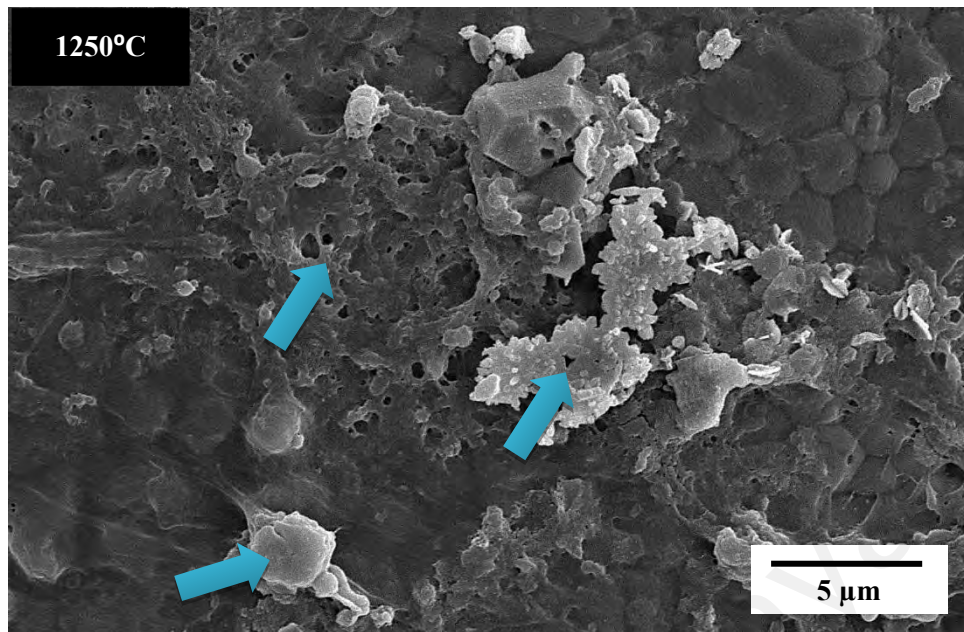


Figure 4.23: SEM picture of exposed scaffolds sintered at 1250°C revealing hMSCs activity (indicated by arrows) after day 11.

4.3.3 Chemical analysis by EDX

The EDX analysis was required to confirm the chemical elements contained in the cultured scaffold used in bio-evolution research. Figure 4.24 shows the EDX spectrum of a cell cultured bovine scaffold surface infiltrated with cells and hydroxyapatite. The weight percentages of chemical elements presented in cultured bovine scaffold are observed as oxygen (O) (20.19%), gold coating (Au) (28.43%), carbon (C) (15.21%), phosphorus (P) (12.98%) and Calcium (Ca) (23.19%). This analysis proves that the impregnation cultured surface only show chemical elements correspond to hydroxyapatite with Ca/P ratio of 1.78 that also discussed in section 4.2.4. This finding also proved that bovine scaffold is chemically stable at culture media and did not dissolve during cell cultural test.

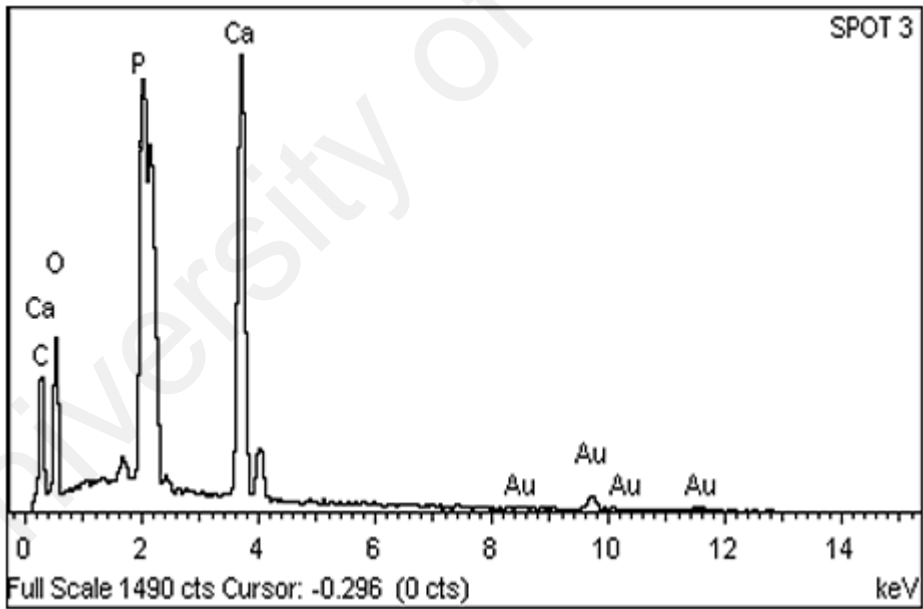
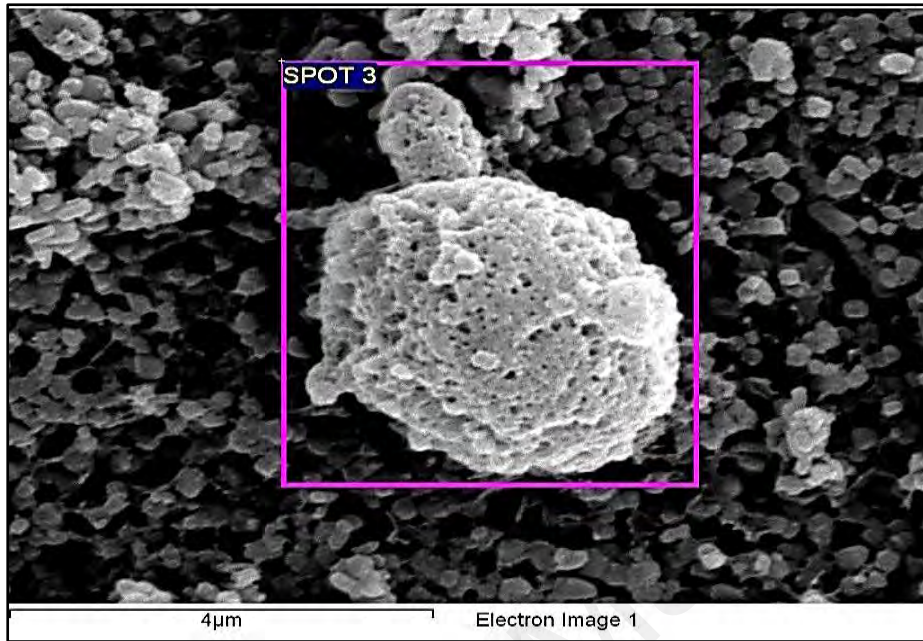


Figure 4.24: EDX of bovine scaffold infiltrated with hMSCs.

4.3.4 Confocal microscopy of cultured scaffold

Confocal microscopy used to confirm the SEM results of cells proliferation on the bovine scaffolds. The confocal microscopy performed on day 14. Samples demonstrated the cell attachment on the surface of different bovine scaffolds prepared at different sintering temperatures from 600°C to 1250°C against control scaffold without cells. As shown in Figure 4.25, cells (bright blue spots) are seen attached to the bovine scaffolds. Confocal microscopy results indicate that the cells are well penetrated to the porous microstructure of bovine scaffold and exhibited a viable bright and shining blue nucleus region for scaffolds from 600°C to 1000°C due to presence of porous surface and they growth as it discussed in section 4.3.2. However, the cells are mostly dispersed as a layer on the surface of scaffold at 1150°C and 1250°C due dense microstructure as shown in Figure 4.26. Figure 4.25 also shows that the cells density of bovine scaffolds at 750°C, 800°C and 900°C are higher than others. The highest cells density (viable nucleus cells) observed at 750°C that also confirm the homogeneity of porous microstructure and ability of cell attachment to the bovine scaffold at this sintering temperature. In all images the bright blue part corresponds to the cells. Various scaffold surfaces behave differently based on the in vitro physiological conditions and cell types. Since few years, efforts have been taken to fabricate an artificial surface mimicking natural ECM; however, not all fabricated materials are biomimetic in nature, because the currently available methodologies are not efficient in pointing out a differentiated cell using imaging studies.

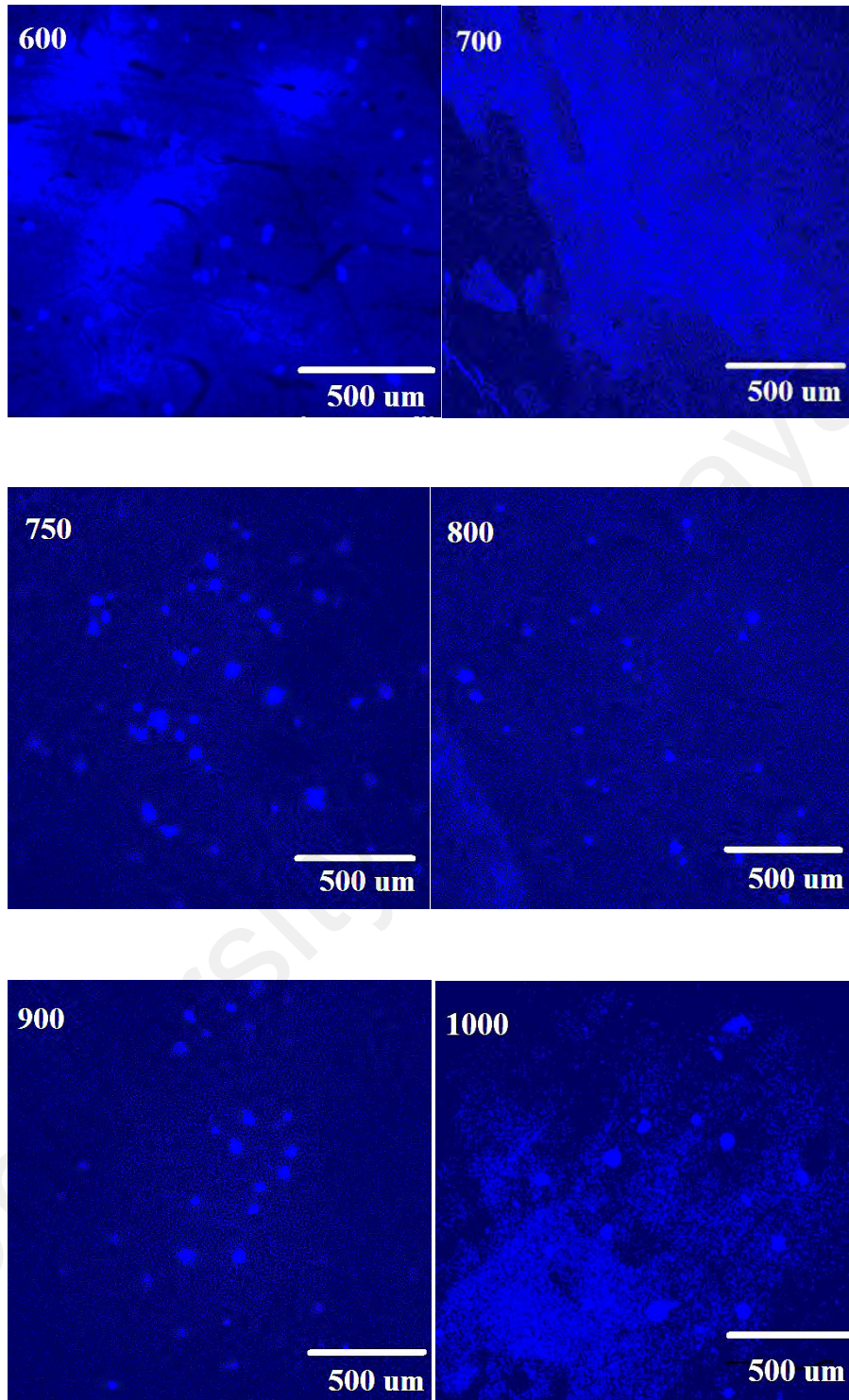


Figure 4.25: Confocal microscopy of cell attachment on bovine scaffolds prepared at varying sintering temperature from 600°C to 1000°C. Bright and shining blue nucleus regions represent the penetrated cells.

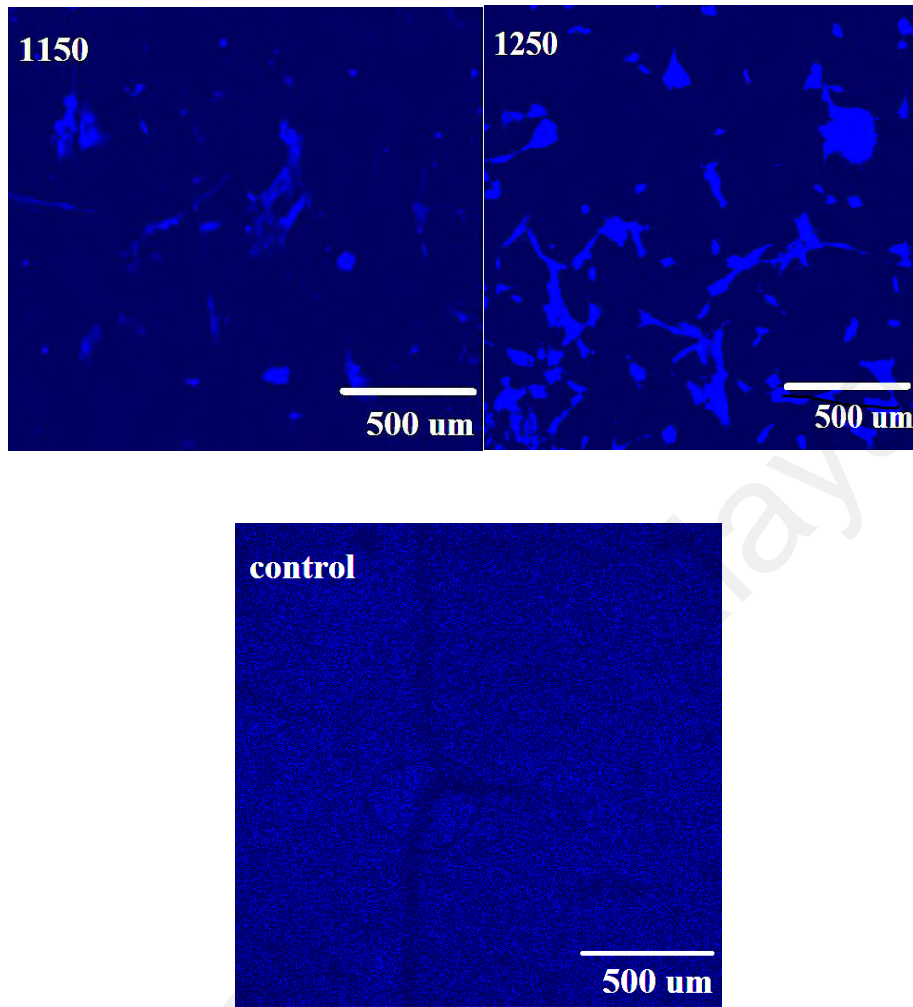


Figure 4.26: Confocal microscopy of cell attachment on bovine scaffolds prepared at sintering temperature of 1150°C and 1250°C against control scaffold without cells.

Bright and shining blue areas represent the dispersed cells.

4.3.5 ALP and osteocalcin assays

To confirm the phase of osteogenic differentiation, we quantified the levels of alkaline phosphate activity (ALP) and osteocalcin (OC) after seeding the cells onto the bovine scaffolds based on the SEM and Alamar Blue assay results. The bovine scaffolds with higher proliferation rate at day 11 (700°C, 750°C, 800°C and 900°C) were chosen for further analysis including ALP and osteocalcin assays.

When hMSCs are cultured in osteogenic media they express markers known to be exhibited by bone forming osteoblasts, which are the cells responsible for laying down the matrix and mineral during new bone formation *in vivo*. The osteogenic differentiation of MSCs *in vitro* has been divided into three stages (Huang et al., 2007). The first stage consists of days one to four where a peak in the number of cells is seen. This is followed by early cell differentiation from days 5 to 14, which is characterized by the transcription and protein expression of alkaline phosphatase (ALP) (Aubin, 2001). After this initial peak of ALP its level starts to decline. The final stage starts from days 14 to 28 that result in a high expression of osteocalcin and osteopontin, followed by calcium and phosphate deposition (Hoemann et al., 2009; Huang et al., 2007).

ALP results as an early-stage marker of osteogenic differentiation was found to gradually increase and reach approximately two folds of its initial level in cells cultured on days 7 ($p < 0.01$). The ALP results also shows significant differentiation on day 14 and 21 for $p < 0.05$ as presented in Figure 4.27. It is known that one of the characteristics of a mature osteoblast phenotype is the ability of the cells to produce ALP.

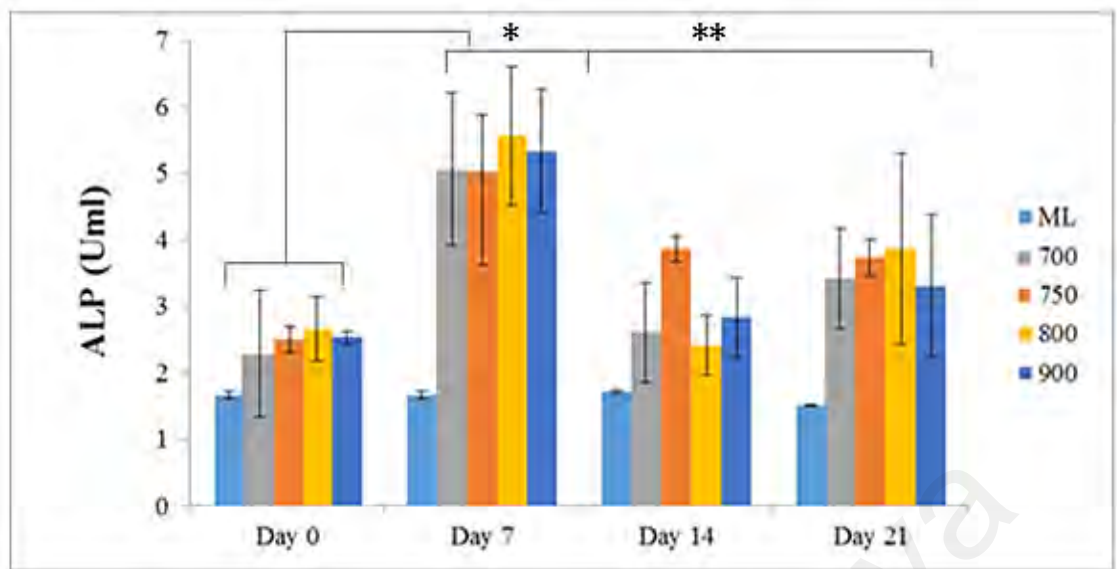


Figure 4.27: Early hMSCs differentiation and ALP of bovine scaffold prepared from 700°C to 900°C with significant value at $P < 0.01$ and $P < 0.05$. The symbol * represent the $P < 0.01$ and ** represent the $P < 0.05$.

OC is a pro-osteoblastic marker that is claimed to play a significant role in modulating mineralization, because it has rich glutamic acid domains with binding affinities to both Ca and HA (Mikuni-Takagaki et al., 1995).

The bar graph in Figure 4.28 presented the production of OC, a late-stage marker of osteogenesis, was significantly enhanced ($P < 0.01$) approximately eleven fold increase in the bovine scaffold prepared at 750°C on day 14, when compared with other time points followed by other bovine scaffold at 700°C, 800°C and 900°C.

Considering the late-stage expression of OC during osteogenesis, it appeared that the cells had progressed along the differentiation phase before migrating into the center of the porous bovine scaffolds. These findings correlate with the levels of proliferation, where proliferation halts and differentiation twitches. It should be noted that it is not easy to achieve a shift from proliferative to differentiate phase in the cells under cell-culture conditions (Balaji Raghavendran et al., 2014).

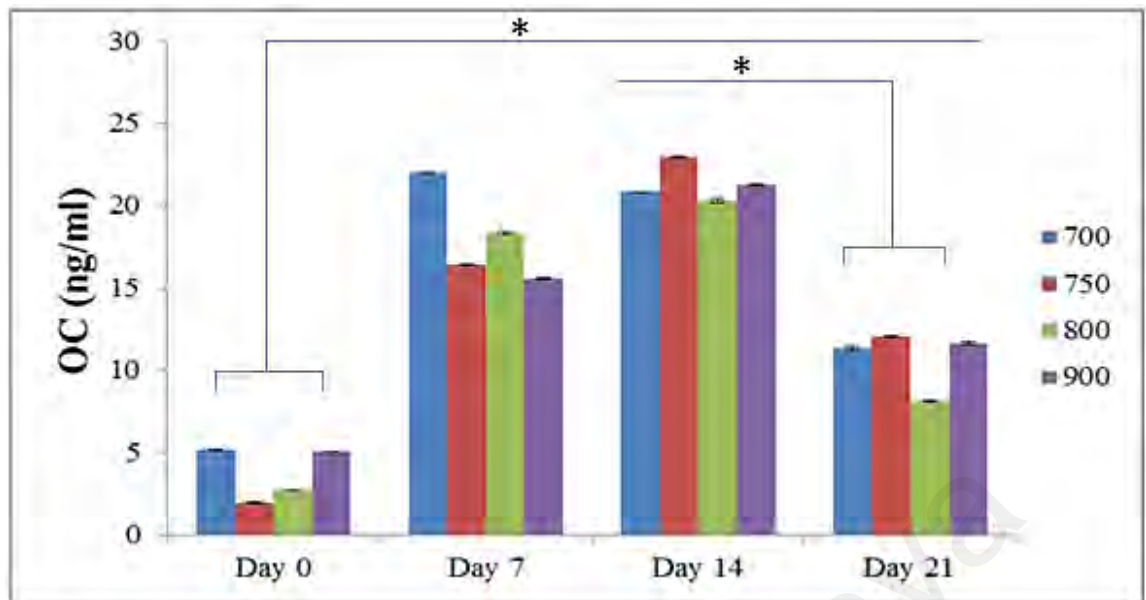


Figure 4.28: Production of osteocalcin (OC) on bovine scaffold prepared from 700°C to 900°C with significant value at $P < 0.01$. The symbol* represent the $P < 0.01$.

An ideal scaffold should exhibit properties such as osteoinductivity, osteoconductivity and osteogenesis. In the present research, the increase in ALP and osteocalcin is consistent in all the four scaffolds, which principally demonstrate that the material could initiate stem cells or progenitors to undergo differentiation process, particularly, to form osteoblast-like cells. From the results obtained in the present work, it was evident that the fabricated porous structure material from sintered bovine bone supported adhesion and proliferation, and that porous bovine scaffold at 750°C could act as a carrier for the mineralization of osteoblasts.

CHAPTER 5

CONCLUSIONS AND RECOMMENDATIONS FOR FUTURE WORKS

5.1 Conclusions

This research was carried out to investigate the viability of using the sintering process to convert bovine bone directly into bovine-HA and to evaluate the phase content, microstructural evolution, mechanical properties as well as the biocompatibility of the derived bovine-HA for potential use in biomedical applications. The objectives of this research have been achieved with the following conclusions:

1. XRD analysis indicated that a pure and single phase HA has successfully being produced from bovine bone, with no secondary phase such as TCP or CaO being detected, when sintered at temperatures ranging up to 1200°C.
2. The characteristic analysis of un-sintered bovine bone by infrared spectroscopy confirmed the presences of vibrational bands corresponded to the organic material as well as the functional groups PO_4^{3-} and OH. However, the organic vibrational bands were not detected after sintering the bovine bone at 750°C. There is a decrease in the intensity of phosphate ion with increasing sintering

temperature up to 1300°C which resulted in phase decomposition of HA at 1250°C and 1300°C.

3. The microstructural analysis revealed that the optimal conventional pressureless sintering profile for the production of a uniform porous-structured bovine-HA was 750°C.
4. All the bovine-HA samples from 700°C to 900°C exhibited a similar grain size trend with increasing temperature, while the HA grain size increased dramatically after 900°C. However, average pore size reduced with increasing temperature. In general, the average pore size of 152 nm and HA grain size ranging from 110 nm to 215 nm was measured for the sintered sample at 750°C.
5. The influence of the sintering temperature on the relative density of sintered samples from 500°C to 1300°C was found to increase linearly with increasing temperature i.e. from 41% at 500°C to 92.9% at 1300°C. The relative density of the sintered sample at 750°C was approximately 50% (i.e. 50% porosity) and hence was within the reported range suitable for use as HA porous scaffolds.
6. The hardness of porous bovine-HA samples increased with increasing of sintering temperature. This increase in hardness was found to be related to the combined influence of both relative density and grain size of sintered samples. With regard to relative density results and morphologies structural of porous samples the average hardness value of 172 MPa was measured for porous HA sample sintered at 750°C.
7. The microstructure analysis clearly demonstrated the presences of a porous network (up to 65.8% porosity level) within the HA matrix of the bovine bones that were sintered below 1100°C.

8. The cell proliferation and cell viability test of bovine-HA scaffolds were carried out by Alamar Blue assay. The Alamar Blue results indicated that cell proliferation rate of all cultured bovine-HA were significantly high thus confirming the nontoxicity of the derived material.
9. The SEM analysis of cultured bovine-HA confirmed that the prepared scaffold at 750°C, having approximately porosity level of 50%, and provided better cell attachment on the porous structure. Furthermore, the confocal microscopy of bovine scaffolds also showed that the hMSCs were well penetrated into the pores of bovine-HA. Furthermore, the EDX analysis of cell cultured bovine-HA only revealed elements corresponded to hydroxyapatite chemical composition, thus confirming that the bovine-HA is chemically stable.
10. The Alkaline phosphate activity (ALP) and osteocalcin (OC) assay indicated that osteocalcin was produced on all bovine-HA by osteoblasts during osteogenic formation. The ALP results confirmed the positive osteogenic differentiation on all cultured bovine scaffolds. The OC results also showed that natural porous bovine scaffold sintered at 750°C produced higher OC level when compare to bovine scaffolds sintered at 700 °C, 800 °C and 900 °C.

5.2 Recommendation for further work

During the period of this research, some interesting results were obtained which provided new opportunities for further research. The current work has also given some ideas, which could be exploited further in order to enhance the properties of sintered bovine HA while retaining its biocompatibility. As indicated in the present work, the control of sintering temperature has led to uniform porous structure within bovine HA

and enhance its cell attachment behavior and biocompatibility. Following are several suggestions for further work:

1. Microwave sintering is an advanced sintering technique that can apply higher heating rates (up to 100°C/min.) during sintering process in order to produce finer grain structure (Ramesh et al., 2007; Yang et al., 2004) and probably produce much uniform porous architecture. A thorough study of the effect of microwave sintering on the properties of bovine bone has yet to be undertaken. It would be beneficial to examine the different microwave sintering profile in order to produce a uniform porosity structure and enhancement in the mechanical properties and bioactivity of the material.
2. In order to measure the fracture toughness of porous bovine HA, the indentation toughness method is used in this study which was not viable. The notch beam test could be helpful to measure the fracture toughness of porous bioceramics.
3. Since the *in vitro* results of sintered bovine HA by using hMSCs were found to be very promising, further work could concentrate on *in vivo* studies of sintered bovine HA that will help to verify the possible use of bovine scaffold for bone substitute and clinical applications.
4. In order to use of sintered bovine HA for clinical application, the effect of stress on the cell cultured scaffold and improvement of mechanical properties of sintered bovine-HA after production of osteocalcin (OC) which has been reported in the literatures could also be investigated.

REFERENCES

- Agrawal, C., & Ray, R. B. (2001). Biodegradable polymeric scaffolds for musculoskeletal tissue engineering. *J Biomed Mater Res*, 55(2), 141-150.
- Agrawal, C. M. (1998). Reconstructing the human body using biomaterials. *JOM*, 50(1), 31-35.
- Akao, M., Aoki, H., & Kato, K. (1981). Mechanical properties of sintered hydroxyapatite for prosthetic applications. *Journal of Materials Science*, 16(3), 809-812.
- Akazawa, T., Itabashi, K., Murata, M., Sasaki, T., Tazaki, J., Arisue, M., Kanno, T. (2005). Osteoinduction by Functionally Graded Apatites of Bovine Origin Loaded with Bone Morphogenetic Protein-2. *Journal of the American Ceramic Society*, 88(12), 3545-3548.
- Albrektsson, T., & Johansson, C. (2001). Osteoinduction, osteoconduction and osseointegration. *European Spine Journal*, 10(2), S96-S101.
- Almirall, A., Larrecq, G., Delgado, J., Martinez, S., Planell, J., & Ginebra, M. (2004). Fabrication of low temperature macroporous hydroxyapatite scaffolds by foaming and hydrolysis of an α -TCP paste. *Biomaterials*, 25(17), 3671-3680.
- Anselme, K. (2000). Osteoblast adhesion on biomaterials. *Biomaterials*, 21(7), 667-681.
- Anselme, K., Broux, O., Noel, B., Bouxin, B., Bascoulergue, G., Dudermel, A.-F., Hardouin, P. (2002). In vitro control of human bone marrow stromal cells for bone tissue engineering. *Tissue engineering*, 8(6), 941-953.
- Anstis, G., Chantikul, P., Lawn, B. R., & Marshall, D. (1981). A Critical Evaluation of Indentation Techniques for Measuring Fracture Toughness. I.--Direct Crack Measurements. *Journal of the American Ceramic Society*, 64(9), 533-538.
- Artico, M., Ferrante, L., Pastore, F. S., Ramundo, E. O., Cantarelli, D., Scopelliti, D., & Iannetti, G. (2003). Bone autografting of the calvaria and craniofacial skeleton: historical background, surgical results in a series of 15 patients, and review of the literature. *Surgical neurology*, 60(1), 71-79.

- Bahrololoom, M., Javidi, M., Javadpour, S., & Ma, J. (2009). Characterisation of natural hydroxyapatite extracted from bovine cortical bone ash. *J. Ceram. Process. Res*, 10, 129-138.
- Balasundaram, G., Sato, M., & Webster, T. J. (2006). Using hydroxyapatite nanoparticles and decreased crystallinity to promote osteoblast adhesion similar to functionalizing with RGD. *Biomaterials*, 27(14), 2798-2805.
- Balázs, C., Wéber, F., Kövér, Z., Horváth, E., & Németh, C. (2007). Preparation of calcium-phosphate bioceramics from natural resources. *Journal of the European Ceramic Society*, 27(2), 1601-1606.
- Barralet, J., Grover, L., Gaunt, T., Wright, A., & Gibson, I. (2002). Preparation of macroporous calcium phosphate cement tissue engineering scaffold. *Biomaterials*, 23(15), 3063-3072.
- Barsoum, M., & Barsoum, M. (2002). *Fundamentals of ceramics*: CRC press.
- Behnamghader, A., Shirazi, R. N., Iost, A., & Najjar, D. (2011). *Surface Cracking and Degradation of Dense Hydroxyapatite through Vickers Microindentation Testing*. Paper presented at the Applied Mechanics and Materials.
- Ben-Nissan, B., Kannangara, G., & Milev, A. (2003). Morphological stability of hydroxyapatite precursor. *Materials Letters*, 57(13), 1960-1965.
- Best, S., Sim, B., Kayser, M., & Downes, S. (1997). The dependence of osteoblastic response on variations in the chemical composition and physical properties of hydroxyapatite. *Journal of Materials Science: Materials in Medicine*, 8(2), 97-103.
- Best, S., Zou, S., Brooks, R. A., Huang, J., Rushton, N., & Bonfield, W. (2008). *The osteogenic behaviour of silicon substituted hydroxyapatite*. Paper presented at the Key Engineering Materials.
- Bigi, A., Boanini, E., Bracci, B., Facchini, A., Panzavolta, S., Segatti, F., & Sturba, L. (2005). Nanocrystalline hydroxyapatite coatings on titanium: a new fast biomimetic method. *Biomaterials*, 26(19), 4085-4089.
- Bigi, A., Boanini, E., Capuccini, C., & Gazzano, M. (2007). Strontium-substituted hydroxyapatite nanocrystals. *Inorganica Chimica Acta*, 360(3), 1009-1016.
- Billotte, W., Bronzino, & D, E. J. (2000). The Biomedical Engineering Handbook, CRC Press LLC, 2000. *Ceramic Biomaterials*.

- Bloemers, F. W., Blokhuis, T. J., Patka, P., Bakker, F. C., Wippermann, B. W., & Haarman, H. J. T. M. (2003). Autologous bone versus calcium-phosphate ceramics in treatment of experimental bone defects. *Journal of Biomedical Materials Research Part B: Applied Biomaterials*, 66(2), 526-531.
- Boyan, B. D., Dean, D. D., Lohmann, C. H., Cochran, D. L., Sylvia, V. L., & Schwartz, Z. (2001). The titanium-bone cell interface in vitro: the role of the surface in promoting osteointegration *Titanium in medicine* (pp. 561-585): Springer.
- Burg, K. J., Porter, S., & Kellam, J. F. (2000). Biomaterial developments for bone tissue engineering. *Biomaterials*, 21(23), 2347-2359.
- Champion, E., Bernache-Assolant, D., Halouani, R., & Ababou, A. (1994). Microstructure and related mechanical properties of hot pressed hydroxyapatite ceramics. *Journal of Materials Science: Materials in Medicine*, 5(8), 563-568.
- Charriere, E., Lemaitre, J., & Zysset, P. (2003). Hydroxyapatite cement scaffolds with controlled macroporosity: fabrication protocol and mechanical properties. *Biomaterials*, 24(5), 809-817.
- Chattopadhyay, P., Pal, S., Wahi, A., Singh, L., & Verma, A. (2007). Synthesis of Crystalline Hydroxyapatite from Coral (*Gergonacea* sp) and Cytotoxicity Evaluation. *Trends in Biomaterials and Artificial Organs*, 20(2).
- Chen, C.-W., Oakes, C. S., Byrappa, K., Riman, R. E., Brown, K., TenHuisen, K. S., & Janas, V. F. (2004). Synthesis, characterization, and dispersion properties of hydroxyapatite prepared by mechanochemical-hydrothermal methods. *Journal of Materials Chemistry*, 14(15), 2425-2432.
- Chen, H., Wang, W., Xie, H., Xu, X., Wu, J., Jiang, Z., Zheng, S. (2009). A pathogenic role of IL-17 at the early stage of corneal allograft rejection. *Transplant immunology*, 21(3), 155-161.
- Chen, J., Wang, Y., Chen, X., Ren, L., Lai, C., He, W., & Zhang, Q. (2011). A simple sol-gel technique for synthesis of nanostructured hydroxyapatite, tricalcium phosphate and biphasic powders. *Materials Letters*, 65(12), 1923-1926.
- Chesnutt, B. M., Viano, A. M., Yuan, Y., Yang, Y., Guda, T., Appleford, M. R., Bumgardner, J. D. (2009). Design and characterization of a novel chitosan/nanocrystalline calcium phosphate composite scaffold for bone regeneration. *J Biomed Mater Res A*, 88(2), 491-502.
- Correia, R., Magalhaes, M., Marques, P., & Senos, A. (1996). Wet synthesis and characterization of modified hydroxyapatite powders. *Journal of Materials Science: Materials in Medicine*, 7(8), 501-505.

- Daglilar, S., & Erkan, M. (2007). A study on bioceramic reinforced bone cements. *Materials Letters*, 61(7), 1456-1459.
- Deatherage, J. (2010). Bone materials available for alveolar grafting. *Oral Maxillofac Surg Clin North Am*, 22(3), 347-352, v.
- Deisinger, U., Stenzel, F., & Ziegler, G. (2004). *Development of hydroxyapatite ceramics with tailored pore structure*. Paper presented at the Key Engineering Materials.
- Deligianni, D., Korovessis, P., Porte-Derrieu, M. C., & Amedee, J. (2005). Fibronectin preadsorbed on hydroxyapatite together with rough surface structure increases osteoblasts' adhesion *in vitro*: The theoretical usefulness of fibronectin preadsorption on hydroxyapatite to increase permanent stability and longevity in spine implants. *Journal of spinal disorders & techniques*, 18(3), 257-262.
- Dey, A., & Mukhopadhyay, A. K. (2011). Fracture Toughness of Microplasma-Sprayed Hydroxyapatite Coating by Nanoindentation. *International journal of applied ceramic technology*, 8(3), 572-590.
- Doostmohammadi, A., Monshi, A., Fathi, M., & Braissant, O. (2011). A comparative physico-chemical study of bioactive glass and bone-derived hydroxyapatite. *Ceramics International*, 37(5), 1601-1607.
- Dorozhkin, S. V. (2007). Calcium orthophosphates. *Journal of Materials Science*, 42(4), 1061-1095.
- Dorozhkin, S. V. (2009). Calcium Orthophosphates in Nature, Biology and Medicine. *Materials*, 2(2), 399-498.
- Dorozhkin, S. V. (2010a). Calcium orthophosphates as bioceramics: state of the art. *J Funct Biomater*, 1(1), 22-107.
- Dorozhkin, S. V. (2010b). Nanosized and nanocrystalline calcium orthophosphates. *Acta Biomater*, 6(3), 715-734.
- Dorozhkin, S. V. (2012). Biphasic, triphasic and multiphasic calcium orthophosphates. *Acta Biomater*, 8(3), 963-977.
- El-Ghannam, A., & Ning, C. (2006). Effect of bioactive ceramic dissolution on the mechanism of bone mineralization and guided tissue growth in vitro. *Journal of Biomedical Materials Research Part A*, 76(2), 386-397.

- Eppley, B. L., & Prevel, C. D. (1997). Nonmetallic fixation in traumatic midfacial fractures. *Journal of Craniofacial Surgery*, 8(2), 103-109.
- Evans, A., & Faber, K. (1981). Toughening of ceramics by circumferential microcracking. *Journal of the American Ceramic Society*, 64(7), 394-398.
- Evis, Z., & Webster, T. J. (2011). Nanosize hydroxyapatite: doping with various ions. *Advances in Applied Ceramics*, 110(5), 311-321.
- Fanovich, M., Castro, M., & Lopez, J. P. (1998). Improvement of the microstructure and microhardness of hydroxyapatite ceramics by addition of lithium. *Materials Letters*, 33(5), 269-272.
- Fathi, M. H., & Hanifi, A. (2007). Evaluation and characterization of nanostructure hydroxyapatite powder prepared by simple sol-gel method. *Materials Letters*, 61(18), 3978-3983.
- Fischgrund, J. S., Chiba, K., Heller, J. G., Patel, T. C., Thalgott, J. S., Truumees, E., Wang, J. C. (2002). Bone grafting alternatives in spinal surgery. *The Spine Journal*, 2(3), 206-215.
- Foster, D. L., & Mucalo, M. R. (2004). A method for avoiding the xanthoproteic-associated discolouration in reprecipitated (nitric-acid-digested) hydroxyapatite prepared from mammalian bone tissue. *Croatica chemica acta*, 77(3), 509-517.
- Georgiade, N. G., Hanker, J., Ruff, G., & Levin, S. (1993). The use of particulate hydroxyapatite and plaster of Paris in aesthetic and reconstructive surgery. *Aesthetic plastic surgery*, 17(2), 85-92.
- Giannoudis, P. V., Dinopoulos, H., & Tsiridis, E. (2005). Bone substitutes: an update. *Injury*, 36 Suppl 3, S20-27.
- Giannoudis, P. V., Dinopoulos, H., & Tsiridis, E. (2005). Bone substitutes: an update. *Injury*, 36(3), S20-S27.
- Groot, K. (1988). Effect of porosity and physicochemical properties on the stability, resorption, and strength of calcium phosphate ceramics. *Annals of the New York Academy of Sciences*, 523(1), 227-233.
- Gross, K. A., & Rodríguez-Lorenzo, L. M. (2004). Sintered hydroxyfluorapatites. Part II: Mechanical properties of solid solutions determined by microindentation. *Biomaterials*, 25(7), 1385-1394.

- Gunzburg, R., & Szpalski, M. (2004). Biology of Bone Grafting: Autograft and Allograft. *The Lumbar Spine*, 247.
- Guo, X., & Xiao, P. (2006). Effects of solvents on properties of nanocrystalline hydroxyapatite produced from hydrothermal process. *Journal of the European Ceramic Society*, 26(15), 3383-3391.
- Guo, Y.-P., Yao, Y.-b., Ning, C.-Q., Guo, Y.-J., & Chu, L.-F. (2011). Fabrication of mesoporous carbonated hydroxyapatite microspheres by hydrothermal method. *Materials Letters*, 65(14), 2205-2208.
- Handbook, A. S. M. (1991). Volume 4. *Heat treating*.
- Hasegawa, S., Neo, M., Tamura, J., Fujibayashi, S., Takemoto, M., Shikinami, Y., Nakamura, T. (2007). In vivo evaluation of a porous hydroxyapatite/poly-DL-lactide composite for bone tissue engineering. *Journal of Biomedical Materials Research Part A*, 81(4), 930-938.
- He, L.-H., Standard, O. C., Huang, T. T., Latella, B. A., & Swain, M. V. (2008). Mechanical behaviour of porous hydroxyapatite. *Acta Biomater*, 4(3), 577-586.
- Hench, L. L. (1998). Biomaterials: a forecast for the future. *Biomaterials*, 19(16), 1419-1423.
- Hench, L. L., & Polak, J. M. (2002). Third-generation biomedical materials. *Science*, 295(5557), 1014-1017.
- Herliansyah, M., Hamdi, M., Ide-Ektessabi, A., Wildan, M., & Toque, J. (2009). The influence of sintering temperature on the properties of compacted bovine hydroxyapatite. *Materials Science and Engineering: C*, 29(5), 1674-1680.
- Herliansyah, M. K., Muzafar, C., & Tontowi, A. E. (2012). Natural Bioceramics Bone Graft: A Comparative Study of Calcite Hydroxyapatite, Gypsum Hydroxyapatite, Bovine Hydroxyapatite and Cuttlefish Shell Hydroxyapatite. *Proceedings of the Asia Pacific Industrial Engineering & Management Systems, Bangkok*, 1135-1145.
- Hing, K. A. (2004). Bone repair in the twenty-first century: biology, chemistry or engineering? *Philos Trans A Math Phys Eng Sci*, 362(1825), 2821-2850.
- Hing, K. A. (2005). Bioceramic bone graft substitutes: influence of porosity and chemistry. *International journal of applied ceramic technology*, 2(3), 184-199.

- Hoemann, C., El-Gabalawy, H., & McKee, M. (2009). In vitro osteogenesis assays: influence of the primary cell source on alkaline phosphatase activity and mineralization. *Pathologie Biologie*, 57(4), 318-323.
- Hojo, Y., Kotani, Y., Ito, M., Abumi, K., Kadosawa, T., Shikinami, Y., & Minami, A. (2005). A biomechanical and histological evaluation of a bioresorbable lumbar interbody fusion cage. *Biomaterials*, 26(15), 2643-2651.
- Hsieh, M.-F., Perng, L.-H., Chin, T.-S., & Perng, H.-G. (2001). Phase purity of sol-gel-derived hydroxyapatite ceramic. *Biomaterials*, 22(19), 2601-2607.
- Hu, J., Russell, J., Ben-Nissan, B., & Vago, R. (2001). Production and analysis of hydroxyapatite from Australian corals via hydrothermal process. *Journal of materials science letters*, 20(1), 85-87.
- Huang, J., Li, G., Li, Y., Zhang, R., Deng, B., Zhang, J., & Aoki, H. (2007). In vitro study on influence of a discrete nano-hydroxyapatite on leukemia P388 cell behavior. *Biomedical Materials and Engineering*, 17(5), 321.
- Ito, A., Ojima, K., Naito, H., Ichinose, N., & Tateishi, T. (2000). Preparation, solubility, and cytocompatibility of zinc-releasing calcium phosphate ceramics. *J Biomed Mater Res*, 50(2), 178-183.
- Ivanchenko, L. A., & Pinchuk, N. D. (2003). Making calcium phosphate biomaterials. *Powder Metallurgy and Metal Ceramics*, 42(7-8), 357-371.
- Ivankovic, H., Ferrer, G. G., Tkalcec, E., Orlic, S., & Ivankovic, M. (2009). Preparation of highly porous hydroxyapatite from cuttlefish bone. *Journal of Materials Science: Materials in Medicine*, 20(5), 1039-1046.
- Jayabalan, M., Shalumon, K. T., Mitha, M. K., Ganesan, K., & Epple, M. (2010). Effect of hydroxyapatite on the biodegradation and biomechanical stability of polyester nanocomposites for orthopaedic applications. *Acta Biomater*, 6(3), 763-775.
- Jensen, S. S., Broggin, N., Hjørting-Hansen, E., Schenk, R., & Buser, D. (2006). Bone healing and graft resorption of autograft, anorganic bovine bone and β -tricalcium phosphate. A histologic and histomorphometric study in the mandibles of minipigs. *Clin Oral Implants Res*, 17(3), 237-243.
- Jillavenkatesa, A., & Condrate Sr, R. (1998). Sol-gel processing of hydroxyapatite. *Journal of Materials Science*, 33(16), 4111-4119.

- Jin, H.-B., Guo, C.-B., Mao, K.-Y., Dorozhkin, S., & Agathopoulos, S. (2010). Preparation of porous biphasic. BETA.-TCP/HA bioceramics with a natural trabecular structure from calcined cancellous bovine bone. *Journal of the Ceramic Society of Japan*, 118(1373), 52-56.
- jingbing, Guilet, D., Marston, A., Randimbivololona, F., & Hostettmann, K. (2003). Antifungal isopimaranes from *Hypoestes serpens*. *Phytochemistry*, 64(2), 543-548.
- Jinlong, N., Zhenxi, Z., & Dazong, J. (2001). Investigation of phase evolution during the thermochemical synthesis of tricalcium phosphate. *Journal of Materials synthesis and Processing*, 9(5), 235-240.
- Jokanovic, V., Izvonar, D., Dramicanin, M. D., Jokanovic, B., Zivojinovic, V., Markovic, D., & Dacic, B. (2006). Hydrothermal synthesis and nanostructure of carbonated calcium hydroxyapatite. *J Mater Sci Mater Med*, 17(6), 539-546.
- Joschek, S., Nies, B., Krotz, R., & Göpferich, A. (2000). Chemical and physicochemical characterization of porous hydroxyapatite ceramics made of natural bone. *Biomaterials*, 21(16), 1645-1658.
- Kalita, S. J., Bhardwaj, A., & Bhatt, H. A. (2007). Nanocrystalline calcium phosphate ceramics in biomedical engineering. *Materials Science and Engineering: C*, 27(3), 441-449.
- Kalita, S. J., & Verma, S. (2010). Nanocrystalline hydroxyapatite bioceramic using microwave radiation: Synthesis and characterization. *Materials Science and Engineering: C*, 30(2), 295-303.
- Kamalanathan, P., Ramesh, S., Bang, L., Niakan, A., Tan, C., Purbolaksono, J., Teng, W. (2014). Synthesis and sintering of hydroxyapatite derived from eggshells as a calcium precursor. *Ceramics International*, 40(10), 16349-16359.
- Kannan, S., Rocha, J. H., Agathopoulos, S., & Ferreira, J. M. (2007). Fluorine-substituted hydroxyapatite scaffolds hydrothermally grown from aragonitic cuttlefish bones. *Acta Biomater*, 3(2), 243-249.
- Katti, K. S. (2004). Biomaterials in total joint replacement. *Colloids and Surfaces B: Biointerfaces*, 39(3), 133-142.
- Kim, D.-H., Kim, K.-L., Chun, H.-H., Kim, T.-W., Park, H.-C., & Yoon, S.-Y. (2014). In vitro biodegradable and mechanical performance of biphasic calcium phosphate porous scaffolds with unidirectional macro-pore structure. *Ceramics International*, 40(6), 8293-8300.

- Kim, H.-W., Noh, Y.-J., Koh, Y.-H., & Kim, H.-E. (2003). Enhanced performance of fluorine substituted hydroxyapatite composites for hard tissue engineering. *Journal of Materials Science: Materials in Medicine*, 14(10), 899-904.
- Kim, I.-S., & Kumta, P. N. (2004). Sol-gel synthesis and characterization of nanostructured hydroxyapatite powder. *Materials Science and Engineering: B*, 111(2-3), 232-236.
- Kim, J. Y., Lee, T. J., Cho, D. W., & Kim, B. S. (2010). Solid free-form fabrication-based PCL/HA scaffolds fabricated with a multi-head deposition system for bone tissue engineering. *J Biomater Sci Polym Ed*, 21(6), 951-962.
- Koester, K. J., Ager, J., & Ritchie, R. (2008). The true toughness of human cortical bone measured with realistically short cracks. *Nature materials*, 7(8), 672-677.
- Kokkinos, P. A., Koutsoukos, P. G., & Deligianni, D. D. (2012). Detachment strength of human osteoblasts cultured on hydroxyapatite with various surface roughness. Contribution of integrin subunits. *J Mater Sci Mater Med*, 23(6), 1489-1498.
- Krishna, D. S. R., Siddharthan, A., Seshadri, S., & Kumar, T. S. (2007). A novel route for synthesis of nanocrystalline hydroxyapatite from eggshell waste. *Journal of Materials Science: Materials in Medicine*, 18(9), 1735-1743.
- Krishnamurithy, G., Murali, M. R., Hamdi, M., Abbas, A., Raghavendran, H. B., & Kamarul, T. (2014). Characterization of bovine-derived porous hydroxyapatite scaffold and its potential to support osteogenic differentiation of human bone marrow derived mesenchymal stem cells. *Ceramics International*, 40(1), 771-777.
- Kruzic, J., Kim, D., Koester, K., & Ritchie, R. (2009). Indentation techniques for evaluating the fracture toughness of biomaterials and hard tissues. *Journal of the Mechanical Behavior of Biomedical Materials*, 2(4), 384-395.
- Kumar, G. S., Girija, E. K., Thamizhavel, A., Yokogawa, Y., & Kalkura, S. N. (2010). Synthesis and characterization of bioactive hydroxyapatite-calcite nanocomposite for biomedical applications. *J Colloid Interface Sci*, 349(1), 56-62.
- Kumar, R., Prakash, K., Cheang, P., & Khor, K. (2004). Temperature driven morphological changes of chemically precipitated hydroxyapatite nanoparticles. *Langmuir*, 20(13), 5196-5200.
- Kwok, C. T., Wong, P. K., Cheng, F. T., & Man, H. C. (2009). Characterization and corrosion behavior of hydroxyapatite coatings on Ti6Al4V fabricated by electrophoretic deposition. *Applied Surface Science*, 255(13-14), 6736-6744.

- Lach, R., Gyurova, L. A., & Grellmann, W. (2007). Application of indentation fracture mechanics approach for determination of fracture toughness of brittle polymer systems. *Polymer testing*, 26(1), 51-59.
- Langstaff, S., Sayer, M., Smith, T., & Pugh, S. (2001). Resorbable bioceramics based on stabilized calcium phosphates. Part II: evaluation of biological response. *Biomaterials*, 22(2), 135-150.
- Lee, C., & Jones, W. (1982). Fracture toughness (KQ) testing with a mini-compact tension (CT) specimen. *Polymer Engineering & Science*, 22(18), 1190-1198.
- Lee, S. J., & Oh, S. H. (2003). Fabrication of calcium phosphate bioceramics by using eggshell and phosphoric acid. *Materials Letters*, 57(29), 4570-4574.
- LeGeros, R. Z. (2002). Properties of osteoconductive biomaterials: calcium phosphates. *Clinical orthopaedics and related research*, 395, 81-98.
- LeGeros, R. Z., Daculsi, G., & LeGeros, J. P. (2008). Bioactive bioceramics *Musculoskeletal Tissue Regeneration* (pp. 153-181): Springer.
- Lemos, A. F., Rocha, J. H. G., Quaresma, S. S. F., Kannan, S., Oktar, F. N., Agathopoulos, S., & Ferreira, J. M. F. (2006). Hydroxyapatite nano-powders produced hydrothermally from nacreous material. *Journal of the European Ceramic Society*, 26(16), 3639-3646.
- Li, J., Dou, Y., Yang, J., Yin, Y., Zhang, H., Yao, F., Yao, K. (2009). Surface characterization and biocompatibility of micro-and nano-hydroxyapatite/chitosan-gelatin network films. *Materials Science and Engineering: C*, 29(4), 1207-1215.
- Li, X., Liu, H., Niu, X., Fan, Y., Feng, Q., Cui, F. z., & Watari, F. (2011). Osteogenic differentiation of human adipose-derived stem cells induced by osteoinductive calcium phosphate ceramics. *Journal of Biomedical Materials Research Part B: Applied Biomaterials*, 97(1), 10-19.
- Lin, F.-H., Liao, C.-J., Chen, K.-S., & Sun, J.-S. (1999). Preparation of a biphasic porous bioceramic by heating bovine cancellous bone with Na₄P₂O₇·10H₂O addition. *Biomaterials*, 20(5), 475-484.
- Liu, D.-M., Troczynski, T., & Tseng, W. J. (2001). Water-based sol-gel synthesis of hydroxyapatite: process development. *Biomaterials*, 22(13), 1721-1730.
- Liu, D.-M., Yang, Q., Troczynski, T., & Tseng, W. J. (2002). Structural evolution of sol-gel-derived hydroxyapatite. *Biomaterials*, 23(7), 1679-1687.

- Low, K. L., Tan, S. H., Zein, S. H., Roether, J. A., Mourino, V., & Boccaccini, A. R. (2010). Calcium phosphate-based composites as injectable bone substitute materials. *J Biomed Mater Res B Appl Biomater*, 94(1), 273-286.
- Meredith, T. L. (2008). Composite Bone Material and Method of Making and Using Same: Google Patents.
- Mikuni-Takagaki, Y., Kakai, Y., Satoyoshi, M., Kawano, E., Suzuki, Y., Kawase, T., & Saito, S. (1995). Matrix mineralization and the differentiation of osteocyte-like cells in culture. *Journal of Bone and Mineral Research*, 10(2), 231-242.
- Mitragotri, S., & Lahann, J. (2009). Physical approaches to biomaterial design. *Nature materials*, 8(1), 15-23.
- Miyazaki, M., Tsumura, H., Wang, J. C., & Alanay, A. (2009). An update on bone substitutes for spinal fusion. *Eur Spine J*, 18(6), 783-799.
- Mkukuma, L., Skakle, J., Gibson, I., Imrie, C., Aspden, R., & Hukins, D. (2004). Effect of the proportion of organic material in bone on thermal decomposition of bone mineral: an investigation of a variety of bones from different species using thermogravimetric analysis coupled to mass spectrometry, high-temperature X-ray diffraction, and Fourier transform infrared spectroscopy. *Calcified tissue international*, 75(4), 321-328.
- Mochales, C., Briak-BenAbdeslam, H. E., Ginebra, M. P., Terol, A., Planell, J. A., & Boudeville, P. (2004). Dry mechanochemical synthesis of hydroxyapatites from DCPD and CaO: influence of instrumental parameters on the reaction kinetics. *Biomaterials*, 25(7-8), 1151-1158.
- Montazeri, L., Javadpour, J., Shokrgozar, M. A., Bonakdar, S., & Javadian, S. (2010). Hydrothermal synthesis and characterization of hydroxyapatite and fluorhydroxyapatite nano-size powders. *Biomed Mater*, 5(4), 045004.
- Mostafa, N. Y. (2005). Characterization, thermal stability and sintering of hydroxyapatite powders prepared by different routes. *Materials Chemistry and Physics*, 94(2-3), 333-341.
- Mucalo, M. R., & Worth, A. J. (2008). Biomedicals from Bone.
- Muralithran, G., & Ramesh, S. (2000). The effects of sintering temperature on the properties of hydroxyapatite. *Ceramics International*, 26(2), 221-230.
- Murugan, R., & Ramakrishna, S. (2005). Aqueous mediated synthesis of bioresorbable nanocrystalline hydroxyapatite. *Journal of Crystal Growth*, 274(1), 209-213.

- Nasiri-Tabrizi, B., Honarmandi, P., Ebrahimi-Kahrizsangi, R., & Honarmandi, P. (2009). Synthesis of nanosize single-crystal hydroxyapatite via mechanochemical method. *Materials Letters*, 63(5), 543-546.
- Navarro, E., Baun, A., Behra, R., Hartmann, N. B., Filser, J., Miao, A.-J., Sigg, L. (2008). Environmental behavior and ecotoxicity of engineered nanoparticles to algae, plants, and fungi. *Ecotoxicology*, 17(5), 372-386.
- Nayar, S., & Guha, A. (2009). Waste utilization for the controlled synthesis of nanosized hydroxyapatite. *Materials Science and Engineering: C*, 29(4), 1326-1329.
- Neira, I. S., Kolen'ko, Y. V., Lebedev, O. I., Van Tendeloo, G., Gupta, H. S., Guitián, F., & Yoshimura, M. (2008). An effective morphology control of hydroxyapatite crystals via hydrothermal synthesis. *Crystal Growth and Design*, 9(1), 466-474.
- Newesely, H. (1963). The nature of carbonate contents in tooth mineral. *Experientia*, 19(12), 620-621.
- Niakan, A., Ramesh, S., Ganesan, P., Tan, C., Purbolaksono, J., Chandran, H., & Teng, W. (2015). Sintering behaviour of natural porous hydroxyapatite derived from bovine bone. *Ceramics International*, 41(2), 3024-3029.
- Niihara, K., Morena, R., & Hasselman, D. (1982). Evaluation of K_{Ic} of brittle solids by the indentation method with low crack-to-indent ratios. *Journal of materials science letters*, 1(1), 13-16.
- Nuss, K. M., & von Rechenberg, B. (2008). Biocompatibility issues with modern implants in bone—a review for clinical orthopedics. *The open orthopaedics journal*, 2, 66.
- Oh, S., Oh, N., Appleford, M., & Ong, J. L. (2006). Bioceramics for tissue engineering applications—a review. *Am J Biochem Biotechnol*, 2(2), 49-56.
- Ooi, C. Y., Hamdi, M., & Ramesh, S. (2007). Properties of hydroxyapatite produced by annealing of bovine bone. *Ceramics International*, 33(7), 1171-1177.
- Orlovskii, V., Komlev, V., & Barinov, S. (2002). Hydroxyapatite and hydroxyapatite-based ceramics. *Inorganic Materials*, 38(10), 973-984.
- Padmanabhan, S. K., Balakrishnan, A., Chu, M.-C., Lee, Y. J., Kim, T. N., & Cho, S.-J. (2009). Sol-gel synthesis and characterization of hydroxyapatite nanorods. *Particuology*, 7(6), 466-470.

- Park, J. W., Bae, S. R., Suh, J. Y., Lee, D. H., Kim, S. H., Kim, H., & Lee, C. S. (2008). Evaluation of bone healing with eggshell-derived bone graft substitutes in rat calvaria: A pilot study. *Journal of Biomedical Materials Research Part A*, 87(1), 203-214.
- Park, Y.-S., Lee, J.-Y., Yun, S.-H., Jung, M.-W., & Oh, I. (2003). Comparison of hydroxyapatite-and porous-coated stems in total hip replacement. *Acta Orthopaedica*, 74(3), 259-263.
- Pena, J., LeGeros, R. Z., Rohanizadeh, R., & LeGeros, J. P. (2000). *CaCO₃/Ca-P biphasic materials prepared by microwave processing of natural aragonite and calcite*. Paper presented at the Key Engineering Materials.
- Petite, H., Viateau, V., Bensaid, W., Meunier, A., de Pollak, C., Bourguignon, M., Guillemain, G. (2000). Tissue-engineered bone regeneration. *Nature biotechnology*, 18(9), 959-963.
- Pinchuk, N., & Ivanchenko, L. (2003). Technological processes of producing calcium-phosphate biomaterials.
- Poinern, G. E. J., Brundavanam, R. K., Le, X. T., & Fawcett, D. (2012). The mechanical properties of a porous ceramic derived from a 30 nm sized particle based powder of hydroxyapatite for potential hard tissue engineering applications. *American Journal of Biomedical Engineering*, 2(6), 278-286.
- Porter, A. E., Best, S. M., Thian, E. S., & Huang, J. (2008). Bioceramics: Past, present and for the future. *Journal of the European Ceramic Society*, 28(7), 1319-1327.
- Porter, A. E., Patel, N., Skepper, J. N., Best, S. M., & Bonfield, W. (2004). Effect of sintered silicate-substituted hydroxyapatite on remodelling processes at the bone-implant interface. *Biomaterials*, 25(16), 3303-3314.
- Porter, M. M., & McKittrick, J. (2014). It's tough to be strong: Advances. *Am. Ceram. Soc. Bull*, 93, 18-24.
- Prabakaran, K., & Rajeswari, S. (2006). Development of hydroxyapatite from natural fish bone through heat treatment. *Trends Biomater Artif Organs*, 20, 20-23.
- Qazi, T. H., Mooney, D. J., Pumberger, M., Geißler, S., & Duda, G. N. (2015). Biomaterials based strategies for skeletal muscle tissue engineering: Existing technologies and future trends. *Biomaterials*, 53, 502-521.

- Qian, J., Kang, Y., Zhang, W., & Li, Z. (2008). Fabrication, chemical composition change and phase evolution of biomorphic hydroxyapatite. *J Mater Sci Mater Med*, 19(11), 3373-3383.
- Quinn, G. D. (2008). Fracture toughness of ceramics by the Vickers indentation crack length method: a critical review. *Mechanical Properties and Performance of Engineering Ceramics II: Ceramic Engineering and Science Proceedings, Volume 27, Issue 2*, 45-62.
- Raghavendran, H. R. B., Puvaneswary, S., Talebian, S., Murali, M. R., Naveen, S. V., Krishnamurthy, G., Kamarul, T. (2014). A comparative study on in vitro osteogenic priming potential of electron spun scaffold PLLA/HA/Col, PLLA/HA, and PLLA/Col for tissue engineering application.
- Ramanan, S. R., & Venkatesh, R. (2004). A study of hydroxyapatite fibers prepared via sol-gel route. *Materials Letters*, 58(26), 3320-3323.
- Ramesh, S., Christopher, P., Tan, C., & Teng, W. (2004). The effect of cold isostatic pressing on the sinterability of synthesized HA. *Biomedical Engineering: Applications, Basis and Communications*, 16(04), 199-204.
- Ramesh, S., Tan, C. Y., Bhaduri, S. B., & Teng, W. D. (2007). Rapid densification of nanocrystalline hydroxyapatite for biomedical applications. *Ceramics International*, 33(7), 1363-1367.
- Ramesh, S., Tan, C. Y., Tolouei, R., Amiriyani, M., Purbolaksono, J., Sopyan, I., & Teng, W. D. (2012). Sintering behavior of hydroxyapatite prepared from different routes. *Materials & Design*, 34, 148-154.
- Raynaud, S., Champion, E., Bernache-Assollant, D., & Thomas, P. (2002). Calcium phosphate apatites with variable Ca/P atomic ratio I. Synthesis, characterisation and thermal stability of powders. *Biomaterials*, 23(4), 1065-1072.
- Reyes-Gasga, J., Garcia-Garcia, R., Arellano-Jimenez, M., Sanchez-Pastenes, E., Tiznado-Orozco, G., Gil-Chavarria, I., & Gómez-Gasga, G. (2008). Structural and thermal behaviour of human tooth and three synthetic hydroxyapatites from 20 to 600 C. *Journal of Physics D: Applied Physics*, 41(22), 225407.
- Reynolds, M. A., Aichelmann-Reidy, M. E., & Branch-Mays, G. L. (2010). Regeneration of periodontal tissue: bone replacement grafts. *Dent Clin North Am*, 54(1), 55-71.
- Rhee, S.-H. (2002). Synthesis of hydroxyapatite via mechanochemical treatment. *Biomaterials*, 23(4), 1147-1152.

- Riman, R. E., Suchanek, W. L., Byrappa, K., Chen, C.-W., Shuk, P., & Oakes, C. S. (2002). Solution synthesis of hydroxyapatite designer particulates. *Solid State Ionics*, 151(1), 393-402.
- Rizzi, S. C., Heath, D., Coombes, A., Bock, N., Textor, M., & Downes, S. (2001). Biodegradable polymer/hydroxyapatite composites: surface analysis and initial attachment of human osteoblasts. *J Biomed Mater Res*, 55(4), 475-486.
- Rocha, J. H. G., Lemos, A. F., Kannan, S., Agathopoulos, S., & Ferreira, J. M. F. (2005). Hydroxyapatite scaffolds hydrothermally grown from aragonitic cuttlefish bones. *Journal of Materials Chemistry*, 15(47), 5007.
- Rose, F. R., & Oreffo, R. O. (2002). Bone tissue engineering: hope vs hype. *Biochem Biophys Res Commun*, 292(1), 1-7.
- Rose, F. R., & Oreffo, R. O. (2002). Bone tissue engineering: hope vs hype. *Biochem Biophys Res Commun*, 292(1), 1-7.
- Roy, D. M., & Linnehan, S. K. (1974). Hydroxyapatite formed from coral skeletal carbonate by hydrothermal exchange.
- Ruehe, B., Niehues, S., Heberer, S., & Nelson, K. (2009). Miniature pigs as an animal model for implant research: bone regeneration in critical-size defects. *Oral Surg Oral Med Oral Pathol Oral Radiol Endod*, 108(5), 699-706.
- Salas, J., Benzo, Z., & González, G. (2004). Synthesis of Hydroxyapatite by Mechanochemical transformation. *Revista Latinoamericana de Metalurgia y Materiales*, 24(1), 12-16.
- Salgado, A. J., Coutinho, O. P., & Reis, R. L. (2004). Bone tissue engineering: state of the art and future trends. *Macromol Biosci*, 4(8), 743-765.
- Sanosh, K., Chu, M.-C., Balakrishnan, A., Kim, T., & Cho, S.-J. (2009). Preparation and characterization of nano-hydroxyapatite powder using sol-gel technique. *Bulletin of Materials Science*, 32(5), 465-470.
- Santos, M. H., Oliveira, M. d., Souza, L. P. d. F., Mansur, H. S., & Vasconcelos, W. L. (2004). Synthesis control and characterization of hydroxyapatite prepared by wet precipitation process. *Materials Research*, 7(4), 625-630.
- Sasikumar, S., & Vijayaraghavan, R. (2006). Low temperature synthesis of nanocrystalline hydroxyapatite from egg shells by combustion method. *Trends Biomater. Artif. Organs*, 19(2), 70-73.

- Schieker, M., Seitz, H., Drosse, I., Seitz, S., & Mutschler, W. (2006). Biomaterials as Scaffold for Bone Tissue Engineering. *European Journal of Trauma*, 32(2), 114-124.
- Shepherd, J. H., Shepherd, D. V., & Best, S. M. (2012). Substituted hydroxyapatites for bone repair. *J Mater Sci Mater Med*, 23(10), 2335-2347.
- Shi, Z., Huang, X., Cai, Y., Tang, R., & Yang, D. (2009). Size effect of hydroxyapatite nanoparticles on proliferation and apoptosis of osteoblast-like cells. *Acta Biomater*, 5(1), 338-345.
- Silva, R., Camilli, J., Bertran, C., & Moreira, N. (2005). The use of hydroxyapatite and autogenous cancellous bone grafts to repair bone defects in rats. *International journal of oral and maxillofacial surgery*, 34(2), 178-184.
- Silvester, L., Lamonier, J.-F., Vannier, R.-N., Lamonier, C., Capron, M., Mamede, A.-S., Dumeignil, F. (2014). Structural, textural and acid–base properties of carbonate-containing hydroxyapatites. *Journal of Materials Chemistry A*, 2(29), 11073.
- Simon, Z., & Watson, P. A. (2002). Biomimetic dental implants-new ways to enhance osseointegration. *Journal-Canadian Dental Association*, 68(5), 286-289.
- Sivakumar, M., Kumar, T. S., Shantha, K., & Rao, K. P. (1996). Development of hydroxyapatite derived from Indian coral. *Biomaterials*, 17(17), 1709-1714.
- Skedros, J. G., Holmes, J. L., Vajda, E. G., & Bloebaum, R. D. (2005). Cement lines of secondary osteons in human bone are not mineral-deficient: new data in a historical perspective. *Anat Rec A Discov Mol Cell Evol Biol*, 286(1), 781-803.
- Ślósarczyk, A., & Piekarczyk, J. (1999). Ceramic materials on the basis of hydroxyapatite and tricalcium phosphate. *Ceramics International*, 25(6), 561-565.
- Ślósarczyk, A., Stobierska, E., & Paszkiewicz, Z. (1999). Porous hydroxyapatite ceramics. *Journal of materials science letters*, 18(14), 1163-1165.
- Sofronia, A. M., Baies, R., Anghel, E. M., Marinescu, C. A., & Tanasescu, S. (2014). Thermal and structural characterization of synthetic and natural nanocrystalline hydroxyapatite. *Materials Science and Engineering: C*, 43, 153-163.
- Sopyan, I., & Kaur, J. (2009). Preparation and characterization of porous hydroxyapatite through polymeric sponge method. *Ceramics International*, 35(8), 3161-3168.

- Sousa, F., & Evans, J. R. (2003). Sintered hydroxyapatite latticework for bone substitute. *Journal of the American Ceramic Society*, 86(3), 517-519.
- Suchanek, W., & Yoshimura, M. (1998). Processing and properties of hydroxyapatite-based biomaterials for use as hard tissue replacement implants. *Journal of Materials Research*, 13(01), 94-117.
- Suchanek, W. L., Byrappa, K., Shuk, P., Riman, R. E., Janas, V. F., & TenHuisen, K. S. (2004). Preparation of magnesium-substituted hydroxyapatite powders by the mechanochemical-hydrothermal method. *Biomaterials*, 25(19), 4647-4657.
- Suchanek, W. L., Riman, R. E., Byrappa, K., Chen, C.-W., Shuk, P., & Oakes, C. S. (2002). Solution synthesis of hydroxyapatite designer particulates. *Solid State Ionics*, 151(1), 393-402.
- Tadic, D., & Epple, M. (2004). A thorough physicochemical characterisation of 14 calcium phosphate-based bone substitution materials in comparison to natural bone. *Biomaterials*, 25(6), 987-994.
- Taniguchi, Y., Tamaki, T., Oura, H., Hashizume, H., & Minamide, A. (1999). Sintered bone implantation for the treatment of benign bone tumours in the hand. *Journal of Hand Surgery (British and European Volume)*, 24(1), 109-112.
- Tian, H., Tang, Z., Zhuang, X., Chen, X., & Jing, X. (2012). Biodegradable synthetic polymers: Preparation, functionalization and biomedical application. *Progress in Polymer Science*, 37(2), 237-280.
- Trentz, O. A., Hoerstrup, S. P., Sun, L. K., Bestmann, L., Platz, A., & Trentz, O. L. (2003). Osteoblasts response to allogenic and xenogenic solvent dehydrated cancellous bone in vitro. *Biomaterials*, 24(20), 3417-3426.
- Tripathi, G., & Basu, B. (2012). A porous hydroxyapatite scaffold for bone tissue engineering: Physico-mechanical and biological evaluations. *Ceramics International*, 38(1), 341-349.
- Truumees, E., & Herkowitz, H. N. (1999). Alternatives to autologous bone harvest in spine surgery. *The University of Pennsylvania Orthopaedic Journal*, 12, 77-88.
- Tuominen, T., Jämsä, T., Tuukkanen, J., Marttinen, A., Lindholm, T., & Jalovaara, P. (2001). Bovine bone implant with bovine bone morphogenetic protein in healing a canine ulnar defect. *International orthopaedics*, 25(1), 5-8.

- Ugarte, J. F. d. O., Sena, L. Á. d., Pérez, C. A. d. C., Aguiar, P. F. d., Rossi, A. M., & Soares, G. A. (2005). Influence of processing parameters on structural characteristics of porous calcium phosphate samples: A study using an experimental design method. *Materials Research*, 8(1), 71-76.
- Vaccaro, A. R., Chiba, K., Heller, J. G., Patel, T. C., Thalgott, J. S., Truumees, E., Wang, J. C. (2002). Bone grafting alternatives in spinal surgery. *The Spine Journal*, 2(3), 206-215.
- Vaccaro, A. R., & Madigan, L. (2002). supnal applications of bioabsorbable implants. *Special Supplements*, 97(4), 407-412.
- Vallet-Regí, M. (2001). Ceramics for medical applications. *Journal of the Chemical Society, Dalton Transactions*(2), 97-108.
- Vallet-Regí, M. (2010). Evolution of bioceramics within the field of biomaterials. *Comptes Rendus Chimie*, 13(1-2), 174-185.
- Vallet-Regí, M., & González-Calbet, J. M. (2004). Calcium phosphates as substitution of bone tissues. *Progress in Solid State Chemistry*, 32(1), 1-31.
- Valletregi, M. (2004). Calcium phosphates as substitution of bone tissues. *Progress in Solid State Chemistry*, 32(1-2), 1-31.
- Van den Vreken, N. M., Pieters, I. Y., Declercq, H. A., Cornelissen, M. J., & Verbeeck, R. M. (2010). Characterization of calcium phosphate cements modified by addition of amorphous calcium phosphate. *Acta Biomater*, 6(2), 617-625.
- Vecchio, K. S., Zhang, X., Massie, J. B., Wang, M., & Kim, C. W. (2007). Conversion of bulk seashells to biocompatible hydroxyapatite for bone implants. *Acta Biomater*, 3(6), 910-918.
- Vecchio, K. S., Zhang, X., Massie, J. B., Wang, M., & Kim, C. W. (2007). Conversion of bulk seashells to biocompatible hydroxyapatite for bone implants. *Acta Biomater*, 3(6), 910-918.
- Villora, J., Callejas, P., Barba, M., & Baudin, C. (2004). Statistical analysis of the fracture behaviour of porous ceramic Raschig rings. *Journal of the European Ceramic Society*, 24(3), 589-594.
- Vogel, M., Voigt, C., Gross, U. M., & Müller-Mai, C. M. (2001). In vivo comparison of bioactive glass particles in rabbits. *Biomaterials*, 22(4), 357-362.

- Wang, C., Duan, Y., Markovic, B., Barbara, J., Howlett, C. R., Zhang, X., & Zreiqat, H. (2004). Phenotypic expression of bone-related genes in osteoblasts grown on calcium phosphate ceramics with different phase compositions. *Biomaterials*, 25(13), 2507-2514.
- Wang, J., & Shaw, L. L. (2009). Nanocrystalline hydroxyapatite with simultaneous enhancements in hardness and toughness. *Biomaterials*, 30(34), 6565-6572.
- Wang, X., Ito, A., Sogo, Y., Li, X., & Oyane, A. (2010). Zinc-containing apatite layers on external fixation rods promoting cell activity. *Acta Biomater*, 6(3), 962-968.
- Webster, T. J., Massa-Schlueter, E. A., Smith, J. L., & Slamovich, E. B. (2004). Osteoblast response to hydroxyapatite doped with divalent and trivalent cations. *Biomaterials*, 25(11), 2111-2121.
- Wei, G., & Ma, P. X. (2004). Structure and properties of nano-hydroxyapatite/polymer composite scaffolds for bone tissue engineering. *Biomaterials*, 25(19), 4749-4757.
- Wei, G., & Ma, P. X. (2004). Structure and properties of nano-hydroxyapatite/polymer composite scaffolds for bone tissue engineering. *Biomaterials*, 25(19), 4749-4757.
- Wei, G., & Ma, P. X. (2008). Nanostructured Biomaterials for Regeneration. *Adv Funct Mater*, 18(22), 3566-3582.
- Weiner, A. A., Bock, E. A., Gipson, M. E., & Shastri, V. P. (2008). Photocrosslinked anhydride systems for long-term protein release. *Biomaterials*, 29(15), 2400-2407.
- Weiner, S., & Dove, P. M. (2003). An overview of biomineralization processes and the problem of the vital effect. *Reviews in Mineralogy and Geochemistry*, 54(1), 1-29.
- Wenz, B., Oesch, B., & Horst, M. (2001). Analysis of the risk of transmitting bovine spongiform encephalopathy through bone grafts derived from bovine bone. *Biomaterials*, 22(12), 1599-1606.
- Worth, A., Mucalo, M., Horne, G., Bruce, W., & Burbidge, H. (2005). The evaluation of processed cancellous bovine bone as a bone graft substitute. *Clin Oral Implants Res*, 16(3), 379-386.

- Worth, A., Thompson, K., Owen, M., Mucalo, M., & Firth, E. (2007). Combined xeno/auto-grafting of a benign osteolytic lesion in a dog, using a novel bovine cancellous bone biomaterial. *New Zealand veterinary journal*, 55(3), 143-148.
- Xu, Y., Wang, D., Yang, L., & Tang, H. (2001). Hydrothermal conversion of coral into hydroxyapatite. *Materials characterization*, 47(2), 83-87.
- Yang, Z., Jiang, Y., Wang, Y., Ma, L., & Li, F. (2004). Preparation and thermal stability analysis of hydroxyapatite derived from the precipitation process and microwave irradiation method. *Materials Letters*, 58(27-28), 3586-3590.
- Yeong, W. Y., Chua, C. K., Leong, K. F., & Chandrasekaran, M. (2004). Rapid prototyping in tissue engineering: challenges and potential. *Trends Biotechnol*, 22(12), 643-652.
- Yoshimura, M., Sujaridworakun, P., Koh, F., Fujiwara, T., Pongkao, D., & Ahniyaz, A. (2004). Hydrothermal conversion of calcite crystals to hydroxyapatite. *Materials Science and Engineering: C*, 24(4), 521-525.
- Yuasa, T., Miyamoto, Y., Ishikawa, K., Takechi, M., Momota, Y., Tatehara, S., & Nagayama, M. (2004). Effects of apatite cements on proliferation and differentiation of human osteoblasts in vitro. *Biomaterials*, 25(7-8), 1159-1166.
- Zakharov, N., Polunina, I., Polunin, K., Rakitina, N., Kochetkova, E., Sokolova, N., & Kalinnikov, V. (2004). Calcium hydroxyapatite for medical applications. *Inorganic Materials*, 40(6), 641-648.
- Zaremba, C. M., Morse, D. E., Mann, S., Hansma, P. K., & Stucky, G. D. (1998). Aragonite-hydroxyapatite conversion in gastropod (abalone) nacre. *Chemistry of materials*, 10(12), 3813-3824.
- Zhang, X., & Vecchio, K. S. (2007). Hydrothermal synthesis of hydroxyapatite rods. *Journal of Crystal Growth*, 308(1), 133-140.
- Zhao, G., Zinger, O., Schwartz, Z., Wieland, M., Landolt, D., & Boyan, B. D. (2006). Osteoblast-like cells are sensitive to submicron-scale surface structure. *Clin Oral Implants Res*, 17(3), 258-264.
- Zhou, H., & Lee, J. (2011). Nanoscale hydroxyapatite particles for bone tissue engineering. *Acta Biomater*, 7(7), 2769-2781.
- Zhou, J., Zhang, X., Chen, J., Zeng, S., & De Groot, K. (1993). High temperature characteristics of synthetic hydroxyapatite. *Journal of Materials Science: Materials in Medicine*, 4(1), 83-85.

Zioupos, P. (2001). Ageing Human Bone: Factors Affecting Its Biomechanical Properties and the Role of Collagen. *Journal of Biomaterials Applications*, 15(3), 187-229.

University of Malaya

List of Publications and Award

Best Biotechnology Award from Japan Intellectual Property Association (JIPA) for Production of hydroxyapatite with natural microstructure from bovine bone, 2014.

Niakan, A., Ramesh, S., Ganesan, P., Tan, C. Y., Purbolaksono, J., Chandran, H., & Teng, W. D. (2015). Sintering behaviour of natural porous hydroxyapatite derived from bovine bone. *Ceramics International*, 41(2), 3024-3029.

Niakan, A., Ramesh, S., Tana, C. Y., Purbolaksono, J., Chandran, H., & Teng, W. D. (2015). Effect of annealing treatment on the characteristics of bovine bone. *Journal of Ceramic Processing Research*, 16(2), 223-226.

Niakan, A., Ramesh, S., Hamdi, M., Jahanshahi, A., Tan, C. Y., Ching, Y. C., & Tolouei, R. (2014). Thermal treatment and properties of bovine hydroxyapatite. *Materials Research Innovations*, 18(S6), S6-117.

Niakan, A., Ramesh, S., Tan, C. Y., Hamdi, M., & Teng, W. D. (2013, October). Characteristics of Sintered Bovine Hydroxyapatite. In *Applied Mechanics and Materials* (Vol. 372, pp. 177-180).